DISSERTATION

Titel der Dissertation

„The role of Raf in Ras mediated skin carcinogenesis"

Verfasser

Mag. Florian Kern

angestrebter akademischer Grad

Doktor der Naturwissenschaften (Dr.rer.nat.)

Wien, 2011

Contents

Part I. Abstract

1   Abstract

"The role of Raf in Ras mediated skin carcinogenesis"

The Erk/MAPK pathway consists of a protein kinase cascade (Raf-Mek-Erk) that can regulate growth, differentiation and apoptosis. Ras activates the first kinase in this cascade, Raf. Three Raf family members are known: A-, B- and C-Raf (also known as Raf-1). While A-Raf knockout mice are viable, but have gastrointestinal and neurological defects, the knockout of B-Raf or Raf-1 in mice is embryonic lethal. Both Ras and Raf are often deregulated in human tumors. We have investigated the role of Raf in Ras-driven epidermal tumorigenesis by combining epidermis-restricted B-Raf or Raf-1 ablation with a transgenic and a chemical tumorigenesis model. The transgenic approach used a membrane-tethered form of SOS expressed under the control of the K5 promoter, resulting in constitutive activation of Ras in the basal layer of the epidermis. As a chemical approach we used the classical DMBA/TPA carcinogenesis protocol.

Conditional ablation in the intact murine epidermis by K5-Cre showed that both Raf-1 and B-Raf are dispensable for normal skin homeostasis. Remarkably, Raf-1-deficient epidermis was completely refractory to tumor formation; even more strikingly, ablation of Raf-1 in established tumors led to complete regression accompanied by increased differentiation. Mechanistically, we could show that Raf-1 acts downstream of Ras as an endogenous inhibitor of the cytoskeleton-based kinase Rok-α, a positive regulator of keratinocyte differentiation. B-Raf deletion also led to an impressive reduction in tumor formation, and ablation in established tumors stopped tumor growth by decreasing proliferation and increasing differentiation. The effects were more subtle than those obtained in Raf-1-ablated mice and correlated with reduced ERK phosphorylation in cells and tissues. Thus, B-Raf and Raf-1 have distinct non-redundant roles in Ras-driven tumorigenesis. Consistent with this, the concomitant deletion of B-Raf and Raf-1 in established tumors led to an extremely rapid regression (tumors disappear within three weeks) accompanied by a decrease in ERK activation and by an increase in Rok-α signaling. These data underscore the therapeutic potential of strategies targeting both Raf-1 and B-Raf.

2   Zusammenfassung

"Die Rolle von Raf in Ras vermittelter Hautkarzinogenese"

Der Erk/MAPK Signalweg besteht aus einer Protein Kinase Kaskade (Raf-Mek-Erk) welche Wachstum, Differenzierung und Apoptose reguliert. Ras aktiviert die erste Kinase in dieser Kaskade, Raf. Drei Raf Familienmitglieder sind bekannt: A-, B- und C-Raf (auch bekannt als Raf-1). Während A-Raf knockout Mäuse lebensfähig sind, aber gastrointestinale und neurologische Defekte aufzeigen, sind die Knockouts von B-Raf oder Raf-1 embryonal lethal. Beide Ras und Raf sind oft dereguliert in humanen Tumoren. Wir haben die Rolle von Raf in Ras-vermittelter Tumorentwicklung durch die Kombination von Epidermis-beschränkter B-Raf oder Raf-1 Ablation mit einem transgenen und einem chemischen Tumormodel untersucht. Der transgene Ansatz verwendet eine Membrangebundene Form von SOS unter der Kontrolle des K5 Promoters. Dies führt zu einer konstitutiven Aktivierung von Ras in der basalen Schicht der Epidermis. Als chemischer Ansatz wurde das klassische DMBA/TPA Karzinogenese Protokoll verwendet.

Konditionale Ablation in der intakten Mausepidermis durch K5-Cre zeigte, dass beide Raf-1 und B-Raf für die normale Hauthomeostase verzichtbar sind. Bemerkenswert ist, dass sich Raf-1 defiziente Epidermis total impermeabel für Tumorentstehung zeigte. Noch auffälliger war, dass die Ablation von Raf-1 in einem entwickelten Tumor zu einer totalen Regression durch einhergehender Differenzierung führte. Mechanistisch konnten wir zeigen, dass Raf-1 unterhalb von Ras als endogener Inhibitor der Zytoskelet-basiernden Kinase Rok-α, einem positiven Regulator von Keratinozytendifferenzierung, wirkt. Die Deletion von B-Raf führte auch zu einer beeindruckenden Reduktion an Tumorentstehung und die Ablation in einem bestehenden Tumor stoppte das Tumorwachstum durch Reduzierung der Proliferation und einhergehender Steigerung der Differenzierung. Diese Effekte waren weniger offensichtlich als in den Raf-1 knockout Mäusen und korrelierten mit reduzierter Erk Phosphorylierung in Zellen und im Gewebe. Demnach haben B-Raf und Raf-1 unterschiedliche nicht-redundante Rollen in der Ras-vermittelten Tumorentstehung. Das ist konsistent mit der Beobachtung, dass die gleichzeitige Deletion von B-Raf und Raf-1 in einem bereits bestehenden Tumor zu einer extrem schnellen Regression führt (die Tumore verschwinden innerhalb von drei Wochen), die mit einer Reduktion der Erk-Aktivierung und einer Steigerung des Rok-α Signalweges einhergeht. Diese Daten unterstreichen das therapeutische Potential von Strategien die auf B-Raf und Raf-1 abzielen.

Part II. Introduction

3   Signal transduction

Cells need to communicate and/or respond to outside cues. Signal transduction is the process by which an extracellular signal (e.g. growth factor molecules) activates a receptor leading to an intracellular reaction. The first step is the binding of the signal molecule to a specific receptor on the cell membrane and its subsequent activation. Second messengers are then used to pass the signal on into the cell and engender processes, that ultimately lead to a cellular response. At each stage, the signal can be altered (e.g. amplified, integrated, split, ...), meaning that one signaling cue can account for many responses and that only the integration of all signaling cues determines the actual outcome (Pearson et al., 2001).

3.1   MAPK pathways

Among the best studied signal transduction pathways are the mitogen-activated protein kinase (MAPK) pathways. Mammals possess more than a dozen MAPK genes. Among the most studied MAPK signaling pathways are the Erk/MAPK, the p38/MAPK, and the JNK/MAPK pathway (Bardwell et al., 2009, Raman et al., 2007). The basic principle of MAPK pathways is that of a cascade passing the activation signal in form of phosphorylation from an entry point (the MAPKKK) via an intermediate kinase (the MAPKK) to the business end (the MAPK; Figure 1).
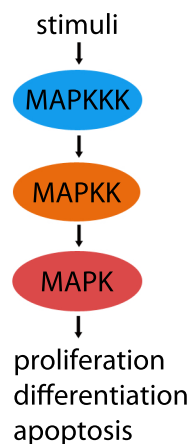

Fig. 1: The mitogen-activated protein kinase (MAPK) pathway principle.
See text for detailed description.

This conserved three tiered module allows signal amplification as well as diversification, en-

abling the MAPK pathways to regulate diverse cellular processes including embryogenesis, proliferation, differentiation and apoptosis (Bardwell et al., 2009, Wimmer and Baccarini, 2010).

3.2   The Erk/MAPK pathway

The Erk/MAPK pathway is one of the longest-studied signaling pathways. Upon mitogenic stimulation (e.g. by EGF), a receptor tyrosine kinase (RTK; e.g. the EGFR) dimerizes and cross-phosphorylates specific tyrosine residues in the carboxy-terminal domains to allow the binding of a complex formed by an adaptor protein (Grb2) and a guanine nucleotide exchange factor, son of sevenless (SOS). The recruitment of the Grb2-SOS complex brings SOS to the membrane and in the proximity of membrane-tethered Ras. SOS leads to the activation of the small GTPase Ras by catalyzing the replacement of GDP with GTP. Activated GTP-bound Ras exerts its effects via discrete downstream effector pathways that include the PI3K/Akt, the RalGDS/Ral, the Tiam1/Rac and the Erk/MAPK pathway, possibly the most prominent one (Khavari and Rinn, 2007). The Erk/MAPK pathway follows the conserved three-tiered module activation. At the level of the MAPKKK three isoforms of Raf, namely A-Raf, B-Raf and C-Raf (or Raf-1), can recruit and phosphorylate the MAPKKs, Mek1 and Mek2 which in turn activate the MAPKs, Erk1 and Erk2 (Figure 2; Mitin et al. 2005).
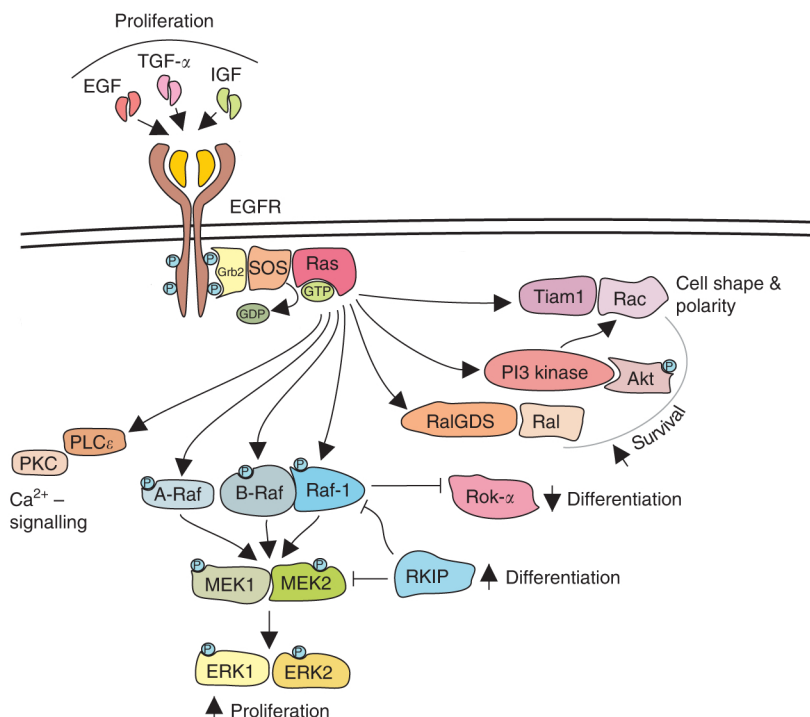

Fig. 2: The Erk/MAPK pathway. Adapted from Kern et al. 2010. See text for detailed description.

Structurally, the Raf proteins can be divided into the regulatory domains (CR1 and CR2; N-terminal) and the kinase domain (CR3; C-terminal). The CR1 region contains the Ras binding domain (RBD), which is essential for Raf activation by Ras (Figure 3; Zhang and Guan 2000).

Normally, the Raf proteins are regulated by the association with scaffold proteins such as 14-3-3 and by intramolecular binding of the regulatory domain to its kinase domain. Upon activation Rafs undergo dephosphorylation events to relieve this intramolecular autoinhibition, are recruited to the membrane and phosphorylation events in the negative charge region (N-region) and the activation loop (AL) lead to activation. Compared to Raf-1, B-Raf possesses a co-translationally phosphorylated serine and an aspartate in the N-region which makes B-Raf activation independent of this phosphorylation events and partially explains its higher kinase activity (Mercer and Pritchard, 2003, Kolch, 2000, Mason et al., 1999, Galabova-Kovacs et al., 2006a).
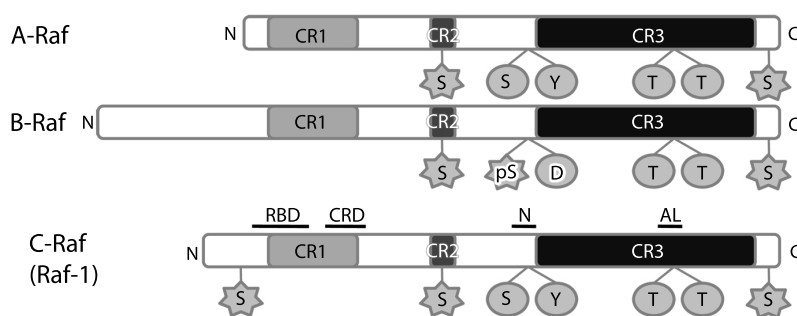
Fig. 3: The structure of Raf kinases. Adapted from Galabova-Kovacs et al. 2006a. See text for detailed description.

Raf kinases are able to form homodimers and to heterodimerize with other Rafs or with structurally similar proteins such as KSR (Rushworth et al., 2006, Rajakulendran et al., 2009). Heterodimerization occurs via the kinase domain, is increased by upstream stimuli (Ras) and results in strong kinase activation. Within the dimer, only one subunit needs to be active as a kinase; this is the basis of the paradox ERK activation observed in normal cells treated with Raf inhibitors which promote the formation of Raf heterodimers (Hatzivassiliou et al., 2010, Heidorn et al., 2010, Poulikakos et al., 2010).

Besides its role in the ERK pathway, Raf-1 was found to implement pathway crosstalk by exerting a kinase-independent function in regulating other pathways through protein-protein interaction. Examples are the interaction of Raf-1 with ASK1 (Chen et al., 2001, Yamaguchi et al., 2004) and MST2 (O'Neill et al., 2004) to promote survival; and our discovery that the regulatory domain of Raf-1 impinges on differentiation through binding and inhibiting the Rho effector Rok-α (Ehrenreiter, 2005, Niault et al., 2009).

3.3 Rho/ROCK Pathway & Effectors

The Rho family of small GTPases, Rho, Rac, and Cdc42 control the organization of actin. Among them, RhoA regulates the assembly of actin stress fibers and focal contacts, through activation of the downstream effectors mDia and the closely related kinases Rok-α (ROCKII) and Rok-β (ROCKI) (Pawlak and Helfman, 2002).

Both isoforms share a high 92% amino acid sequence identity across their kinase domains but neither Rok-α nor Rok-β can compensate for loss of the other isoform during murine embryonic development. Structurally similar to Raf, their modular structure is comprised of a kinase domain (N-terminal), a coiled-coil domain containing a Rho binding (RBD) site and a pleckstrin homology (PH) domain (C- terminal; Figure 3).

Fig. 4: The structure of Rok. Adapted from Sebbagh et al. (2005). See text for detailed description.

As in Raf-1, this modular assembly allows inhibition of the kinase domain via intramolecular interaction with the regulatory domain to keep an inactive, closed-conformation state. Intramolecular inhibition is relieved upon the binding of small GTPases Rho to the negative regulatory domain of the proteins, leading to kinase activation (Niault et al., 2009, Wimmer and Baccarini, 2010). The autoinhibitory regions of Raf-1 and Rok-α are very similar and contain a cysteine-rich domain within the plecstrin homology region. This similarity in structure and autoinhibitory regulation to Raf-1 allows direct protein-protein interaction between the regulatory domain of Raf and the kinase domain of Rok, and the inhibition of Rok activity *in trans*, a novel form of kinase regulation discussed below in Niault et al. (2009).

Activation of Rok leads to the formation of stress fibers and focal contact formation. Rok increases actomyosin-based contractility directly via its downstram targets myosin light chain (MLC) and myosin phosphatases (MYPT). Rok also activates LIMK, which subsequently leads to the phosphorylation of cofilin, which inhibits its actin-depolymerizing activity and therefore contributes to the stabilization of actin stress fibers (Pawlak and Helfman, 2002). Moreover, it was recently found that LIMK-mediated cofilin phosphorylation negatively regulates Myc and Stat3 and thereby keratinocyte proliferation (Honma et al., 2006).

4   Skin & Cancer

The mammalian skin is comprised of subcutaneous tissue, dermis and epidermis, that protects the body from water loss and the environmental insults. The outermost layer of the skin is the epidermis which is a stratifying squamous tissue comprised of several layers of keratinocytes. These layers can be distinguished by their distinct stages of keratinocyte differentiation. The innermost layer, the basal layer, contains undifferentiated, proliferating keratinocytes adhering to the basal lamina comprised of ECM proteins, including fibronectin, collagens and laminins. Upon withdrawal from the cell cycle and disruption of the integrin-ECM binding the keratinocytes migrate outwards to the differentiated suprabasal layers, the stratum spinosum and granulosum. Eventually they differentiate terminally, enucleate and reach the outermost layer, the stratum corneum, where they are continuously shed off. Therefore, the basal layer keratinocytes constantly replenish cells of the outer compartments with a turnover of a about a month. Thus, processes such as proliferation and differentiation need to be tightly controlled to maintain epidermal homeostasis, and any alteration might lead to severe conditions like inflammation, skin-barrier defects, hyperplasia and even cancer (Lock and Hotchin, 2009, Khavari and Rinn, 2007, Bardwell et al., 2009).
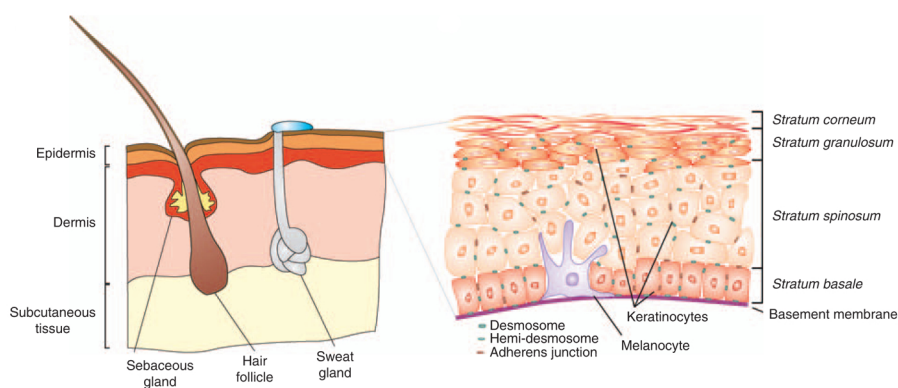
Fig. 5: Structure of the skin and epidermis (Kern et al., 2010). See text for detailed description.

Activating mutations of RAS and B-RAF are often found in human cancers, while RAF-1 is often found overexpressed. Special attention is given to skin cancers as they are the most commonly diagnosed type of cancer mainly caused by ultraviolet radiation-induced DNA damage and genetic mutations. The three most prevalent malignant types of skin cancers are basal cell carcinoma (BCC), squamous cell carcinoma (SCC), and melanoma (Alam and Ratner, 2001, Narayanan et al., 2010). According to the WHO up to 3 million new NMSC cases per year of non-melanoma skin cancer (NMSC) and almost 160.000 new melanoma cases per year worldwide are diagnosed.

4.1   Melanoma

Although the occurrence of melanoma is only about 4-5% of all cancers, in 10-15% of patients the cancer metastasizes. Metastatic melanoma (Stage IV) has a poor prognosis, with a median survival of 8 to 18 months after diagnosis. Estimated death rates range from 1.8 in 100.000 in Western Europe to 3.5 in 100.000 in Australia and New Zealand (Arkenau et al., 2010, Chapman et al., 2011, Ferlay et al., 2010). In up to 60% of melanoma the most frequent point mutation results in a single amino-acid substitution at valine 600 to glutamic acid in the activating segment of B-Raf (V600E). (Arkenau et al., 2010, Bollag et al., 2010, Flaherty et al., 2010). BRAF V600E mutation has highly elevated kinase activity compared to wild type BRAF and leads to constitutive phosphorylation of MEK and ERK, resulting in melanoma formation if expressed in melanocytes (Davies et al., 2002, Dhomen et al., 2009).

Therefore, RAF kinase inhibitors were designed and tested to treat melanoma patients. The first potent RAF kinase inhibitor was sorafenib (Bay 43-9006) which showed almost no tumor response in human xenograft models and negligible clinical activity in melanoma patients (Arkenau et al., 2010). Lately a new ATP competitive small molecule inhibitor, namely PLX4032 (also called vemurafenib or zelboraf) achieved unprecedented 80% response in patients in phase I clinical trials, but revealed distressing side effects. Among these are arthralgia, rash, fatigue, alopecia, photosensitivity, nausea, and diarrhea but, more disquietingly, drug-related keratoacanthoma and squamous-cell carcinoma (Chapman et al., 2011).

4.2   Non-melanoma skin cancers

About 80 percent of non-melanoma skin cancers are BCCs, and 20 percent are SCCs. In contrast to the majority of BCCs, cutaneous SCCs have a considerable risk of metastasis (Alam and Ratner, 2001). Aberrant sonic hedgehog/patched signaling is enough to induce hallmark features of BCC in human and murine epidermis, while activation of Ras paralleled by an inhibition of NF-xB function is sufficient to transform normal human epidermis into tumor tissue with all the key attributes of SCC (Ridky and Khavari, 2004). RAS, RAF and TP53 have often been found mutated in SCCs and seem to play pivotal roles in the development of skin cancers. Although TP53 mutations are the most prevalent mutation in SCCs it alone is not sufficient to induce neoplasia but most likely facilitates a second hit that leads to cancer (Khavari and Rinn, 2007). RAS is found activated in a majority of human SCCs and plays a major role in murine models of SCC. B-RAF is mostly downregulated and RAF-1 is often found overexpressed in SCCs (Riva et al., 1995, Zaravinos et al., 2009). Together, these observations implicate RAS and its downstream effectors

as critical regulators in epidermal neoplasia (Khavari and Rinn, 2007).

Unlike cancers of internal organs, primary skin cancer can be easily monitored. Treatment normally includes surgical resection with accompanying chemotherapy to prevent metastases. The 10-year survival rate for primary SCCs is excellent. For patients with metastatic SCC the long-term prognosis is rather poor with a 10-year survival rate of less than 20 percent (Alam and Ratner, 2001).

In the light of recent findings, as mentioned above, therapy-induced SCCs have attracted attention as they were found to arise as a side-effect in small molecule inhibitor-treated melanoma patients. Although less dangerous and easier to treat than melanoma, the development of drug-related SCC rings an alarm bell as it implies that the treatment with PLX4032 that shows tremendous effect against BRAFV600E mutated cells sensitizes wildtype cells to become tumorigenic upon a second hit that causes upstream pathway activation (Arkenau et al., 2010, Chapman et al., 2011) reviewed in Wimmer and Baccarini (2010).

In general the data presented below exemplify how signal transduction and signaling pathways are plastic entities that amplify, integrate and split signals leading to context-dependent pathway crosstalk and regulate diverse cellular programs including embryogenesis, proliferation, differentiation and apoptosis (Raman et al., 2007, Wimmer and Baccarini, 2010) and play important roles in tumorigenesis through these processes.

Part III. Publications

5 Introductory Summary

This thesis is comprised of several publications including a review and a submitted article all with the common theme of signaling mechanisms in epidermal carcinogenesis. The main focus lies on the role of Raf in Ras-driven skin-tumorigenesis, either as a kinase regulating the Erk/MAPK cascade in the case of B-Raf or through the kinase independent function of Raf-1 that regulates the activity of Rok-α by protein-protein interaction. A further model of non-melanoma skin cancers (NMSC) broadens the scope of this thesis by examining human papillomavirus 8 (HPV8)-induced skin cancer and its dependency on proper STAT3 signaling.

The review "Ras and Raf pathways in epidermis development and carcinogenesis" published in the British Journal of Cancer provides a good overview of the skin and its epidermal compartment and nicely lays out the role of the Erk/MAPK pathway in this context. Especially, how the Erk/MAPK pathway sustains epidermal homeostasis by controlling proliferation and differentiation. The review mainly focuses on the essential role of Raf-1, but we have recently demonstrated an essential role of B-Raf in mediating the full fledged ERK activation and skin tumorigenesis, addressed in the submitted manuscript "Essential ERK-dependent and -independent roles of Raf in Ras-driven skin carcinogenesis".

The report "From autoinhibition to inhibition in trans: the Raf-1 regulatory domain inhibits Rok-alpha kinase activity" published in the Journal of Cell Biology investigates the kinase independent protein-protein interaction of Raf-1 and Rok-α and elaborates on the underlying molecular mechanisms that regulate kinase activity of Rok-α through Raf-1 *in vitro*. Using immunofluorescence, immunoprecipitation, FRET/FLIM, and *in vitro* kinase assays in Raf-1 knockout mouse embryonic fibroblasts and other cell lines for overexpression studies the relevant interaction properties of Raf-1 and Rok-α are delineated. Particular emphasis is put on the fact that Raf-1 mediates this inhibition of Rok-α *in trans*, which is an entirely new concept in kinase regulation.

The article "Raf-1 Addiction in Ras-Induced Skin Carcinogenesis" published in Cancer Cell establishes an exceptional relevance of this *in trans* regulation of Rok-α via Raf-1 *in vivo*. As the conventional knockout of Raf-1 leads to embryonic lethality (Mikula et al., 2001) a viable keratinocyte-restricted conditional knock out of Raf-1 (Ehrenreiter, 2005) is used in two skin tumor models, namely the chemical two steps carcinogenesis model DMBA/TPA (Quintanilla et al., 1986) and a genetic model using a transgenic epidermis-restricted membrane tethered form of SOS (SOS-F) to cause tonic Ras activation (Sibilia et al., 2000). Moreover, a tamoxifen inducible

Raf-1 knockout was employed to examine the role of Raf-1 knockout in preexisting neoplasms. This and the chemical inhibition of Rok-α via topical application of Y27632 to counteract the Rok-α hyperactivation in Raf-1 deleted epidermis strengthen the link between Raf-1 and a recently found Rok-α/LIMK/Cofilin/STAT3/c-myc signaling pathway (Honma et al., 2006) that has a major impact on keratinocyte differentiation and hence on tumorigenesis. Altogether this shows the relevance of Raf-1 and in particular the role of the Raf-1/Rok-α interaction in tumor onset, progression and even maintenance.

As already noted above, the article "Keratinocyte-specific Stat3 heterozygosity impairs development of skin tumors in human papillomavirus 8 transgenic mice" published in Cancer Research has, in regards to the role of Raf, only the more loosely connected aspect of the involvement of STAT3 in skin carcinogenesis. A conditional epidermis-restricted STAT3 knockout along an epidermis-restricted genetic human papillomavirus driven mouse tumor model is used to elucidate a critical and dose dependent role of STAT3 in this context. As the epidermis-restricted Raf-1 knockout likewise affects Ras-driven tumorigenesis through altering phospho-STAT3 levels via the above mentioned Rok-α/LIMK/Cofilin signaling, this might demonstrate that STAT3 plays a more general role in skin tumor formation.

Together with several other reports on the *in vivo* importance of the kinase-independent interactions of Raf-1 e.g. with ASK1 (Yamaguchi et al., 2004) and MST2 (O'Neill et al., 2004) to promote survival as well as our discovery that Raf-1 impinges on differentiation through Rok-α proves that the role of Raf-1 extends beyond the Erk/MAPK pathway and exerts its influence over several key regulatory pathways, although this was only demonstrated *in vivo* for the Raf-1/Rok-a interaction.

In contrast, the article "Essential ERK-dependent and -independent roles of Raf in Ras-driven skin carcinogenesis" submitted to Cancer Cell, deals with the fundamental role of B-Raf restricted to the activation of Erk. The same epidermis-restricted knockout systems and tumor models as described above in "Raf-1 Addiction in Ras-Induced Skin Carcinogenesis" are used to show the role of B-Raf alone or in combination with the role of Raf-1. A profound function of B-Raf *in vivo* and even an indirect link through ERK activation to Rok-α activity was observed. The concomitant and inducible epidermis-restricted knockout of B-Raf and Raf-1 is used to elucidate that the essential roles of either Raf are independent but act synergistic in tumor regression studies.

Hence, the main focus of this thesis lies on investigating the role of B-Raf and Raf-1 in Ras-mediated skin carcinogenesis and the underlying mechanisms, with a side project extending the scope to a viral induced skin tumor model and its dependency on STAT3.

6   Ras and Raf pathways in epidermis development and carcinogenesis

F Kern[1], T Niault[1,2] and M Baccarini[*,1]

[1]University of Vienna, Center for Molecular Biology, Max F. Perutz Laboratories, Doktor-Bohr-Gasse 9, A-1030 Vienna, Austria

[2]Current address: Microbes and Host Barriers Group, Inserm Avenir U604, Institut Pasteur, 25 Rue du Docteur Roux, 75724 Paris Cedex 15, France

[*]Correspondence: Professor M. Baccarini; E-mail: manuela.baccarini@univie.ac.at

Relevance & Contribution: This review deals with the role of Ras and Raf in the regulation of the homeostasis of the largest organ of the body, the skin. Moreover, it discusses our findings that Ras-driven tumorigenesis are addicted to Raf-1, and their implications also in regard to possible novel therapeutic avenues. The manuscript was written by M.B. and F.K., parts of the introduction and Figure 1 were contributed by T.N..

Minireview

Ras and Raf pathways in epidermis development and carcinogenesis

F Kern[1], T Niault[1,2] and M Baccarini*[,1]

[1]University of Vienna, Center for Molecular Biology, Max F. Perutz Laboratories, Doktor-Bohr-Gasse 9, A-1030 Vienna, Austria

The epidermis is the outermost layer of the body and protects it from environmental insults. This crucial function is sustained by a continuous process of self-renewal involving the carefully balanced proliferation and differentiation of progenitor cells constantly replacing the mature cells at the surface of the epidermis. Genetic changes in the signalling pathways controlling keratinocyte proliferation and differentiation disrupt this balance and lead to pathological changes including carcinogenesis. This review discusses the role of Ras, an oncogene critically involved in the development of skin neoplasia, and its downstream effector Raf in epidermal homeostasis and tumourigenesis. In particular, we will focus on the recently established role of Raf-1 as the decisive element that, by restraining keratinocyte differentiation, allows the development and maintenance of Ras-driven tumours.
British Journal of Cancer (2011) **104,** 229–234. doi:10.1038/sj.bjc.6606009   www.bjcancer.com
Published online 16 November 2010
© 2011 Cancer Research UK

The epidermis is the outer layer of the skin, a stratified squamous epithelium that forms a protective barrier against environmental insults and prevents body dehydration. The epidermis is primarily composed of keratinocytes in which pigment cells (melanocytes), immune cells (Langerhans cells and T cells) and nerve-ending cells (Merkel cells) are embedded. Invaginating into the dermis, the epidermis gives rise to various appendages: the hair, produced by the hair follicles, the sebaceous glands that lubricate the skin and the sweat glands that extrude water and salts (Figure 1A). The epidermis is separated from the dermis by the basement membrane, which is rich in extracellular matrix, and is organised into four major layers: the *stratum basale*, the *stratum spinosum*, the *stratum granulosum* and the *stratum corneum*. The *stratum basale* contains the keratinocyte progenitors required for skin renewal. These can either divide to generate further progenitor or give rise to suprabasal keratinocytes (reviewed in Blanpain and Fuchs, 2009). As they progress to the *stratum spinosum* and to the *stratum granulosum*, the keratinocytes produce the network of keratin filaments anchored in intercellular junctions that provide structural support to the skin; the cells flatten and exocytose lamellar granules containing the precursors of the lipids that contribute to the *stratum corneum* barrier. The *stratum corneum* contains the last stage of differentiation, the enucleated corneocytes, which are continuously sloughed off and must be replaced by differentiation of the lower layers (Figure 1B).

To preserve the integrity of the epidermal barrier, the epidermis turns over throughout life. Alterations in this process, such as keratinocyte proliferation/differentiation defects, or inflammation can lead to cancer or skin barrier defects; thus, the many signalling pathways involved in epidermal homeostasis must be tightly controlled.

RAS PATHWAYS IN THE EPIDERMIS

The epidermal growth factor receptor (EGFR) is a critical regulator of epidermal homeostasis (Figure 1C). Binding of EGFR to its ligands, EGF, TGF-α and IGF, promotes keratinocyte proliferation; in contrast, inhibitory ligands of EGFR, Lrig1 and Mig6 are involved in maintaining stem cell quiescence, as ablation of either protein leads to hyperproliferation of keratinocytes (Fuchs, 2009). Downstream of EGFR, activation of Ras induces keratinocyte proliferation and inhibits differentiation (Khavari and Rinn, 2007). Ras isoforms are small G-nucleotide-binding proteins that oscillate between a GDP-bound, inactive state, and a GTP-bound state in which they can bind and activate their downstream effectors. In growth factor signalling, the transition between the inactive and the activated state is engendered by the binding of a guanine nucleotide exchange factor (GEF) that displaces GDP. Once GDP is displaced, GTP, whose intracellular concentration is ten-fold higher than that of GDP, will bind to Ras, converting it into an active form. Active Ras will then proceed to stimulate a number of effectors, including the prominent classical effectors phosphoinositide-3 kinase (PI-3K) and Raf; Ral-GDS and Tiam-1, exchange factors leading to the activation of small GTPases Ral and Rac; and several other less well-defined effectors (Figure 1C; Karnoub and Weinberg, 2008). These molecules control aspects of keratinocyte biology ranging from the regulation of proliferation, traditionally attributed to the Raf/MEK/ERK pathway (see below), or of survival, linked to the activation of PI-3K and its downstream target Akt (Sibilia *et al*, 2000; Calautti *et al*, 2005) and Ral-GDS (Gonzalez-Garcia *et al*, 2005), to the establishment of cell–cell

*Correspondence: Professor M Baccarini; E-mail: manuela.baccarini@univie.ac.at
[2]Current address: Microbes and Host Barriers Group, Inserm Avenir U604, Institut Pasteur, 25 Rue du Docteur Roux, 75724 Paris Cedex 15, France
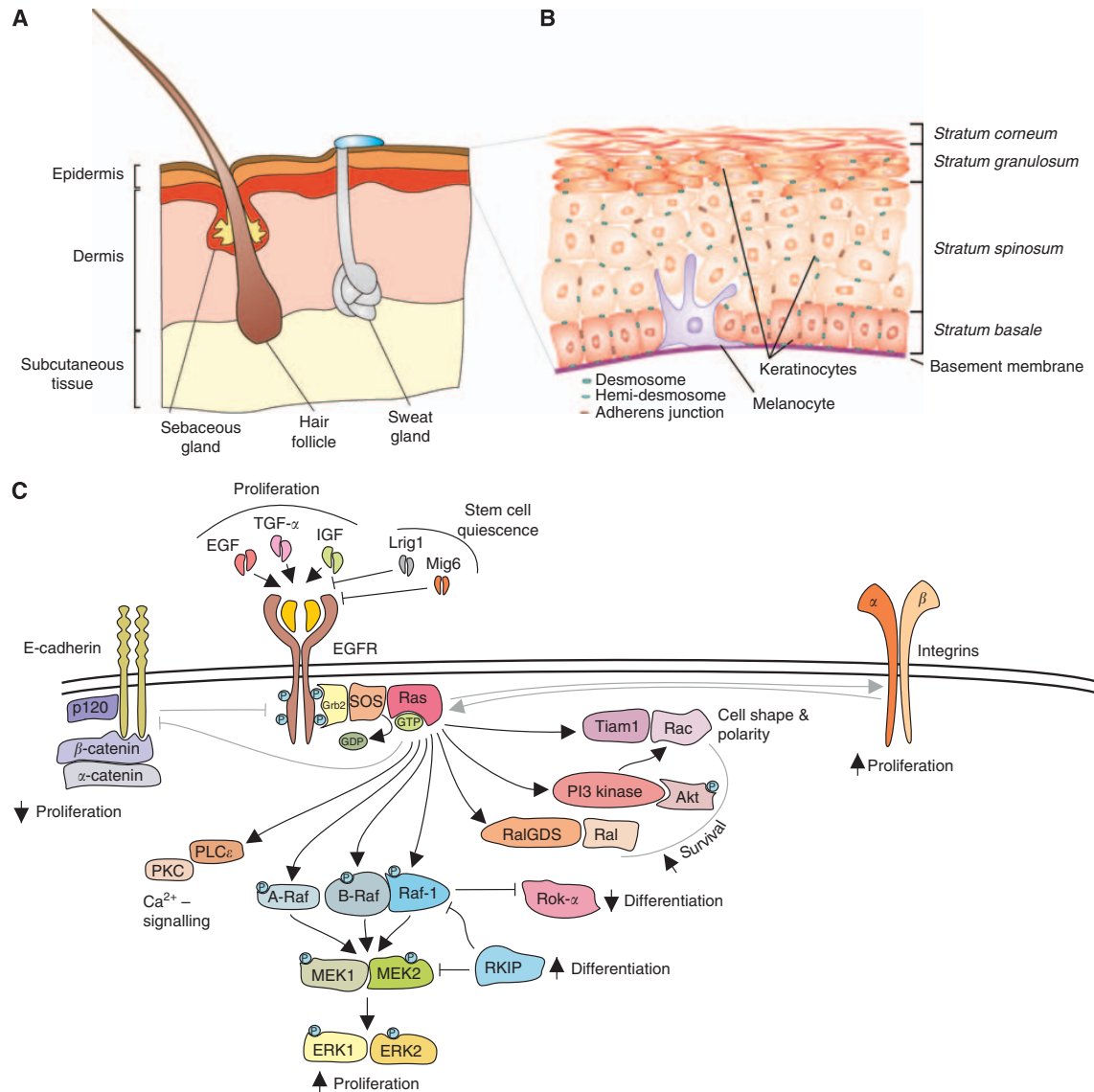
230

Figure 1 Ras pathways in the epidermis. (**A**) Schematic representation of mammalian skin. The skin consists of subcutaneous tissue, dermis and epidermis. Hair follicles and sebaceous glands invaginate into the dermis. (**B**) Structure of the epidermis. The epidermis is mainly composed of keratinocytes in various stages of differentiation. We distinguish four strata: the *stratum basale*, comprising the proliferating, undifferentiated basal keratinocytes; the *strata spinosum* and *granulosum*, containing differentiating keratinocytes; and the *stratum corneum*, with the terminally differentiated, enucleated corneocytes that are continuously removed and replaced by cells from the differentiating strata below. (**C**) The Ras pathway in the epidermis. Ras can be activated downstream of the EGFR and integrins, and can be inhibited by adhesion molecules, such as E-cadherins, inducing growth arrest. With its host of downstream effectors, Ras can mediate survival, proliferation, and can inhibit differentiation (see text for details). Arrows denote induction, blunt arrows indicate inhibition. Arrows pointing upwards signify increase, and arrows pointing downwards symbolise decrease.

adhesion, polarity and redox balance, controlled by Tiam1 (Mertens *et al*, 2005; Pegtel *et al*, 2007; Rygiel *et al*, 2008). Thus, activation of the Ras pathway by growth factors must be kept under tight control to provide just the right balance of proliferation/differentiation signals required for epidermal homeostasis.

Adhesion molecules, such as integrins and cadherins, have a crucial role in the modulation of growth factor signalling in the epidermis. In general, integrin activation supports proliferation, whereas cadherins can both support or inhibit it (Figure 1C); E-cadherin and desmosomal cadherins, for instance, modulate the

EGF response to signal growth arrest (Muller *et al*, 2008). In line with its crucial role in proliferative signalling, the Ras pathway is activated by integrins (Janes and Watt, 2006) and negatively regulated by cell–cell adhesion: ablation of either α-catenin or p120-catenin in the epidermis causes a reduction of adherens junctions, which does not affect skin barrier and intercellular adhesion but leads to hyperplasia and to sustained activation of the Ras/ERK pathway (Vasioukhin *et al*, 2001; Perez-Moreno *et al*, 2006).

Activating Ras mutations stabilise this signalling-competent, GTP-bound state. These mutations are frequent in human cancer

16

(33%; higher frequency in epithelial cancers and melanoma; http://www.sanger.ac.uk/genetics/CGP/cosmic). The number of tumours (particularly squamous cell carcinomas) containing GTP-bound Ras is however much higher, likely owing to the autocrine/paracrine activation and/or to mutation in receptor tyrosine kinases such as the EGFR (Khavari and Rinn, 2007). Expression of constitutively active Ras mutants in the basal layer of mouse epidermis induces proliferation and inhibits differentiation (Vitale-Cross *et al*, 2004; Khavari and Rinn, 2007); the activation of endogenous Ras by the transgenic expression of the Ras GEFs SOS (Sibilia *et al*, 2000) and Rasgrp1 (Oki-Idouchi and Lorenzo, 2007) in the same epidermal compartment produces similar phenotypes. Consistent with an essential role of Ras in skin tumourigenesis, H-Ras ablation impairs tumour development in mouse models of chemical carcinogenesis (Ise *et al*, 2000).

The consequences of Ras activation in the epidermis can be mimicked, at least in part, by the expression of gain-of-function mutants of Ras downstream effectors. Constitutively active Akt mutants promote proliferation in skin (Murayama *et al*, 2007); conversely, the knock-in of a PI-3K mutant incapable of binding to Ras reduces tumour load in a chemical model of epidermal carcinogenesis (Gupta *et al*, 2007). Ablation of other Ras targets such as Tiam1 (Malliri *et al*, 2002) and its downstream target Rac1 (Wang *et al*, 2010), Ral-GDS (Gonzalez-Garcia *et al*, 2005) and PLCepsilon (Bai *et al*, 2004) has similar effects, but only in the case of Rac1 it is clear that the phenotype is cell autonomous.

RAF PATHWAYS IN THE EPIDERMIS

The Raf/MEK/ERK cascade is the longest-studied and probably the best-described Ras effector pathway. The term 'cascade' already suggests the chain reaction that propels the signal, in the form of sequential phosphorylation, from an entry point to an intermediate kinase and finally to ERK, the business end of the pathway. ERK stimulation results in the phosphorylation of transcription factors, structural proteins and metabolic enzymes, and ultimately engenders both short- and long-term changes in cellular behaviour. This basic three-tiered module is robust and plastic at the same time, allowing not only the amplification but also the diversification and temporal modulation of the signal at each and every node; in mammals, it is found in four mitogen-activated protein kinase (MAPK) pathways that contribute to implementing biological outcomes as diverse as proliferation, apoptosis, differentiation, motility and response to stress and cytokines.

One outstanding feature of the Raf/MEK/ERK pathway in mammals is redundancy. Mammals have three Raf isoforms (A-Raf, B-Raf and Raf-1, also known as C-Raf), two MEK and two ERK isoforms. All three Rafs can bind to Ras and phosphorylate MEK, although B-Raf is much more efficient than the other two and is necessary for ERK activation *in vivo* (reviewed in Galabova-Kovacs *et al*, 2006a; Niault and Baccarini, 2010). Both MEKs can phosphorylate ERK1/2; and whether ERK1/2 have non-redundant functions or not is still unclear (see below).

Consistent with its prominent role as a MEK kinase, B-Raf is the component of the ERK pathway most often mutated in human tumours, with a particularly high frequency (43%) in human melanoma. The most frequent B-Raf mutation, V600E, results in constitutive catalytic activity and MEK/ERK activation. Recently, a kinase drug selectively inhibiting B-Raf V600E has achieved an unprecedented response rate of 80% in phase 1 clinical trials involving metastatic melanoma patients, opening new therapeutic avenues for this deadly disease (Bollag *et al*, 2010; Flaherty *et al*, 2010). Less frequent BRAF mutations reduce intrinsic catalytic activity but drive MEK/ERK activation by stimulating the formation of B-Raf/Raf-1 heterodimers in which mutant B-Raf activates wild-type Raf-1 in trans (reviewed in Niault and Baccarini, 2010; Wimmer and Baccarini, 2010).

Unlike B-Raf, Raf-1 is infrequently mutated in human cancer (overall frequency of 1%; http://www.sanger.ac.uk/genetics/CGP/cosmic). The rare mutations detected in human cancer cell lines and in patients with therapy-related acute myeloid leukaemia do not drive tumourigenesis *per se*, but can do so upon somatic loss of a negative regulator of Raf-mediated MEK/ERK activation, the Raf kinase inhibitory protein RKIP (Niault and Baccarini, 2010). Interestingly, RKIP promotes differentiation of human keratinocytes (Yamazaki *et al*, 2004), and both RKIP and B-Raf are downregulated in human SCC (Zaravinos *et al*, 2009), whereas Raf-1 is overexpressed (Riva *et al*, 1995). Mutations or overexpression of MEK or ERK in human SCC have not been reported.

The data summarised above suggest that Raf-1 is an important player in the development of human SCC. Support for this idea came in the unexpected form of recent findings concerning small-molecule inhibitors of Raf. These compounds, some of which are already being used in the clinic, efficiently inhibit MEK/ERK activation in cells harbouring the B-Raf V600E mutation (Bollag *et al*, 2010; Flaherty *et al*, 2010), but can activate the ERK pathway to different extents in normal cells and in cells expressing Ras mutations. At the molecular level, the inhibitors promote the formation of dimers in which wild-type Raf-1 is activated in trans (reviewed in Brower, 2010; Cichowski and Janne, 2010; Wimmer and Baccarini, 2010). Before these reports, potentially deleterious effects of Raf inhibitors because of ERK inhibition in normal cells were expected to limit their clinical use. In stark contrast, these studies now predict that these inhibitors may be dangerous because they may activate Raf-1 and MEK/ERK in B-Raf wild-type cells prone to deregulated proliferation because of other mutations. Intriguingly, although the inhibitors are administered systemically, keratoacanthomas and SCC *in situ* develop in patients treated with Raf inhibitors (Brower, 2010; Cichowski and Janne, 2010; Wimmer and Baccarini, 2010), underscoring the connection between Raf-1 activation and epidermal proliferation and tumourigenesis.

The role of the Raf/MEK/ERK pathway in epidermal proliferation has been clearly established in animal models, in which inducible activation of Raf or MEK in the epidermis results in massive cutaneous hyperplasia and reduced differentiation (Khavari and Rinn, 2007). In apparent contrast, knockout of B-Raf (Galabova-Kovacs *et al*, 2006b), Raf-1 (Ehrenreiter *et al*, 2005), MEK1, MEK2 (Scholl *et al*, 2007), ERK1 and ERK2 (Dumesic *et al*, 2009) has no effect on epidermis development and/or homeostasis. In the MEK and ERK knockouts, this lack of phenotype may result from functional redundancy within the pathway. Indeed, epidermis-restricted compound MEK1/MEK2 knockout causes severe barrier function defects and marked epidermis hypoplasia leading to perinatal death (Scholl *et al*, 2007); and simultaneous ERK1/ERK2 ablation inhibits keratinocyte division (Dumesic *et al*, 2009). MEK1/2 gene dosage also appears to be the rate-limiting factor in the hyperplastic response of mouse epidermis to activated Ras (Scholl *et al*, 2009a); in contrast, however, MEK1 (but not MEK2) and ERK1 are required for full-fledged chemical carcinogenesis (Bourcier *et al*, 2006; Scholl *et al*, 2009b). Together, these results confirm the role of the ERK pathway in promoting proliferation and restraining differentiation in the epidermis.

However, recent conditional gene ablation experiments have revealed that one of the Raf kinases has ERK-independent roles in keratinocyte biology and tumourigenesis. As mentioned above, mice harbouring epidermis-restricted Raf-1 ablation do not show any major anomalies, with the exception of a curly fur and whiskers that subside after the first hair cycle. Wound healing, however, is delayed in these mice, and their keratinocytes show defects in adhesion and migration (Ehrenreiter *et al*, 2005). These phenotypes do not correlate with defects in ERK phosphorylation; rather, we have been able to trace them to the cytoskeleton-based Rho effector Rok-α, which is hyperactive in Raf-1-deficient cells (Ehrenreiter *et al*, 2005, 2009; Niault *et al*, 2009).

232

Although these data do not exclude that Raf-1 may have function(s) connected with its ability to phosphorylate MEK or other substrates, they do indicate that the essential role of Raf-1, at least in the epidermis, is independent of its kinase activity. But what happens if one stresses the system, for instance, by inducing tumourigenesis *in vivo*? We have answered this question by combining a chemical and a genetic tumourigenesis protocol with epidermis-restricted Raf-1 ablation in mice. Both models rely on the activation of Ras, caused by mutations in the DMBA/TPA chemical carcinogenesis model (Ise *et al*, 2000) or by tethering the Ras activator SOS to the membrane of basal keratinocytes (Sibilia *et al*, 2000); this results in the constitutive activation of endogenous Ras, observed more frequently than Ras mutations in human SCC (Dajee *et al*, 2003). The results were striking: Raf-1-deficient epidermis was completely refractory to tumour formation in both models; in addition, using the genetic model we could show that Raf-1 ablation enforces complete, rapid regression of established lesions that never recur, although Ras activation persists throughout the life of the animals (Figure 2; Ehrenreiter *et al*, 2009). Tumour regression is characterised by massive, runaway differentiation, which was a surprise in view of the well-established role of Raf-1 in proliferation and of its essential antiapoptotic function in other cell types (Galabova-Kovacs *et al*, 2006a). These data identify Raf-1 as the single key Ras effector absolutely required for both development and maintenance of Ras-driven tumours *in vivo*. They evoke the concept of 'non-oncogene addiction', intended as the absolute dependence of cancer cells on a non-mutated component of a signalling pathway to prevent system failure in the form of apoptosis or, as in this case, differentiation. Downstream of Ras, activated Raf-1 binds to Rok-α, reducing its activity (Figure 2); Rok-α, in turn, has been previously implicated in keratinocyte differentiation (McMullan *et al*, 2003) and, via the phosphorylation of Cofilin, can prevent the activation of the STAT3/Myc axis (Honma *et al*, 2006).

The relevance of the Raf-1/Rok-α interaction for tumourigenesis is illustrated by the fact that Ras-driven dedifferentiation, STAT3 phosphorylation and Myc expression occur both in wild-type and in Raf-1-deficient epidermis treated with a chemical Rok inhibitor

(Ehrenreiter *et al*, 2009). These data establish Raf-1 as an endogenous Rok-α inhibitor operating downstream of Ras to regulate keratinocyte differentiation, and imply that caution is in order when using Rok inhibitors, especially in the treatment of Ras-driven tumours (Figure 2).

Rok-α inhibition by Raf-1 requires physical interaction between the two proteins. In growth factor-stimulated or Ras-transformed cells, the kinase domain of Rok-α interacts with, and is inhibited by, the regulatory domain of Raf-1, which is structurally very similar to Rok-α's own autoinhibitory domain (Niault *et al*, 2009). This kind of 'inhibition in trans' has never been reported before, and represents a new paradigm of kinase regulation and pathway cross-talk.

Our results have implications for future therapeutic strategies targeting the Raf-1/Rok-α interaction, for instance, by silencing the Raf-1 gene or by using small-molecule inhibitors to disrupt the complex. The predicted outcome of such interventions is an increase in Rok-α activity, resulting in turn in epithelial cell differentiation. The success of these therapies, however, might be highly context dependent. We must bear in mind that Rok-α was found upregulated in human SSC samples, and that its over-expression confers features of malignancy to human tumours in mouse xenograft models (Lefort *et al*, 2007). It is possible that treatments aimed at increasing Rok-α activation might be beneficial only in the context of epithelial tumours driven by Ras activation. Alternatively, tumour cells might accumulate mutations, downstream of Rok-α or in other pathways, which enable them to tolerate high Rok-α activity without undergoing differentiation. Thus, as in the case of other approaches, the success of a Rok-α activation therapy might depend both on the type of tumour and on the stage of the tumour at the time of intervention.

CONCLUSIONS

The evidence summarised above is consistent with a pivotal role of Ras and its downstream effectors in epidermal tumourigenesis. Ras effectors have been reported to induce proliferation and
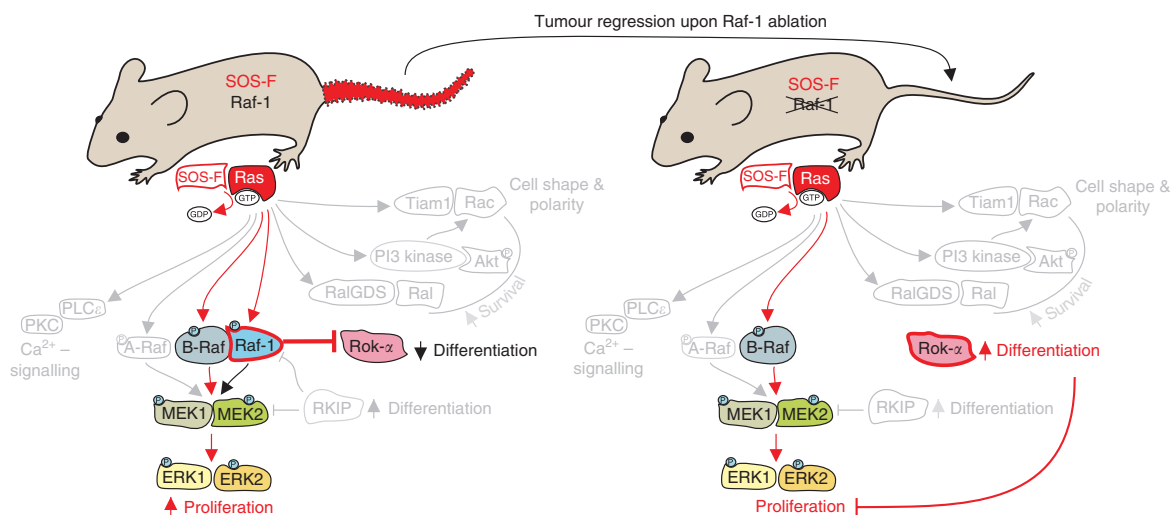
Figure 2 Ras-driven tumours are addicted to Raf-1. Ras-driven tumours, induced by the keratinocyte-restricted expression of membrane-tethered SOS (SOS-F transgenic mice; red, irregularly shaped tail) regress upon keratinocyte-specific ablation of Raf-1, indicating an essential role of this molecule in tumour maintenance. Downstream of Ras, Raf-1 is involved in at least two pathways: the canonical Raf/MEK/ERK pathway, where Raf-1 acts as an activator, likely in the context of a Ras-induced heterodimer with B-Raf; and the Rok-α pathway, where Raf-1 acts as an inhibitor via direct protein–protein interaction (left panel). Upon Raf-1 ablation (right panel; Raf-1 crossed out), ERK phosphorylation continues undisturbed, likely sustained by B-Raf; Rok-α, however, is strongly activated, leading to increased differentiation, and to tumour regression.

prevent apoptosis; recently, the differentiation block enforced by Raf-1-mediated Rok-α has been added to the potentially 'druggable' events required for Ras-driven tumourigenesis. The prediction of our *in vivo* work is that freeing Rok-α from its interaction with Raf-1, for instance, by silencing the Raf-1 gene or by using small-molecule inhibitors aimed to disrupt the complex,

will increase Rok-α activity and result in epithelial cell differentiation, at least within a window of opportunity. Such a strategy should be useful in the co-therapy of Ras-driven epidermis tumours, much in the way that differentiation therapy has radically increased the success rate of leukaemia treatment (Wang and Chen, 2008).

REFERENCES

Bai Y, Edamatsu H, Maeda S, Saito H, Suzuki N, Satoh T, Kataoka T (2004) Crucial role of phospholipase Cepsilon in chemical carcinogen-induced skin tumor development. *Cancer Res* **64:** 8808–8810

Blanpain C, Fuchs E (2009) Epidermal homeostasis: a balancing act of stem cells in the skin. *Nat Rev Mol Cell Biol* **10:** 207–217

Bollag G, Hirth P, Tsai J, Zhang J, Ibrahim PN, Cho H, Spevak W, Zhang C, Zhang Y, Habets G, Burton EA, Wong B, Tsang G, West BL, Powell B, Shelloe R, Marimuthu A, Nguyen H, Zhang KY, Artis DR, Schlessinger J, Su F, Higgins B, Iyer R, D'Andrea K, Koehler A, Stumm M, Lin PS, Lee RJ, Grippo J, Puzanov I, Kim KB, Ribas A, McArthur GA, Sosman JA, Chapman PB, Flaherty KT, Xu X, Nathanson KL, Nolop K (2010) Clinical efficacy of a RAF inhibitor needs broad target blockade in BRAF-mutant melanoma. *Nature* **467:** 596–599

Bourcier C, Jacquel A, Hess J, Peyrottes I, Angel P, Hofman P, Auberger P, Pouyssegur J, Pages G (2006) p44 mitogen-activated protein kinase (extracellular signal-regulated kinase 1)-dependent signaling contributes to epithelial skin carcinogenesis. *Cancer Res* **66:** 2700–2707

Brower V (2010) BRAF inhibitors: research accelerates in wake of positive findings. *J Natl Cancer Inst* **102:** 214–215

Calautti E, Li J, Saoncella S, Brissette JL, Goetinck PF (2005) Phosphoinositide 3-kinase signaling to Akt promotes keratinocyte differentiation versus death. *J Biol Chem* **280:** 32856–32865

Cichowski K, Janne PA (2010) Drug discovery: inhibitors that activate. *Nature* **464:** 358–359

Dajee M, Lazarov M, Zhang JY, Cai T, Green CL, Russell AJ, Marinkovich MP, Tao S, Lin Q, Kubo Y, Khavari PA (2003) NF-kappaB blockade and oncogenic Ras trigger invasive human epidermal neoplasia. *Nature* **421:** 639–643

Dumesic PA, Scholl FA, Barragan DI, Khavari PA (2009) Erk1/2 MAP kinases are required for epidermal G2/M progression. *J Cell Biol* **185:** 409–422

Ehrenreiter K, Kern F, Velamoor V, Meissl K, Galabova-Kovacs G, Sibilia M, Baccarini M (2009) Raf-1 addiction in Ras-induced skin carcinogenesis. *Cancer Cell* **16:** 149–160

Ehrenreiter K, Piazzolla D, Velamoor V, Sobczak I, Small JV, Takeda J, Leung T, Baccarini M (2005) Raf-1 regulates Rho signaling and cell migration. *J Cell Biol* **168:** 955–964

Flaherty KT, Puzanov I, Kim KB, Ribas A, McArthur GA, Sosman JA, O'Dwyer PJ, Lee RJ, Grippo JF, Nolop K, Chapman PB (2010) Inhibition of mutated, activated BRAF in metastatic melanoma. *N Engl J Med* **363:** 809–819

Fuchs E (2009) Finding one's niche in the skin. *Cell Stem Cell* **4:** 499–502

Galabova-Kovacs G, Kolbus A, Matzen D, Meissl K, Piazzolla D, Rubiolo C, Steinitz K, Baccarini M (2006a) ERK and beyond: insights from B-Raf and Raf-1 conditional knockouts. *Cell Cycle* **5:** 1514–1518

Galabova-Kovacs G, Matzen D, Piazzolla D, Meissl K, Plyushch T, Chen AP, Silva A, Baccarini M (2006b) Essential role of B-Raf in ERK activation during extraembryonic development. *Proc Natl Acad Sci USA* **103:** 1325–1330

Gonzalez-Garcia A, Pritchard CA, Paterson HF, Mavria G, Stamp G, Marshall CJ (2005) RalGDS is required for tumor formation in a model of skin carcinogenesis. *Cancer Cell* **7:** 219–226

Gupta S, Ramjaun AR, Haiko P, Wang Y, Warne PH, Nicke B, Nye E, Stamp G, Alitalo K, Downward J (2007) Binding of ras to phosphoinositide 3-kinase p110alpha is required for ras-driven tumourigenesis in mice. *Cell* **129:** 957–968

Honma M, Benitah SA, Watt FM (2006) Role of LIM kinases in normal and psoriatic human epidermis. *Mol Biol Cell* **17:** 1888–1896

Ise K, Nakamura K, Nakao K, Shimizu S, Harada H, Ichise T, Miyoshi J, Gondo Y, Ishikawa T, Aiba A, Katsuki M (2000) Targeted deletion of the H-ras gene decreases tumor formation in mouse skin carcinogenesis. *Oncogene* **19:** 2951–2956

Janes SM, Watt FM (2006) New roles for integrins in squamous-cell carcinoma. *Nat Rev Cancer* **6:** 175–183

Karnoub AE, Weinberg RA (2008) Ras oncogenes: split personalities. *Nat Rev Mol Cell Biol* **9:** 517–531

Khavari TA, Rinn J (2007) Ras/Erk MAPK signaling in epidermal homeostasis and neoplasia. *Cell Cycle* **6:** 2928–2931

Lefort K, Mandinova A, Ostano P, Kolev V, Calpini V, Kolfschoten I, Devgan V, Lieb J, Raffoul W, Hohl D, Neel V, Garlick J, Chiorino G, Dotto GP (2007) Notch1 is a p53 target gene involved in human keratinocyte tumor suppression through negative regulation of ROCK1/2 and MRCKalpha kinases. *Genes Dev* **21:** 562–577

Malliri A, van der Kammen RA, Clark K, van der Valk M, Michiels F, Collard JG (2002) Mice deficient in the Rac activator Tiam1 are resistant to Ras-induced skin tumours. *Nature* **417:** 867–871

McMullan R, Lax S, Robertson VH, Radford DJ, Broad S, Watt FM, Rowles A, Croft DR, Olson MF, Hotchin NA (2003) Keratinocyte differentiation is regulated by the Rho and ROCK signaling pathway. *Curr Biol* **13:** 2185–2189

Mertens AE, Rygiel TP, Olivo C, van der Kammen R, Collard JG (2005) The Rac activator Tiam1 controls tight junction biogenesis in keratinocytes through binding to and activation of the Par polarity complex. *J Cell Biol* **170:** 1029–1037

Muller EJ, Williamson L, Kolly C, Suter MM (2008) Outside-in signaling through integrins and cadherins: a central mechanism to control epidermal growth and differentiation? *J Invest Dermatol* **128:** 501–516

Murayama K, Kimura T, Tarutani M, Tomooka M, Hayashi R, Okabe M, Nishida K, Itami S, Katayama I, Nakano T (2007) Akt activation induces epidermal hyperplasia and proliferation of epidermal progenitors. *Oncogene* **26:** 4882–4888

Niault T, Sobczak I, Meissl K, Weitsman G, Piazzolla D, Maurer G, Kern F, Ehrenreiter K, Hamerl M, Moarefi I, Leung T, Carugo O, Ng T, Baccarini M (2009) From autoinhibition to inhibition in Trans: the Raf-1 regulatory domain inhibits Rok-alpha kinase activity. *J Cell Biol* **187:** 335–342

Niault TS, Baccarini M (2010) Targets of Raf in tumorigenesis. *Carcinogenesis* **31:** 1165–1174

Oki-Idouchi CE, Lorenzo PS (2007) Transgenic overexpression of RasGRP1 in mouse epidermis results in spontaneous tumors of the skin. *Cancer Res* **67:** 276–280

Pegtel DM, Ellenbroek SI, Mertens AE, van der Kammen RA, de Rooij J, Collard JG (2007) The Par-Tiam1 complex controls persistent migration by stabilizing microtubule-dependent front-rear polarity. *Curr Biol* **17:** 1623–1634

Perez-Moreno M, Davis MA, Wong E, Pasolli HA, Reynolds AB, Fuchs E (2006) p120-catenin mediates inflammatory responses in the skin. *Cell* **124:** 631–644

Riva C, Lavieille JP, Reyt E, Brambilla E, Lunardi J, Brambilla C (1995) Differential c-myc, c-jun, c-raf and p53 expression in squamous cell carcinoma of the head and neck: implication in drug and radioresistance. *Eur J Cancer B Oral Oncol* **31:** 384–391

Rygiel TP, Mertens AE, Strumane K, van der Kammen R, Collard JG (2008) The Rac activator Tiam1 prevents keratinocyte apoptosis by controlling ROS-mediated ERK phosphorylation. *J Cell Sci* **121:** 1183–1192

Scholl FA, Dumesic PA, Barragan DI, Charron J, Khavari PA (2009a) Mek1/2 gene dosage determines tissue response to oncogenic Ras signaling in the skin. *Oncogene* **28:** 1485–1495

Scholl FA, Dumesic PA, Barragan DI, Harada K, Bissonauth V, Charron J, Khavari PA (2007) Mek1/2 MAPK kinases are essential for Mammalian development, homeostasis, and Raf-induced hyperplasia. *Dev Cell* **12:** 615–629

Scholl FA, Dumesic PA, Barragan DI, Harada K, Charron J, Khavari PA (2009b) Selective role for Mek1 but not Mek2 in the induction of epidermal neoplasia. *Cancer Res* **69:** 3772–3778

234

Sibilia M, Fleischmann A, Behrens A, Stingl L, Carroll J, Watt FM, Schlessinger J, Wagner EF (2000) The EGF receptor provides an essential survival signal for SOS- dependent skin tumor development. *Cell* **102:** 211–220

Vasioukhin V, Bauer C, Degenstein L, Wise B, Fuchs E (2001) Hyperproliferation and defects in epithelial polarity upon conditional ablation of alpha-catenin in skin. *Cell* **104:** 605–617

Vitale-Cross L, Amornphimoltham P, Fisher G, Molinolo AA, Gutkind JS (2004) Conditional expression of K-ras in an epithelial compartment that includes the stem cells is sufficient to promote squamous cell carcinogenesis. *Cancer Res* **64:** 8804–8807

Wang Z, Pedersen E, Basse A, Lefever T, Peyrollier K, Kapoor S, Mei Q, Karlsson R, Chrostek-Grashoff A, Brakebusch C (2010) Rac1 is crucial for Ras-dependent skin tumor formation by controlling Pak1-Mek-Erk hyperactivation and hyperproliferation in vivo. *Oncogene* **29:** 3362–3373

Wang ZY, Chen Z (2008) Acute promyelocytic leukemia: from highly fatal to highly curable. *Blood* **111:** 2505–2515

Wimmer R, Baccarini M (2010) Partner exchange: protein–protein interactions in the Raf pathway. *Trends Biochem Sci*, e-pub ahead of print 9 July 2010; doi:10.1016/j.tibs.2010.06.001

Yamazaki T, Nakano H, Hayakari M, Tanaka M, Mayama J, Tsuchida S (2004) Differentiation induction of human keratinocytes by phosphatidylethanolamine-binding protein. *J Biol Chem* **279:** 32191–32195

Zaravinos A, Kanellou P, Baritaki S, Bonavida B, Spandidos DA (2009) BRAF and RKIP are significantly decreased in cutaneous squamous cell carcinoma. *Cell Cycle* **8:** 1402–1408

7   From autoinhibition to inhibition in trans: the Raf-1 regulatory domain inhibits Rok-alpha kinase activity

Théodora Niault[1], Izabela Sobczak[1], Katrin Meissl[1], Gregory Weitsman[2,3,4], Daniela Piazzolla[1], Gabriele Maurer[1], Florian Kern[1], Karin Ehrenreiter[1], Matthias Hamerl[1], Ismail Moarefi[5], Thomas Leung[6], Oliviero Carugo[1,7], Tony Ng[2,3,4], and Manuela Baccarini[*,1]

[1]Max F. Perutz Laboratories, Center for Molecular Biology, University of Vienna, 1030 Vienna, Austria

[2]Richard Dimbleby Department of Cancer Research,

[3]Randall Division of Cell and Molecular Biophysics, and

[4]Division of Cancer Studies, King's College London, WC2R 2LS London, England, UK

[5]CRELUX GmbH, 82152 Martinsried, Germany

[6]Institute of Molecular and Cell Biology, Singapore 138673

[7]Department of General Chemistry, University of Pavia, 27100 Pavia, Italy

[*]Correspondence: Professor M. Baccarini; E-mail: manuela.baccarini@univie.ac.at

Relevance & Contribution: This report discusses in detail the kinase-independent mechanism by which Raf-1 interacts with and regulates the kinase activity of Rok-α *in vitro*. For the first time protein-protein interaction *in trans* is shown to regulate kinase activity. Furthermore this new concept is shown to be enhanced but not dependent on upstream activation e.g. through SOS or Ras. This important link between the mechanistic details and the function and relevance on the cellular level was contributed by F.K..

From autoinhibition to inhibition in trans: the Raf-1 regulatory domain inhibits Rok-α kinase activity

Théodora Niault,[1] Izabela Sobczak,[1] Katrin Meissl,[1] Gregory Weitsman,[2,3,4] Daniela Piazzolla,[1] Gabriele Maurer,[1] Florian Kern,[1] Karin Ehrenreiter,[1] Matthias Hamerl,[1] Ismail Moarefi,[5] Thomas Leung,[6] Oliviero Carugo,[1,7] Tony Ng,[2,3,4] and Manuela Baccarini[1]

[1]Max F. Perutz Laboratories, Center for Molecular Biology, University of Vienna, 1030 Vienna, Austria
[2]Richard Dimbleby Department of Cancer Research, [3]Randall Division of Cell and Molecular Biophysics, and [4]Division of Cancer Studies, King's College London, WC2R 2LS London, England, UK
[5]CRELUX GmbH, 82152 Martinsried, Germany
[6]Institute of Molecular and Cell Biology, Singapore 138673
[7]Department of General Chemistry, University of Pavia, 27100 Pavia, Italy

The activity of Raf-1 and Rok-α kinases is regulated by intramolecular binding of the regulatory region to the kinase domain. Autoinhibition is relieved upon binding to the small guanosine triphosphatases Ras and Rho. Downstream of Ras, Raf-1 promotes migration and tumorigenesis by antagonizing Rok-α, but the underlying mechanism is unknown. In this study, we show that Rok-α inhibition by Raf-1 relies on an intermolecular interaction between the Rok-α kinase domain and the cysteine-rich Raf-1 regulatory domain (Raf-1reg), which is similar to Rok-α's own autoinhibitory region. Thus, Raf-1 mediates Rok-α inhibition in trans, which is a new concept in kinase regulation. This mechanism is physiologically relevant because Raf-1reg is sufficient to rescue all Rok-α–dependent defects of Raf-1–deficient cells. Downstream of Ras and Rho, the Raf-1–Rok-α interaction represents a novel paradigm of pathway cross talk that contributes to tumorigenesis and cell motility.

Introduction

The GTPases Rho, Rac, and Cdc42 control fundamental processes including cell shape, polarity, and migration but also gene expression and cell cycle progression. Thus, Rho GTPases and their effectors are promising therapeutic targets for several diseases, including cancer (Heasman and Ridley, 2008; Olson, 2008).

The Rho effectors Rok-α and -β (Riento and Ridley, 2003; Zhao and Manser, 2005) are serine/threonine kinases with a modular structure comprising an N-terminal catalytic domain, a coiled-coil region containing the Ras/Rho-binding domain (RBD), and a C-terminal regulatory region with an unusual pleckstrin homology (PH) domain interrupted by a cysteine-rich domain (CRD; Riento and Ridley, 2003). Roks are regulated by autoinhibition; their C-terminal regulatory region, particularly the PH/CRD domain, binds to the kinase domain and inhibits its activity (Amano et al., 1999; Chen et al., 2002). Interaction of two RhoA molecules with the RBD domains arranged in a parallel coiled-coil dimer relieves autoinhibition (Amano et al., 1999; Shimizu et al., 2003; Dvorsky et al., 2004) and leads to kinase domain dimerization, transautophosphorylation, and activation (Riento and Ridley, 2003; Zhao and Manser, 2005).

Raf-1, a serine/threonine kinase member of the Ras/extracellular signal-regulated kinase (ERK) signaling pathway, interacts with Rok-α (Ehrenreiter et al., 2005; Piazzolla et al., 2005). In Raf-1 knockout (KO) cells, hyperactive Rok-α causes cytoskeletal changes, leading to inhibition of cell migration

JCB   335

THE JOURNAL OF CELL BIOLOGY

(Ehrenreiter et al., 2005) and hypersensitivity to Fas-induced apoptosis (Piazzolla et al., 2005). Intriguingly, Raf-1–mediated inhibition of Rok-α is also essential for Ras-induced tumorigenesis in vivo (Ehrenreiter et al., 2009).

Like Rok-α, Raf-1 is part of a family of kinases recruited to the cell membrane and activated by a small GTPase, in this case, Ras. Raf kinases share a structure featuring three conserved regions (CRs): (1) CR1, with the RBD and the CRD, (2) CR2, rich in S/T residues, and (3) CR3, encompassing the kinase domain. Like Roks, Rafs are regulated by autoinhibition; their N-terminal regulatory domain, particularly the CRD, binds to the kinase domain, suppressing its catalytic activity (Cutler et al., 1998). Raf activation requires Ras binding, membrane recruitment, and phosphorylation of S/T sites in the activation loop of the CR3 region (Wellbrock et al., 2004).

All Raf kinases can activate the MAPK/ERK kinase (MEK)–ERK module, yet the main in vivo roles of Raf-1 in migration, survival, and Ras-induced tumorigenesis are MEK–ERK independent and rely on Raf-1's ability to interact with and inhibit other kinases such as Rok-α (Ehrenreiter et al., 2005; Piazzolla et al., 2005; Ehrenreiter et al., 2009), MST2 (O'Neill et al., 2004), and ASK-1 (Yamaguchi et al., 2004). Until now, the mechanisms underlying this inhibition were unknown.

Negative regulation of the activity of a kinase by other kinases can occur in the context of a negative feedback loop, as does the inhibition of MEK1 by ERK (Eblen et al., 2004; Catalanotti et al., 2009), or in the context of pathway cross talk, as exemplified by the down-regulation of Raf-1 by Akt or PKA (Wellbrock et al., 2004). In these and other cases, negative regulation is achieved by direct phosphorylation of one kinase by the other. In this study, we report a novel form of kinase regulation and pathway cross talk mediated by protein–protein interaction instead of phosphorylation. Upon growth factor stimulation, GTPase binding to Raf-1 and Rok-α relieves autoinhibition, engendering a change from a closed, inactive state to an open, active conformation essential for Raf-1–Rok-α interaction. In the open state, the Raf-1 regulatory domain (Raf-1reg) binds to the kinase domain of Rok-α and inhibits its enzymatic activity directly. This kinase-independent inhibition in trans represents a new paradigm in pathway cross talk and regulation of kinase activity.

Results and discussion

Activation increases Raf-1–Rok-α interaction

In mouse embryonic fibroblasts (MEFs), Raf-1 binds to Rok-α, limiting its activation and cell membrane localization (Ehrenreiter et al., 2005). Raf-1 could conceivably prevent binding of Rok-α to RhoA by competing for or masking the Rho-binding site. Alternatively, Raf-1 could interact with the negative regulatory PH/CRD domain or the kinase domain of Rok-α and stabilize intramolecular autoinhibition. To test these possibilities, we examined the interaction of full-length (FL) Raf-1 with a series of Rok-α deletion mutants (Fig. 1 A). A mutant lacking the PH/CRD domain (ΔPH/CRD) and a truncated protein containing the kinase domain (Rok-α–K) bound to Raf-1 more efficiently than

FL Rok-α (Fig. 1, B and C; and Fig. S1 A). In contrast, Raf-1 hardly interacted with the Rok-α regulatory domain (Rok-αreg; Fig. 1 B). Next, we used multiphoton fluorescence resonance energy transfer (FRET)/fluorescent lifetime imaging microscopy (FLIM) to directly monitor protein–protein interactions in cells. The fraction of FL Raf-1 bound to FL Rok-α in asynchronously growing cells was under the detection limit. However, robust interaction was detected upon coexpression of active RhoA with the FL proteins or using Rok-α–K as an acceptor (Fig. 1, D and E). FRET efficiency was much higher in cell protrusions (28%; Fig. 1 D, inset), suggesting protein accumulation and increased interaction in these locations. In line with the coimmunoprecipitation experiments, these results show that Raf-1 preferentially binds to the kinase domain of Rok-α. They rule out the possibility that Raf-1 inhibits Rok-α activation by competing with RhoA and suggest instead that RhoA favors intermolecular interaction between Rok-α and Raf-1 by disrupting the intramolecular interaction between the kinase and Rok-αreg.

Ras binding similarly disrupts the interaction between the regulatory and kinase domains of Raf-1, rendering both more accessible for intermolecular interactions (Terai and Matsuda, 2005). Indeed, EGF stimulation increased complex formation between endogenous (Fig. 2 A) or ectopically expressed proteins, as shown by both FRET/FLIM and coimmunoprecipitation experiments (Fig. 2, B and C; and Fig. S1 B). Constitutively active Ras or activation of endogenous Ras by a membrane-tethered form of the Ras guanine nucleotide exchange factor SOS (Sibilia et al., 2000) also stimulated Raf-1–Rok-α interaction (Fig. 2 D). Conversely, mutating the Raf-1 RBD (R89L) or CRD (CC165/168SS; CC/SS) significantly reduced complex formation (Fig. 2, E–G). Thus, activation by Ras is both necessary and sufficient to promote Raf-1–Rok-α interaction.

Ras binding induces a conformational change in Raf-1 and recruits it to the membrane to be phosphorylated by activating kinases (Bondeva et al., 2002). Tethering Raf-1 to the membrane by fusing it to the Ki-Ras membrane-targeting signal (Raf-1 CAAX) activates the MEK–ERK pathway (Leevers et al., 1994), but it abolished binding to Rok-α (Fig. 2 E). Thus, the change from a closed to an open conformation mediated by Ras binding is essential both for MEK–ERK activation and Raf-1–Rok-α interaction, but these two functions of Raf-1 take place in distinct subcellular compartments. Indeed, single fluorophore video tracking of Raf proteins has shown that Raf-1 binds to Ras-GTP and activates MEK–ERK in the context of membrane nanoclusters but redistributes to the cytosol when these structures dissolve (Tian et al., 2007). It is tempting to speculate that the activated Raf-1 molecules leaving the membrane may be those that bind Rok-α in vivo.

Raf-1reg binds to Rok-α and inhibits its kinase activity

The R89L and CC/SS mutations may prevent or weaken Ras binding, thus precluding the conformational change that makes Raf-1reg accessible for Rok-α; alternatively, they may be more directly involved in the interaction with Rok-α. To distinguish between these possibilities, we introduced the R89L and CC/SS mutations in Raf-1reg, which lacks the Raf-1 kinase domain.
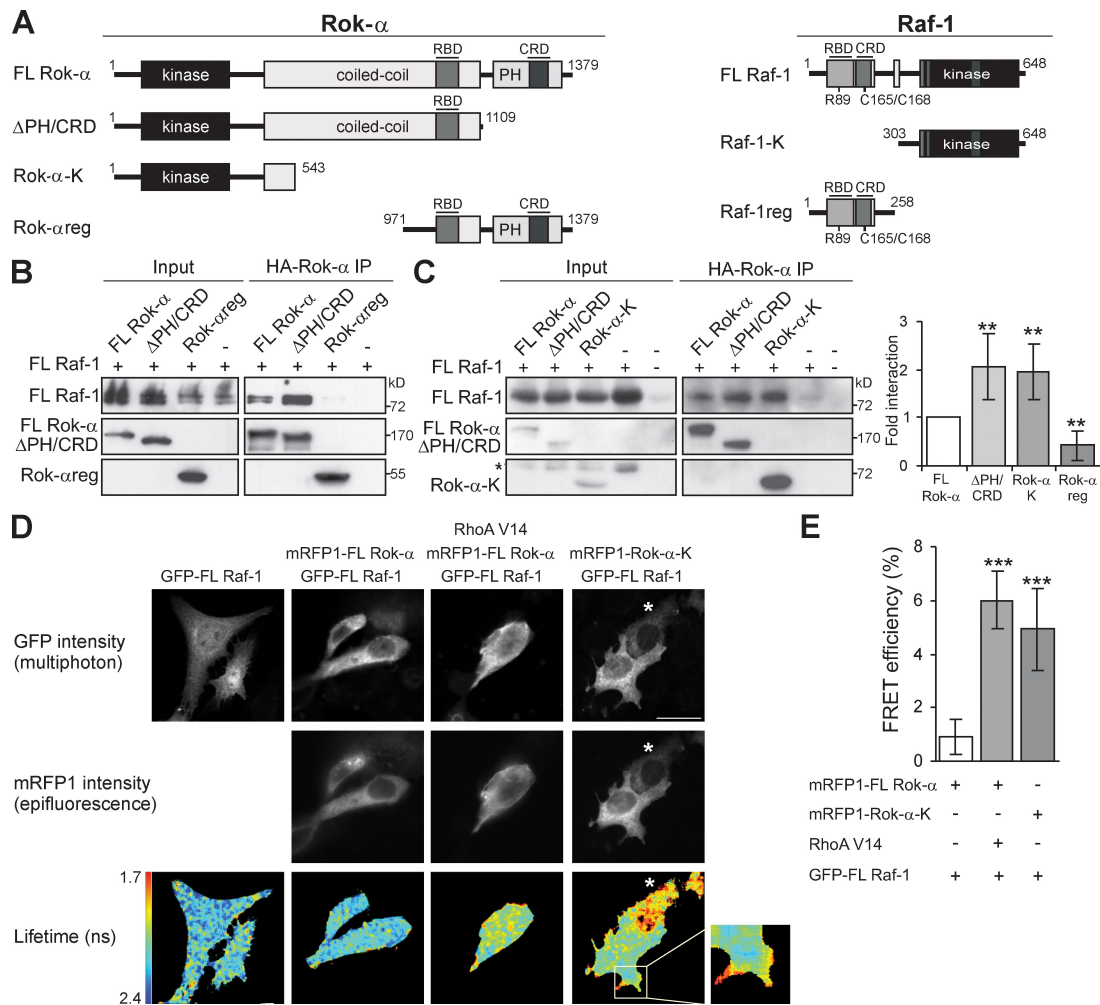
Figure 1.   **Raf-1 interacts with the Rok-α kinase domain.** (A) Rok-α and Raf-1 proteins used in this study are shown. The phosphorylation and Ras-binding site mutants are indicated. (B and C) HA-tagged Rok-α was immunoprecipitated from COS-1 cells cotransfected with Rok-α and FL Raf-1. Input (1.5%) and the immunoprecipitates (IP) were immunoblotted with Raf-1, HA (B), or Rok-α (C) antibodies. *, unspecified band. The amount of Raf-1 coprecipitating with the Rok-α mutant proteins is plotted as fold of FL Raf-1–Rok-α interaction (set as 1; mean ± SD of four experiments). (D) Fluorescence lifetime (τ), GFP intensity, and mRFP1 intensity in MCF-7 cells transfected with the indicated constructs. RhoAV14 expression was verified by staining with Flag antibody. The cell marked with the asterisks was excluded from the cumulative FRET efficiency analysis in E because of insufficient photon counts (see Material and methods). Inset shows a magnified view of the boxed region. (E) Percentage of FRET efficiency (mean ± SD of three experiments) is shown. **, P < 0.01; ***, P < 0.005. Bars, 20 μm.

In contrast to FL Raf-1 R89L, Raf-1reg R89L retained the ability to coimmunoprecipitate with Rok-α (Fig. 3 A). Thus, binding of Ras-GTP to FL Raf-1 is required solely to disrupt the interaction between the regulatory and kinase domains of Raf-1. Interfering with Ras binding did not increase complex formation with Rok-α, indicating that Ras and Rok-α do not compete for Raf-1.

In contrast, Raf-1reg CC/SS, which binds to Ras but not to the Raf-1 kinase domain (Cutler et al., 1998), failed to associate with Rok-α, implying that the CRD plays a critical role in Raf-1–Rok-α complex formation (Fig. 3 B).

Raf-1 CRD might restrain the activity of Rok-α by binding directly to its kinase domain. Indeed, recombinant GST–

Raf-1reg interacted with Rok-α–K in vitro, pulling down ∼25% of the Rok-α–K input, whereas GST–Raf-1reg CC/SS was much less efficient (Fig. 3 C). GST–Raf-1reg, but not a CC/SS mutant, reduced Rok-α–K activity in an in vitro kinase assay (Fig. S2). Moreover, Raf-1reg inhibited recombinant Rok-α–K in a dose-dependent manner (≥70% inhibition at approximately equimolar concentrations of Raf-1reg and MLC2; Fig. 3 D). The calculated half-maximal inhibitory concentration of 2.65 μM is fairly high, but this does not prejudice the physiological relevance of the interaction per se, as exemplified by the even lower affinity (20 μM) of the Raf CRD for Ras-GTP (Williams et al., 2000). Besides, it is unclear how a half-maximal inhibitory concentration calculated in vitro using recombinant proteins relates
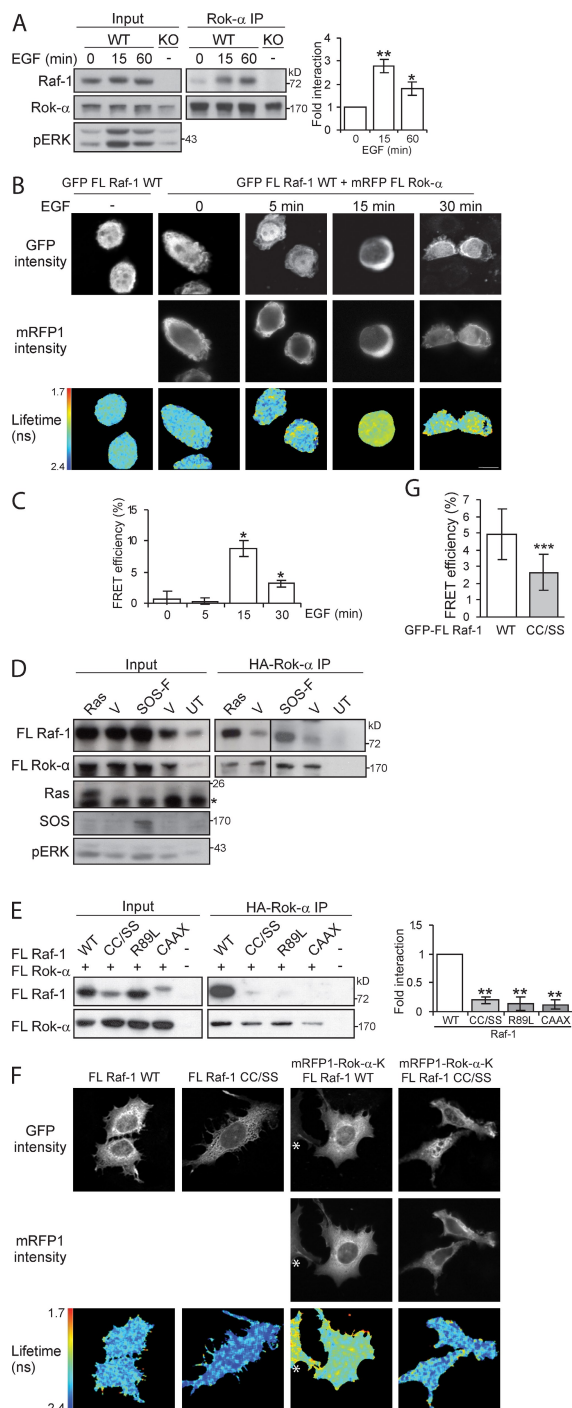
Figure 2.   **Activated Raf-1 preferentially interacts with Rok-α.** (A–C) EGF increases the Rok-α–Raf-1 interaction. (A) MEFs were stimulated with 10 ng/ml EGF, and endogenous Rok-α was immunoprecipitated at the indicated time points. (B and C) Fluorescence lifetime (τ), GFP intensity, and RFP intensity in MDA-MB-468 transfected with GFP-FL Raf-1 and mRFP–FL Rok-α upon stimulation with 100 ng/ml EGF. (C) Percentage of FRET efficiency is shown. Error bars indicate SEM ($n > 3$). (D) Activated Ras promotes Rok-α–Raf-1 interaction. COS-1 cells were transfected with HA-tagged FL Rok-α, FL Raf-1, constitutively active Ras (RasV12), or membrane-tethered SOS-F, resulting in the constitutive activation of endogenous Ras and the corresponding vectors (V). UT, untransfected COS-1 cells; *, endogenous Ras. Black lines indicate that intervening lanes have been spliced out. (E–G) Ras binding and subcellular localization affect Rok-α–Raf-1 interaction. (E) COS-1 cells were transfected with HA-tagged FL Rok-α and the indicated FL Raf-1 mutants. HA immunoprecipitates were analyzed and quantified as described in Fig. 1. (F) Fluorescence lifetime, GFP intensity, and mRFP1 intensity in MCF-7 cells transfected with GFP-FL Raf-1 WT or CC/SS mutant (donor) and mRFP1–Rok-α–K (acceptor). The cell marked with the asterisks was excluded from the cumulative FRET efficiency analysis in G as a result of insufficient photon counts (see Materials and methods). (G) Percentage of FRET efficiency is shown. (A, E, and G) Error bars indicate SD of three experiments. *, $P < 0.05$; **, $P < 0.01$; ***, $P < 0.005$. Bars: (B) 20 μm; (F) 30 μm.

to the binding affinity of the two FL, posttranslationally modified proteins in vivo. Indeed, when expressed at near-endogenous levels in KO MEFs, Raf-1reg wild type (WT), and much less so CC/SS, associated with Rok-α and decreased its kinase activity to levels similar to those observed in WT MEFs (Fig. 3 E).
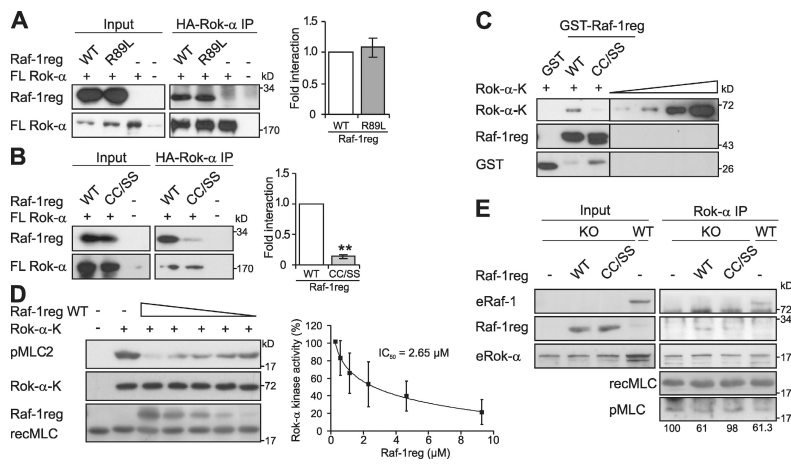
Concentration of the partners in relevant subcellular compartments will also drive protein–protein interaction in vivo. FL Raf-1 and Rok-α accumulate in membrane protrusions (Fig. 1 D), and both Raf-1 (Ehrenreiter et al., 2005) and Raf-1reg colocalize with Rok-α on filamentous structures (Fig. 4 A) corresponding to the vimentin cytoskeleton. Vimentin is a direct substrate of Rok-α, which by phosphorylating it contributes to its depolymerization (Sin et al., 1998). Vimentin collapses in juxtanuclear aggregates in Raf-1–deficient cells, a phenotype rescued by Raf-1reg (Fig. 4 B). Thus, Raf-1reg is sufficient to mediate the correct localization of Rok-α to the vimentin cytoskeleton and to inhibit Rok-α activity, preventing the collapse of these intermediate filaments. In addition to the vimentin defects, Raf-1 KO cells are contracted and characterized by cortical actin bundles. They contain higher amounts of phosphorylated ezrin than WT cells, and their migration is impaired (Fig. 4, C–E). Finally, the death receptor Fas is found in characteristic clusters on the surface of Fas of Raf-1 KO cells, which are more sensitive to Fas-induced cell death (Fig. S3, A and B). All of these defects are caused by Rok-α hyperactivity and can be rescued by chemical inhibition of Rok-α, by expressing dominant-negative Rok-α, or by silencing the Rok-α gene (Ehrenreiter et al., 2005; Piazzolla et al., 2005).

Raf-1reg, but not the CRD mutant, also corrected all defects of Raf-1 KO cells: it significantly improved migration (Fig. 4 C), normalized cell shape, cortical actin bundles, and ezrin phosphorylation (Fig. 4, D and E). Finally, Raf-1reg reduced Fas surface clusters and cell death in Raf-1 KO cells (Fig. S3, A and B). These results demonstrate the biological relevance of the interaction between Rok-α and Raf-1reg and formally rule out a contribution of Raf-1 kinase activity to the regulation of cell shape, migration, and Fas expression.

Raf-1reg and Rok-αreg inhibit Rok-α–K in vivo

Our data suggest that the activity of the Rok-α kinase domain, restrained in cis by its own regulatory domain (Rok-αreg) before activation (Amano et al., 1999), is inhibited in trans by

Figure 3. **Raf-1reg interacts with Rok-α and inhibits its kinase activity.** (A and B) CRD but not RBD mutation disrupts the binding of Raf-1reg to Rok-α. HA immunoprecipitates (IP) were analyzed as in Fig. 1. The mean ± SD of at least three experiments is shown. **, P < 0.01. (C) Rok-α–K interacts in vitro with Raf-1reg WT but not with Raf-1reg CC/SS. 2 µg GST, GST–Raf-1reg WT, or GST–Raf-1reg CC/SS on glutathione Sepharose beads were incubated with 25 ng His-tagged Rok-α–K. Rok-α–K and GST proteins were detected by immunoblotting with His and GST antibody. 3.125–25 ng recombinant Rok-α–K was loaded as a reference on the same gel. One representative experiment out of three is shown. Black lines indicate that intervening lanes have been spliced out. (D) Dose-dependent inhibition of Rok-α–K by purified Raf-1reg. 0.29–9.3 µM Raf-1reg was incubated with 100 ng Rok-α–K (0.05 µM) before a Rok kinase assay with 7 µM recombinant MLC2 (recMLC2) as a substrate. The mean ± SD of three experiments is shown. (E) Raf-1reg inhibits Rok-α activity in vivo. The activity of endogenous Rok-α (eRok-α), immunoprecipitated from WT and KO MEFs, and from KO MEFs transfected with Raf-1reg WT or Raf-1reg CC/SS was assessed as in D. Rok-α activity, expressed as pMLC/MLC ratio and normalized by the amount of Rok-α present in the assay, is indicated below each lane. Rok-α activity of Raf-1 KO MEFs is set to 100%.

Raf-1reg once activation has occurred. A computational model of the Rok-α CRD, based on the structure of the autoinhibitory CRD of Raf-1 (Mott et al., 1996), is compatible with this idea (Fig. 5 A). More importantly, both Rok-αreg and Raf-1reg inhibit the activity of cotransfected Rok-α–K in vivo, reducing the phosphorylation of Rok-α downstream targets by a comparable extent (Fig. 5 B). Finally, Rok-αreg and Raf-1reg, but not Raf-1reg CC/SS, reduced the hyperphosphorylation of ezrin as a result of hyperactive endogenous Rok-α in Raf-1 KO cells (Fig. 5 C). Thus, the regulatory domains of Rok-α and Raf-1 are similarly effective in regulating Rok-α activity in vivo, supporting a model in which activated Raf-1 modulates Rok-α
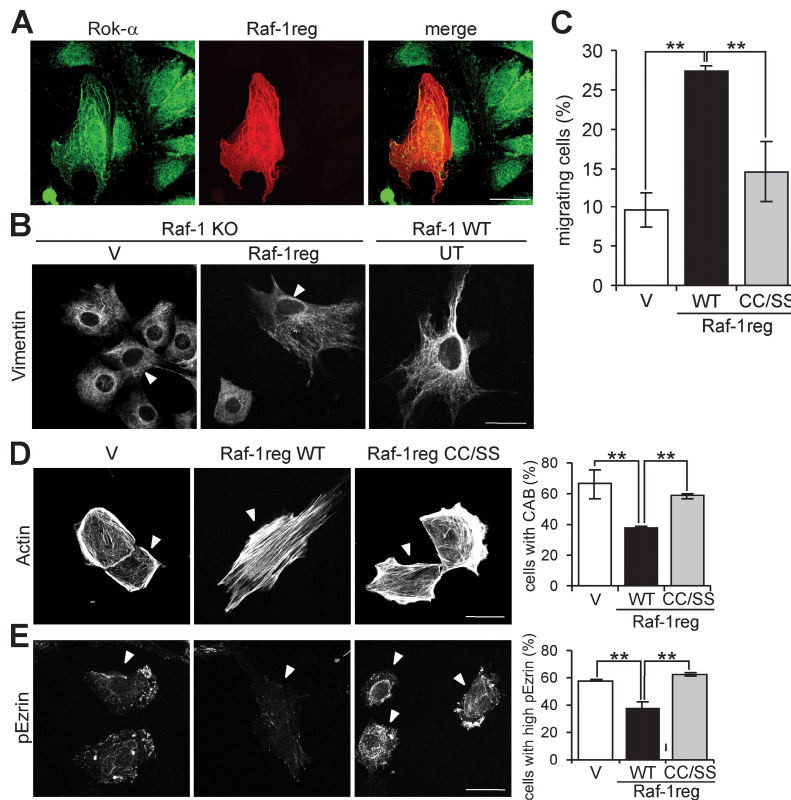

Figure 4. **Raf-1reg colocalizes with Rok-α and rescues all phenotypes of Raf-1 KO MEFs.** (A) Raf-1 KO MEFs expressing Raf-1reg were identified by staining with antibodies against Raf-1. The localization of Raf-1 and Rok-α in migrating MEFs was determined by immunofluorescence. (B–D) Raf-1reg improves cytoskeletal organization and migration. (B) Raf-1reg rescues vimentin cytoskeleton collapse in Raf-1 KO MEFs. Raf-1 KO MEFs cotransfected with pEGFP and pCMV (V) or pCMV Raf-1reg were stained with vimentin antibodies and analyzed by confocal microscopy. UT, untransfected cells. (C) Migration of Raf-1 KO MEFs transfected with the indicated pEGFP constructs was assessed using 10% FCS as a chemoattractant. The percentage of transfected cells migrating to the lower compartment of a Boyden chamber in 2.5 h is plotted. (D and E) Raf-1 KO MEFs were cotransfected with pEGFP and the indicated pCMV constructs, stained with phalloidin to visualize filamentous actin (D) or with anti-ezrin[pT567] (E), and analyzed by confocal microscopy. The number of cells displaying cortical actin bundles (CAB) or prominent ezrin phosphorylation is plotted on the right. Arrowheads indicate EGFP-expressing cells. Error bars indicate SD of three experiments. **, P < 0.01. Bars, 20 µm.
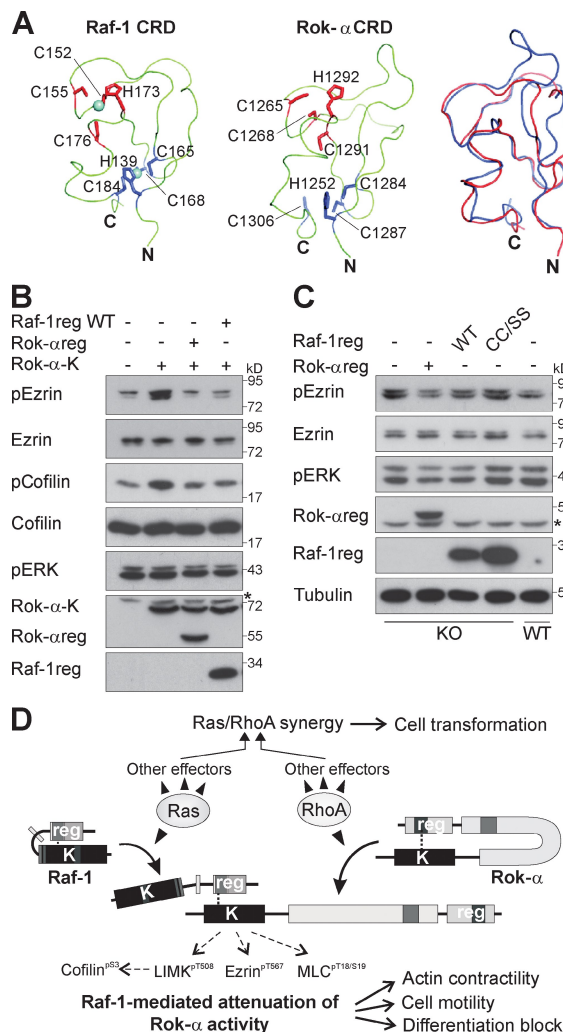
Figure 5. **The regulatory domains of Raf-1 and Rok-α act as inhibitors of Rok-α kinase activity in vivo.** (A) Comparison of the experimental solution structure of Raf-1 CRD (left) and the computational model of the Rok-α CRD (middle). Zinc cations are shown as spheres, and the side chains of the residues coordinating the cations are shown as lines: red in one metal biosite and blue in the other. (right) Superposition of the Raf-1 and Rok-α CRDs. (B and C) COS-1 cells (B) and MEFs (C) were transfected with the indicated constructs. 24 h after transfection, cells were lysed and analyzed by immunoblotting. KO, Raf-1 KO MEFs; *, unspecific band. (D) Model of the regulation of Rok-α by Raf-1. GTPase binding disrupts intramolecular interaction between the regulatory and kinase domains of Raf-1 and Rok-α, upon which Raf-1reg binds to the kinase domain of Rok-α, restraining Rho-induced Rok-α kinase activity. Inhibition in trans limits the phosphorylation of Rok-α downstream targets, regulating cell motility and differentiation.

by providing inhibition in trans (Fig. 5 D). Another GTPase-activated kinase, Pak1, is inhibited in trans in its basal state in the context of a homodimer in which the regulatory domain of one molecule inhibits the kinase domain of the other. However, although disruption of the dimer by activated GTPases allows Pak1 activation (Parrini et al., 2002), GTPase binding to both Raf-1 and Rok-α promotes the formation of complexes within which Rok-α activity is restrained by Raf-1.

Thus far, we don't have any evidence that Rok-α modulates Raf-1 activity. The Raf-1 kinase domain does not bind to Rok-α, and the regulatory domain is not a Rok-α substrate in vitro (unpublished data). It is possible that Rok-α regulates Raf-1 by promoting its localization to intermediate filaments, thereby bringing it in the proximity of specific substrates. Further studies will be needed to clarify this issue.

Implications for transformation

Ras, Rho, and their downstream effectors are implicated in tumorigenesis. A good example of Ras–Rho cross talk is the suppression of Rho signaling by Ras/ERK in transformed cells, leading to increased motility. This is achieved either at the level of integrin-mediated Rho activation, which is impaired by the product of the ERK target gene *fra-1* (Vial et al., 2003) or, more specifically, by uncoupling Rho activation from its downstream effector Rok. In particular, Rok expression can be reduced by ERK activation in Ras-transformed cells with high levels of active Rho (Sahai et al., 2001; Pawlak and Helfman, 2002b) and in v-src–transformed cells (Pawlak and Helfman, 2002a).

Our data identify a novel, ERK-independent mechanism by which Ras selectively regulates Rho signaling by promoting interaction between the top-tier kinases Raf-1 and Rok-α. We have recently shown the significance of this interaction in a model of Ras-driven epidermal tumorigenesis (Ehrenreiter et al., 2009) in which Ras causes transformation by inducing proliferation and survival (Sibilia et al., 2000) and by selectively blocking differentiation. We found that Ras mediates this block by promoting Raf-1–Rok-α interaction and the inhibition of Rok-α activity. If Raf-1 is ablated, both development and maintenance of the Ras-driven tumors are abrogated (Ehrenreiter et al., 2009). Understanding the mechanisms underlying the interaction between Raf-1 and Rok-α may hold promise for the design of novel, specific inhibitors for therapeutic treatments.

Materials and methods

28

Migration assay

Migration was assessed in a modified Boyden chamber as described previously (Ehrenreiter et al., 2005). Migrating and nonmigrating EGFP-transfected cells were visualized and quantified (≥450 cells/sample) by epifluorescence microscopy.

Immunofluorescence

Raf-1, Rok-α, vimentin, actin, ezrin^{pT567}, and Fas were performed as described previously (Ehrenreiter et al., 2005; Piazzolla et al., 2005). For Raf-1 and Rok-α staining, cells plated on fibronectin (Invitrogen) were permeabilized (0.01% Triton X-100), fixed in 4% PFA, and blocked with 0.2% gelatin before incubation with primary antibodies (Raf-1 and Rok-α; BD) and staining with the appropriate Alexa Fluor 488– or 594–conjugated secondary antibodies (Invitrogen). Rhodamine-conjugated phalloidin (Invitrogen) was used to visualize actin filaments.

To visualize vimentin, intermediate filaments cells were fixed in methanol containing 5 mM EDTA and permeabilized with 0.5% Triton X-100. Cells were subsequently stained with vimentin antibody (Sigma-Aldrich) followed by Alexa Fluor 594–conjugated secondary antibodies.

For ezrin^{pT567} staining, cells were fixed in cold methanol/5 mM EDTA and blocked (10% goat serum/1% BSA) before incubation with phospho ezrin–radixin–moesin antibody (pT567; Cell Signaling Technology) followed by Alexa Fluor 594–conjugated secondary antibodies.

For Fas staining, cells were fixed in cold methanol/5 mM EDTA for 10 min at room temperature followed by Alexa Fluor 594–conjugated secondary antibodies. Antifade reagent (ProLong Antifade; Invitrogen) was used as a mounting medium.

Confocal microscopy was performed at room temperature with a microscope (Axiovert 100M; Carl Zeiss, Inc.) fitted with a Plan Apochromat 63×/1.40 NA oil objective and equipped with the confocal laser-scanning module (LSM 510; Carl Zeiss, Inc.). Immersol (518; Carl Zeiss, Inc.) was used as imaging medium. Images were acquired using the LSM 510 software (version 2.3; Carl Zeiss, Inc.). Representative z stacks are shown. 600 transfected cells were counted for the quantification.

Cell lysates, immunoprecipitation, and immunoblotting

Cells were washed with ice-cold PBS and lysed in 200 mM Tris-HCl, pH 7.4, 2 mM EDTA, and 1% Triton X-100 with protease and phosphatase inhibitors. Lysates and HA–Rok-α immunoprecipitates were prepared from subconfluent cells 24–48 h after transfection and analyzed by immunoblotting using the following antibodies: Rok-α (Millipore), HA (12CA5), Rok-α, Raf-1, SOS (BD), pCofilin^{S3}, Cofilin, pMLC$^{T18/S19}$ (Santa Cruz Biotechnology, Inc.), pERK, pEzrin^{T567}, ezrin–radixin–moesin (Cell Signaling Technology), tubulin (Sigma-Aldrich), and pan-Ras^{V12} (EMD). The amount of Raf-1 proteins in the immunoprecipitation was quantified by densitometry (ImageQuant [GE Healthcare] or AlphaEase [Alpha Innotech]) and normalized to the amount of immunoprecipitated Rok-α.

Protein expression and purification

GST–Raf-1reg proteins were expressed in *Escherichia coli* Rosetta (DE3; EMD) by induction with 1 mM IPTG and incubation in minimal medium overnight at 22°C (Korz et al., 1995). GST–Raf-1reg proteins were purified by binding to glutathione Sepharose beads (GE Healthcare) and eluted with 20 mM reduced glutathione in 50 mM Tris-HCl, pH 8.0. Recombinant Raf-1reg and MLC2 were obtained by thrombin cleavage (6 U/ml overnight at 4°C) as previously described (Wyckoff et al., 2006).

GST pull-down and Rok-α in vitro kinase assays

GST–Raf-1reg immobilized on glutathione Sepharose was incubated with Rok-α–K (Millipore) for 15 min at 30°C, washed, and eluted by boiling in SDS sample buffer. Complex formation was determined by immunoblotting with anti-5His (QIAGEN) or anti-GST antibodies. Rok activity was assayed using 7 µM MLC2 as a substrate. Phosphorylation was detected by immunoblotting with pMLC$^{T18/S19}$ antibody, normalized to MLC2 content, and quantified using an infrared imaging system (Odyssey; LI-COR Biosciences).

FRET determination by multiphoton FLIM

Time domain FLIM was performed at room temperature with a multiphoton microscope system comprised of a solid state–pumped (Verdi 8W; Coherent, Inc.), femtosecond self-mode–locked Ti:Sapphire laser system (Mira; Coherent, Inc.), an in-house–developed scan head, and an inverted microscope (TE2000E; Nikon; Peter et al., 2005; Festy et al., 2007). FRET was monitored by the conventional equation: FRET efficiency = $1 - \tau_{da}/\tau_{control}$, where τ_{da} is the lifetime of GFP–Raf-1 in cells that coexpress mRFP1–Rok-α,

and $\tau_{control}$ is the GFP–Raf-1 lifetime measured in the absence of an acceptor. Because ≤100-ps time resolution is achieved with our instrumentation, for a $\tau_{control}$ value of 2.35 ns, FRET efficiencies as low as 3% can be determined accurately. Pixel by pixel lifetime determination was achieved using a modified Levenberg–Marquardt fitting technique (Barber et al., 2005). The error in fitting the monoexponential decay model for fluorescence lifetime determination is <0.4% for signals with a peak of ≥500 photon counts. Also, in general, the lifetime of the interacting population (FRET species) can only be accurately determined with a peak photon count of ≥500 (Barber et al., 2009). We have therefore routinely excluded cells that have insufficient photon counts (<500 photons at the peak) from lifetime analysis.

Computational analysis of Raf-1 and Rok-α CRD

Rok-α CRD was modeled on the basis of the experimental structure of Raf-1 CRD (Protein Data Bank accession no. 1FAR; Mott et al., 1996) using Modeller (http://salilab.org/modeller/; Martí-Renom et al., 2000) and refined with Jackal (full atom Amber force field; http://wiki.c2b2.columbia.edu/honiglab_public/index.php/Software:Jackal; Petrey et al., 2003) in the absence of the two zinc ions. The presence of two metal-binding sites was confirmed by two independent approaches, CheD (Babor et al., 2008) and MetSite (http://bioinf.cs.ucl.ac.uk/MetSite/MetSite.html; Sodhi et al., 2004).

Statistical analysis

All values are expressed as mean ± SD of at least three independent experiments unless indicated otherwise. P-values were calculated using the unpaired, two-tailed Student's t test. $P \leq 0.05$ is considered statistically significant.

Online supplemental material

Fig. S1 shows that FL Raf-1 and Raf-1reg, but not the Raf-1 kinase domain, interact with FL Rok-α and ΔPH/CRD Rok-α. Fig. S2 shows that Raf-1reg, but not Raf-1reg CC/SS, inhibits the kinase activity of Rok-α in vitro. Fig. S3 shows that expression of Raf-1reg prevents the formation of Fas clusters at the cell surface of Raf-1 KO cells and reduces their sensitivity to Fas-induced cell death. Online supplemental material is available at http://www.jcb.org/cgi/content/full/jcb.200906178/DC1.

References

Amano, M., K. Chihara, N. Nakamura, T. Kaneko, Y. Matsuura, and K. Kaibuchi. 1999. The COOH terminus of Rho-kinase negatively regulates rho-kinase activity. *J. Biol. Chem.* 274:32418–32424. doi:10.1074/jbc.274.45.32418

Babor, M., S. Gerzon, B. Raveh, V. Sobolev, and M. Edelman. 2008. Prediction of transition metal-binding sites from apo protein structures. *Proteins.* 70:208–217. doi:10.1002/prot.21587

Barber, P., S.M. Ameer-Beg, J. Gilbey, R.J. Edens, I. Ezike, and B. Vojnovic. 2005. Global and pixel kinetic data analysis for FRET detection by multi-photon time-domain FLIM. *Proc. SPIE.* 5700:171–181. doi:10.1117/12.590510

Barber, P.R., S.M. Ameer-Beg, J. Gilbey, L.M. Carlin, M. Keppler, T.C. Ng, and B. Vojnovic. 2009. Multiphoton time-domain fluorescence lifetime imaging microscopy: practical application to protein–protein interactions using global analysis. *J. R. Soc. Interface.* 6:S93–S105. doi:10.1098/rsif.2008.0451.focus

Bondeva, T., A. Balla, P. Várnai, and T. Balla. 2002. Structural determinants of Ras-Raf interaction analyzed in live cells. *Mol. Biol. Cell.* 13:2323–2333. doi:10.1091/mbc.E02-01-0019

Bruder, J.T., G. Heidecker, and U.R. Rapp. 1992. Serum-, TPA-, and Ras-induced expression from Ap-1/Ets-driven promoters requires Raf-1 kinase. *Genes Dev.* 6:545–556. doi:10.1101/gad.6.4.545

Catalanotti, F., G. Reyes, V. Jesenberger, G. Galabova-Kovacs, R. de Matos Simoes, O. Carugo, and M. Baccarini. 2009. A Mek1-Mek2 heterodimer determines the strength and duration of the Erk signal. *Nat. Struct. Mol. Biol.* 16:294–303. doi:10.1038/nsmb.1564

Chen, X.Q., I. Tan, C.H. Ng, C. Hall, L. Lim, and T. Leung. 2002. Characterization of RhoA-binding kinase ROKalpha implication of the pleckstrin homology domain in ROKalpha function using region-specific antibodies. *J. Biol. Chem.* 277:12680–12688. doi:10.1074/jbc.M109839200

Cutler, R.E. Jr., R.M. Stephens, M.R. Saracino, and D.K. Morrison. 1998. Autoregulation of the Raf-1 serine/threonine kinase. *Proc. Natl. Acad. Sci. USA.* 95:9214–9219. doi:10.1073/pnas.95.16.9214

Dvorsky, R., L. Blumenstein, I.R. Vetter, and M.R. Ahmadian. 2004. Structural insights into the interaction of ROCKI with the switch regions of RhoA. *J. Biol. Chem.* 279:7098–7104. doi:10.1074/jbc.M311911200

Eblen, S.T., J.K. Slack-Davis, A. Tarcsafalvi, J.T. Parsons, M.J. Weber, and A.D. Catling. 2004. Mitogen-activated protein kinase feedback phosphorylation regulates MEK1 complex formation and activation during cellular adhesion. *Mol. Cell. Biol.* 24:2308–2317. doi:10.1128/MCB.24.6.2308-2317.2004

Ehrenreiter, K., D. Piazzolla, V. Velamoor, I. Sobczak, J.V. Small, J. Takeda, T. Leung, and M. Baccarini. 2005. Raf-1 regulates Rho signaling and cell migration. *J. Cell Biol.* 168:955–964. doi:10.1083/jcb.200409162

Ehrenreiter, K., F. Kern, V. Velamoor, K. Meissl, G. Galabova-Kovacs, M. Sibilia, and M. Baccarini. 2009. Raf-1 addiction in Ras-induced skin carcinogenesis. *Cancer Cell.* 16:149–160. doi:10.1016/j.ccr.2009.06.008

Festy, F., S.M. Ameer-Beg, T. Ng, and K. Suhling. 2007. Imaging proteins in vivo using fluorescence lifetime microscopy. *Mol. Biosyst.* 3:381–391. doi:10.1039/b617204k

Filmus, J., M.N. Pollak, R. Cailleau, and R.N. Buick. 1985. MDA-468, a human breast cancer cell line with a high number of epidermal growth factor (EGF) receptors, has an amplified EGF receptor gene and is growth inhibited by EGF. *Biochem. Biophys. Res. Commun.* 128:898–905. doi:10.1016/0006-291X(85)90131-7

Heasman, S.J., and A.J. Ridley. 2008. Mammalian Rho GTPases: new insights into their functions from in vivo studies. *Nat. Rev. Mol. Cell Biol.* 9:690–701. doi:10.1038/nrm2476

Korz, D.J., U. Rinas, K. Hellmuth, E.A. Sanders, and W.D. Deckwer. 1995. Simple fed-batch technique for high cell density cultivation of *Escherichia coli. J. Biotechnol.* 39:59–65. doi:10.1016/0168-1656(94)00143-Z

Kubicek, M., M. Pacher, D. Abraham, K. Podar, M. Eulitz, and M. Baccarini. 2002. Dephosphorylation of Ser-259 regulates Raf-1 membrane association. *J. Biol. Chem.* 277:7913–7919. doi:10.1074/jbc.M108733200

Leevers, S.J., H.F. Paterson, and C.J. Marshall. 1994. Requirement for Ras in Raf activation is overcome by targeting Raf to the plasma membrane. *Nature.* 369:411–414. doi:10.1038/369411a0

Leung, T., X.Q. Chen, E. Manser, and L. Lim. 1996. The p160 RhoA-binding kinase ROK alpha is a member of a kinase family and is involved in the reorganization of the cytoskeleton. *Mol. Cell. Biol.* 16:5313–5327.

Martí-Renom, M.A., A.C. Stuart, A. Fiser, R. Sánchez, F. Melo, and A. Sali. 2000. Comparative protein structure modeling of genes and genomes. *Annu. Rev. Biophys. Biomol. Struct.* 29:291–325. doi:10.1146/annurev.biophys.29.1.291

Mikula, M., M. Schreiber, Z. Husak, L. Kucerova, J. Rüth, R. Wieser, K. Zatloukal, H. Beug, E.F. Wagner, and M. Baccarini. 2001. Embryonic lethality and fetal liver apoptosis in mice lacking the c-raf-1 gene. *EMBO J.* 20:1952–1962. doi:10.1093/emboj/20.8.1952

Mott, H.R., J.W. Carpenter, S. Zhong, S. Ghosh, R.M. Bell, and S.L. Campbell. 1996. The solution structure of the Raf-1 cysteine-rich domain: a novel ras and phospholipid binding site. *Proc. Natl. Acad. Sci. USA.* 93:8312–8317. doi:10.1073/pnas.93.16.8312

O'Neill, E., L. Rushworth, M. Baccarini, and W. Kolch. 2004. Role of the kinase MST2 in suppression of apoptosis by the proto-oncogene product Raf-1. *Science.* 306:2267–2270. doi:10.1126/science.1103233

Olson, M.F. 2008. Applications for ROCK kinase inhibition. *Curr. Opin. Cell Biol.* 20:242–248. doi:10.1016/j.ceb.2008.01.002

Parrini, M.C., M. Lei, S.C. Harrison, and B.J. Mayer. 2002. Pak1 kinase homodimers are autoinhibited in trans and dissociated upon activation by Cdc42 and Rac1. *Mol. Cell.* 9:73–83. doi:10.1016/S1097-2765(01)00428-2

Pawlak, G., and D.M. Helfman. 2002a. MEK mediates v-Src-induced disruption of the actin cytoskeleton via inactivation of the Rho-ROCK-LIM kinase pathway. *J. Biol. Chem.* 277:26927–26933. doi:10.1074/jbc.M202261200

Pawlak, G., and D.M. Helfman. 2002b. Post-transcriptional down-regulation of ROCKI/Rho-kinase through an MEK-dependent pathway leads to cytoskeleton disruption in Ras-transformed fibroblasts. *Mol. Biol. Cell.* 13:336–347. doi:10.1091/mbc.01-06-0302

Peter, M., S.M. Ameer-Beg, M.K. Hughes, M.D. Keppler, S. Prag, M. Marsh, B. Vojnovic, and T. Ng. 2005. Multiphoton-FLIM quantification of the EGFP-mRFP1 FRET pair for localization of membrane receptor-kinase interactions. *Biophys. J.* 88:1224–1237. doi:10.1529/biophysj.104.050153

Petrey, D., Z. Xiang, C.L. Tang, L. Xie, M. Gimpelev, T. Mitros, C.S. Soto, S. Goldsmith-Fischman, A. Kernytsky, A. Schlessinger, et al. 2003. Using multiple structure alignments, fast model building, and energetic analysis in fold recognition and homology modeling. *Proteins.* 53(Suppl 6):430–435. doi:10.1002/prot.10550

Piazzolla, D., K. Meissl, L. Kucerova, C. Rubiolo, and M. Baccarini. 2005. Raf-1 sets the threshold of Fas sensitivity by modulating Rok-α signaling. *J. Cell Biol.* 171:1013–1022. doi:10.1083/jcb.200504137

Riento, K., and A.J. Ridley. 2003. Rocks: multifunctional kinases in cell behaviour. *Nat. Rev. Mol. Cell Biol.* 4:446–456. doi:10.1038/nrm1128

Roy, S., A. Lane, J. Yan, R. McPherson, and J.F. Hancock. 1997. Activity of plasma membrane-recruited Raf-1 is regulated by Ras via the Raf zinc finger. *J. Biol. Chem.* 272:20139–20145. doi:10.1074/jbc.272.32.20139

Sahai, E., M.F. Olson, and C.J. Marshall. 2001. Cross-talk between Ras and Rho signalling pathways in transformation favours proliferation and increased motility. *EMBO J.* 20:755–766. doi:10.1093/emboj/20.4.755

Shimizu, T., K. Ihara, R. Maesaki, M. Amano, K. Kaibuchi, and T. Hakoshima. 2003. Parallel coiled-coil association of the RhoA-binding domain in Rho-kinase. *J. Biol. Chem.* 278:46046–46051. doi:10.1074/jbc.M306458200

Sibilia, M., A. Fleischmann, A. Behrens, L. Stingl, J. Carroll, F.M. Watt, J. Schlessinger, and E.F. Wagner. 2000. The EGF receptor provides an essential survival signal for SOS-dependent skin tumor development. *Cell.* 102:211–220. doi:10.1016/S0092-8674(00)00026-X

Sin, W.C., X.Q. Chen, T. Leung, and L. Lim. 1998. RhoA-binding kinase alpha translocation is facilitated by the collapse of the vimentin intermediate filament network. *Mol. Cell. Biol.* 18:6325–6339.

Sodhi, J.S., K. Bryson, L.J. McGuffin, J.J. Ward, L. Wernisch, and D.T. Jones. 2004. Predicting metal-binding site residues in low-resolution structural models. *J. Mol. Biol.* 342:307–320. doi:10.1016/j.jmb.2004.07.019

Terai, K., and M. Matsuda. 2005. Ras binding opens c-Raf to expose the docking site for mitogen-activated protein kinase kinase. *EMBO Rep.* 6:251–255. doi:10.1038/sj.embor.7400349

Tian, T., A. Harding, K. Inder, S. Plowman, R.G. Parton, and J.F. Hancock. 2007. Plasma membrane nanoswitches generate high-fidelity Ras signal transduction. *Nat. Cell Biol.* 9:905–914. doi:10.1038/ncb1615

Vial, E., E. Sahai, and C.J. Marshall. 2003. ERK-MAPK signaling coordinately regulates activity of Rac1 and RhoA for tumor cell motility. *Cancer Cell.* 4:67–79. doi:10.1016/S1535-6108(03)00162-4

Wellbrock, C., M. Karasarides, and R. Marais. 2004. The RAF proteins take centre stage. *Nat. Rev. Mol. Cell Biol.* 5:875–885. doi:10.1038/nrm1498

Williams, J.G., J.K. Drugan, G.S. Yi, G.J. Clark, C.J. Der, and S.L. Campbell. 2000. Elucidation of binding determinants and functional consequences of Ras/Raf-cysteine-rich domain interactions. *J. Biol. Chem.* 275:22172–22179. doi:10.1074/jbc.M000397200

Wyckoff, J.B., S.E. Pinner, S. Gschmeissner, J.S. Condeelis, and E. Sahai. 2006. ROCK- and myosin-dependent matrix deformation enables protease-independent tumor-cell invasion in vivo. *Curr. Biol.* 16:1515–1523. doi:10.1016/j.cub.2006.05.065

Yamaguchi, O., T. Watanabe, K. Nishida, K. Kashiwase, Y. Higuchi, T. Takeda, S. Hikoso, S. Hirotani, M. Asahi, M. Taniike, et al. 2004. Cardiac-specific disruption of the c-raf-1 gene induces cardiac dysfunction and apoptosis. *J. Clin. Invest.* 114:937–943.

Zhang, L., M. Bewick, and R.M. Lafrenie. 2002. Role of Raf-1 and FAK in cell density-dependent regulation of integrin-dependent activation of MAP kinase. *Carcinogenesis.* 23:1251–1258. doi:10.1093/carcin/23.7.1251

Zhao, Z.S., and E. Manser. 2005. PAK and other Rho-associated kinases—effectors with surprisingly diverse mechanisms of regulation. *Biochem. J.* 386:201–214. doi:10.1042/BJ20041638

30

8   Raf-1 Addiction in Ras-Induced Skin Carcinogenesis

Karin Ehrenreiter[1], Florian Kern[1], Vanishree Velamoor[1], Katrin Meissl[1], Gergana Galabova-Kovacs[1], Maria Sibilia[2], and Manuela Baccarini[*,1]

[1]Max F. Perutz Laboratories, Department of Microbiology and Immunobiology, University of Vienna, 1030 Vienna, Austria

[2]Department of Medicine I, Institute for Cancer Research, Medical University of Vienna, 1090 Vienna, Austria

[*]Correspondence: Professor M. Baccarini; E-mail: manuela.baccarini@univie.ac.at

Relevance & Contribution: This article introduces the concept of non-oncogene addiction to Raf-1 in Ras-mediated skin carcinogenesis. Moreover, it remarkably proofs the role of the previously described Raf-1/Rok-α interaction in two *in vivo* tumor models as an essential regulator to sustain tumorigenesis by restraining the default differentiation program. The knockout of Raf-1 that abolishes this interaction not only leads to a complete protection against Ras-driven epidermal tumorigenesis but even leads to a complete regression in an established solid tumor. This regression is mainly mediated by the Rok-α hyperactivation and consequent keratinocyte hyperdifferentiation upon Raf-1 ablation. The manuscript was written by M.B., K.E. and F.K.. The initial experiments were carried out by K.E., F.K. contributed key experiments showing the relevance of the implicated Raf-1-Rok-α mechanisms *in vivo* and collaborated with K.E. on the final experiments of the project.

Article

Raf-1 Addiction in Ras-Induced Skin Carcinogenesis

Karin Ehrenreiter,[1] Florian Kern,[1] Vanishree Velamoor,[1] Katrin Meissl,[1] Gergana Galabova-Kovacs,[1] Maria Sibilia,[2] and Manuela Baccarini[1,*]
[1]Max F. Perutz Laboratories, Department of Microbiology and Immunobiology, University of Vienna, 1030 Vienna, Austria
[2]Department of Medicine I, Institute for Cancer Research, Medical University of Vienna, 1090 Vienna, Austria
*Correspondence: manuela.baccarini@univie.ac.at
DOI 10.1016/j.ccr.2009.06.008

SUMMARY

Ras activation is common to many human cancers and promotes cell proliferation and survival by initiating multiple signaling cascades. Accordingly, Ras-transformed cells are generally considered too resourceful to become addicted to a single effector. In contrast to this tenet, we now demonstrate an absolute, cell autonomous requirement for Raf-1 in the development and maintenance of Ras-induced skin epidermis tumors. Mechanistically, Raf-1 functions as an endogenous inhibitor dimming the activity of the Rho-dependent kinase Rok-α in the context of a Ras-induced Raf-1:Rok-α complex. Raf-1-induced Rok-α inhibition allows the phosphorylation of STAT3 and Myc expression and promotes dedifferentiation in Ras-induced tumors. These data link the Raf-1:Rok-α complex to STAT3/Myc activation and delineate a pathway crucial for cell fate decision in Ras-induced tumorigenesis.

INTRODUCTION

The epidermis shields the body from the potentially, or frankly, harmful effects of the environment. Due to the wear and tear to which it is subjected, the epidermis is in a constant state of self-renewal. This process requires the proliferation of basal keratinocytes, which, after detaching from the underlying basement membrane of extracellular matrix, withdraw from the cell cycle and differentiate while migrating toward the skin surface. The disruption of the balance between keratinocyte proliferation and their ability to differentiate and/or to undergo apoptosis causes several pathological conditions, including tumorigenesis. Squamous cell carcinoma (SCC), one of the most common human skin cancers, results from such an imbalance between proliferation, differentiation, and apoptosis (Ridky and Khavari, 2004). The pathways required to convert normal epidermis into SCC are still incompletely defined, but there is strong evidence indicating that activation of Ras signaling concomitant with inhibition of NF-κB function is sufficient to transform normal human epidermis into SCC (Green and Khavari, 2004).

Ras GTPases are activated by a variety of extracellular signals and are mutated in 33% of human cancers. Activated Ras stim-

ulates multiple effectors, including the Raf/MEK/ERK pathway, the phosphoinositide-3 kinases (PI-3K)/Akt pathway, and the guanine nucleotide exchange factors Ral-GDS and Tiam-1, which lead to the activation of the small GTPases Ral and Rac, respectively (Repasky et al., 2004). These different effectors of Ras contribute to distinct aspects of transformation. While the PI-3K pathway (Gupta et al., 2007; Sibilia et al., 2000) and Ral-GDS (Gonzalez-Garcia et al., 2005) have been implicated in cell survival, the ERK pathway has long been regarded as the mitogenic branch of Ras signaling. Deregulation of this pathway has been reported in more than 30% of common cancers. In the specific case of SCC, the majority of spontaneous human tumors display Ras and ERK activation in the absence of somatic Ras mutations, suggesting that other factors, such as the overexpression of receptor tyrosine kinases, may activate the pathway in tumors (Dajee et al., 2003).

Consistent with the mitogenic role attributed to the Ras/ERK pathway, studies in mouse and human epidermal cells in vivo have associated the activation of its components with increased proliferation and decreased differentiation (Dajee et al., 2002; Haase et al., 2001; Scholl et al., 2004; Tarutani et al., 2003), although constitutive Ras/Raf activation can arrest growth and

SIGNIFICANCE

Our data show that Ras-driven carcinogenesis requires the continuous presence of Raf-1 to restrain Rok-α activity and prevent differentiation. Since Raf-1 is dispensable for epidermal homeostasis, this discovery paves the way for the design of molecule-targeted therapies, which may include Raf-1 interference or allosteric inhibitors capable of disrupting the Raf-1: Rok complex. The combination of chemotherapy and induction of tumor cell differentiation (differentiation therapy) has revolutionized the treatment of leukemia. The complete differentiation induced by Raf-1 ablation in vivo provides proof of principle that such differentiation therapy may be applied to solid tumors and raises hopes that a combination of Raf-1-targeted and conventional therapies may be beneficial at least in the treatment of skin epidermis tumors containing active Ras.
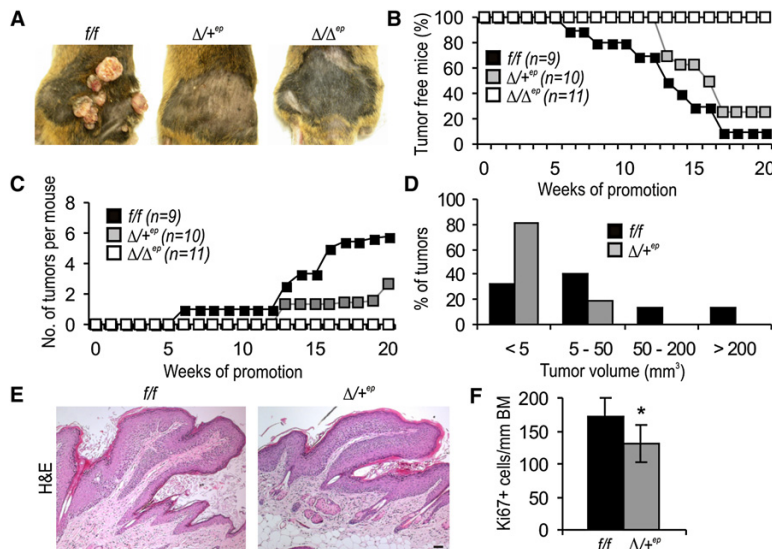
Figure 1. Raf-1 Ablation in Keratinocytes Prevents Chemically Induced Skin Carcinogenesis

Eight- to twelve-week-old *f/f*, $\Delta/+^{ep}$ and Δ/Δ^{ep} mice were subjected to chemical two-stage carcinogenesis with DMBA and TPA.

(A–D) Δ/Δ^{ep} mice are completely resistant and $\Delta/+^{ep}$ mice are partially resistant to chemically-induced skin carcinogenesis. (A) shows representative pictures of *f/f*, $\Delta/+^{ep}$ and Δ/Δ^{ep} animals. (B) shows tumor incidence (C) shows the average number of tumors per mouse. (D) shows tumor size. (E) Lack of major structural differences in $\Delta/+^{ep}$ and *f/f* tumor sections stained with hematoxylin and eosin. The scale bar represents 100 µm.

(F) Mitotic index of *f/f* and $\Delta/+^{ep}$ tumors. Proliferation was determined as the number of Ki67+ cells per millimeter of basal membrane (BM). Three millimeters of BM/mouse were analyzed. The plot shows the results of the analysis of at least three animals/genotype. Error bars indicate SD of the mean. *$p < 0.01$ according to Student's t test.

induce features of terminal differentiation in cultured murine keratinocytes (Lin and Lowe, 2001; Roper et al., 2001). Therefore, the Raf/MEK/ERK arm of Ras signaling represents an attractive target for the therapy of skin cancer. As a caveat to this statement, human tumor cells harboring Ras mutations are quite resistant to the inhibition of MEK (Solit et al., 2006), and while the Raf/MEK/ERK pathway is important in tumor induction, other Ras effectors may be more relevant for the maintenance of established tumors, at least in a xenograft model (Lim and Counter, 2005).

Rho family GTPases have also been implicated in the control of keratinocyte proliferation and differentiation, in the context of both epidermal homeostasis and tumor development (Benitah et al., 2005; Grossi et al., 2005; Lefort et al., 2007; Malliri et al., 2002; Wu et al., 2006). Particularly, RhoA effectors have been reported to both promote (McMullan et al., 2003) and antagonize (Grossi et al., 2005; Lefort et al., 2007) keratinocyte differentiation.

Well-characterized transgenic and chemical models of skin carcinogenesis are available in which both the onset and progression of tumors can be readily monitored. Recently, we have generated a transgenic mouse model in which constitutive activation of the endogenous Ras pathway is achieved by the expression of a dominant active Son of Sevenless (SOS) in the epidermis (*K5-SOS-F* transgenic mice; Sibilia et al., 2000). In the presence of a functional EGFR, required to provide an essential survival signal to tumor cells, *K5-SOS-F* mice develop skin tumors that share features of human SCC (Sibilia et al., 2000).

In the classical chemical carcinogenesis protocol, tumors are initiated by the topical application of 7,12-dimethylbenz[*a*] anthracene (DMBA), which causes a mutation in codon 61 of the *H-ras* gene (Quintanilla et al., 1986), and promoted by the repeated application of 12-O-tetradecanoylphorbol 13-acetate (TPA). The development of these chemically induced tumors critically depends on inflammation (Mueller, 2006) and is reduced to various degrees by the ablation of H-Ras (Ise et al., 2000), of the Rac GEF Tiam-1 (Malliri et al., 2002), and of RalGDS (Gonzalez-Garcia et al., 2005) in the whole animal. Whether the effects of

Tiam1 or RalGDS ablation on carcinogenesis reflect the interruption of Ras signaling in the tumor target cell, or defects in accessory cells (inflammatory cells and tumor-associated fibroblasts) or a combination of both, remains to be conclusively established. We have generated an epidermis-restricted Raf-1 knockout (*K5-Cre;c-raf-1^{flox/flox}* mice; hereafter referred to as Δ/Δ^{ep} [Ehrenreiter et al., 2005]), which enables us to investigate the function of Raf-1 in keratinocytes during skin carcinogenesis. Δ/Δ^{ep} animals develop normally, except for a mild waved fur phenotype that disappears after the first hair cycle and a significant delay in repairing full-thickness wounds, which correlates with a migratory defect of the keratinocytes. The molecular basis of this defect is the hyperactivity of the Rho effector Rok-α, whose activation in wild-type cells is inhibited by Raf-1 in a kinase-independent manner. In contrast, activation of ERK is not affected by Raf-1 ablation (Ehrenreiter et al., 2005). Here, we use the Δ/Δ^{ep} animals as well as a mouse strain allowing tamoxifen-inducible, epidermis-restricted Raf-1 ablation (Indra et al., 1999) to investigate the role of Raf-1 in Ras-driven epidermis carcinogenesis.

RESULTS

Raf-1 Ablation Prevents Ras-Dependent Tumor Formation

We assessed the role of Raf-1 in Ras-dependent tumor formation by combining epidermis-restricted Raf-1 ablation (Δ^{ep}, deleted in epidermis [Ehrenreiter et al., 2005]) with the DMBA/TPA chemical carcinogenesis protocol. In wild-type (*f/f*) mice, this protocol resulted in the development of visible tumors within 6 weeks of application of DMBA/TPA on dorsal skin, with a 50% penetrance by week 13. In heterozygous ($\Delta/+^{ep}$) littermates tumor development was severely retarded, starting at week 13 and reaching an incidence of 50% by week 17 (Figure 1B). In addition, the average number of tumors/mouse was significantly reduced in the $\Delta/+^{ep}$ group (two to three tumors/mouse compared with

Ras Addicted to Raf-1

five to six tumors/mouse in the wild-type cohort; Figures 1A and 1C). The *Δ/+^ep* tumors were much smaller than the *f/f* tumors and most of them did not reach a volume of >5 mm^3 at week 20 (Figures 1A and 1D). Tumor development was completely blocked in homozygous *Δ/Δ^ep* mice (Figures 1A and 1B). Histological examination at week 20 did not reveal any major differences in *f/f* and *Δ/+^ep* tumors of similar size, all of which were papillomas with a clear cut border, projecting above the surrounding tissue (Figure 1E). The numbers of proliferating Ki67+ cells were slightly but significantly reduced in *Δ/+^ep* tumors (Figure 1F). Few apoptotic cells could be visualized by TUNEL staining and their numbers were indistinguishable in *f/f* and *Δ/+^ep* tumors of the same size (see Figure S4A available online). Thus, Raf-1 gene dosage is a critical determinant in DMBA-induced tumor initiation, as shown by the reduced numbers and delayed appearance of tumors in the heterozygotes, and contributes to TPA-induced tumor promotion, as reflected by the decreased proliferative index observed in *Δ/+^ep* tumors.

Typically, DMBA induces tumor initiation by causing an activating mutation in codon 61 of the *ras* gene (Quintanilla et al., 1986). Therefore, the data above strongly suggest a requirement for Raf-1 in Ras-driven skin tumorigenesis. In the majority of human SCCs, however, endogenous Ras signaling is activated in the absence of such activating mutations (Dajee et al., 2003). To mimic this condition, we used a genetic model in which an activated form of the Ras-GEF SOS is expressed under the control of the K5 promoter in basal keratinocytes and in the outer root sheath of the hair follicles, resulting in the synchronous formation of fast-growing tumors, mostly papillomas (Sibilia et al., 2000). These tumors grow predominantly on the tail, behind the ears, and at sites subjected to scratching and biting. This distribution has also been observed in transgenic animals expressing activated Ha-Ras from a keratin 10 (K10) promoter and suggests that minor injuries promote tumor development (Bailleul et al., 1990). In the 129 genetic background, 100% of *f/f* and *Δ/+^ep* mice developed visible tumors by the first and second month of life, respectively (Figure 2A). As already noted for the chemical carcinogenesis protocol, *Δ/+^ep* tumors were much smaller than those arising in *f/f* mice (Figure 2B). The *Δ/Δ^ep* mice did not develop any tumors until 6 months of age (Figure 2A); thereafter, visible tumors started growing very slowly in 20% of the mice. These tumors were identified as escapers in which Raf-1 deletion was incomplete and were not analyzed further (Figure S1).

We next analyzed small, medium, and large *f/f* and *Δ/+^ep* tumors (from 0.3–1.2 cm diameter). The gross histological appearance of size-matched tumors was similar (Figure 2C); however, the cells in the *Δ/+^ep* lesions were smaller in size than *f/f* tumor cells and showed a higher degree of compaction (Figure 2C). Loss of an orderly basal layer, keratin pearls, and clusters or strands of K5$^+$ tumor cells in the dermis, as well as microinvasions, were observed in the large *f/f* (Figures 2C, 2D, and 3D) and occasionally in the *Δ/+^ep* lesions (data not shown). *Δ/+^ep* tumors featured less BrdU$^+$ proliferating cells, which were confined to the basal layer (Figure 2E and data not shown). In addition, whereas ≤25% of the cells in wild-type tumors expressed the differentiation marker K10 (Grade 3–4 according to Broder's classification), *Δ/+^ep* papillomas contained around ≥75% K10$^+$ cells (Grade 1; Figure 2F). Conversely, the expression of integrin β1, enriched in epidermal stem cells and correlated with the inhi-

bition of keratinocyte differentiation (Levy et al., 2000), was strongly increased in basal and suprabasal cells in *f/f* tumors, but much less so in *Δ/+^ep* papillomas (Figure 2G). *K5-SOS-F;Δ/ Δ^ep* epidermis contained only sporadic integrin β1+ cells. An increase in well-differentiated tumors could also be observed in the DMBA/TPA model (5% of wild-type tumors were well differentiated versus 36% *Δ/+^ep* papillomas; Figure S2A). The number of apoptotic cells was very low and indistinguishable in *f/f* and *Δ/+^ep* *K5-SOS-F+* tumors (Figure S4B).

Raf-1 Is Necessary for the Maintenance of *K5-SOS-F*-Induced Tumors

To determine whether Raf-1 was required for the maintenance of the SOS-F-induced tumors, we used *K5-SOS-F;K5-Cre-ER(T);c-raf-1^f/f* mice, which express the Cre recombinase as a fusion protein with the mutated ligand-binding domain of the human estrogen receptor (ER). Binding to 4-hydroxy-tamoxifen (TX), but not to estradiol, stimulates Cre activity (Indra et al., 1999). To induce *c-raf-1* ablation, we injected tumor-bearing *K5-SOS-F;K5-Cre-ER(T);c-raf-1^f/f* and their *K5-SOS-F;c-raf-1^f/f* littermates with TX (1 mg/day intraperitoneally, five consecutive injections). At the time of injection (P26–P41), the diameter of the lesions was between 0.5 and 0.75 cm. *f/f* tumors continued to grow and doubled or even tripled their size within 2 weeks from the last TX injection. In contrast, the lesions from conditional knockout mice (*Δ/Δ^epTX*) decreased in size and became covered in white squames (Figures 3A and 3B), which eventually disappeared (by week 7–8). Most lesions resolved completely and never recurred throughout the life span of the animals. In some cases, the bulk of the tumor was dramatically reduced, but persisting small lesions became evident by week 6 (Figure S3A). The *f/f* allele was not completely converted to *Δ/Δ* in these lesions, indicating that their persistence was due to incomplete recombination (Figure S3B). Importantly, tumor regression was not observed in mice harboring *K5-SOS-F;K5-Cre-ER(T)* (B.M. Lichtenberger and M.S., unpublished data). The regression of the *Δ/Δ^epTX* tumors was accompanied by an increase in cell compaction and tissue stratification (Figure 3D) and by a striking decrease in the number of proliferating and integrin β1+ cells (Figures 3C and 3E), which became absolutely restricted to the basal level (Figure 3E and data not shown). Conversely, suprabasal K10 staining was restored to the *Δ/Δ^epTX* tumors (Figure 3F). The regressing tumors contained hardly any apoptotic cells (Figure S4C). Together, the data indicate that the regression of Raf-1 knockout tumors is due to a massive increase in the terminal differentiation of the tumor cells (Figure 3F), ultimately shed by the epidermis as squames, which, in combination with the sharp decrease in cell proliferation (Figure 3C), results in net cell loss.

Raf-1 Ablation Promotes the Differentiation of *K5-SOS-F+* Keratinocytes In Vitro

The increased differentiation induced by the chronic or acute ablation of Raf-1 in tumors could be a default program entered by cells with a reduced proliferative ability; alternatively, an intrinsic propensity of the cells to differentiate could bring about the decrease in proliferation. To discriminate between these two possibilities, we isolated primary keratinocytes from *K5-SOS-F+* and *K5-SOS-F−* mice to test their ability to proliferate and
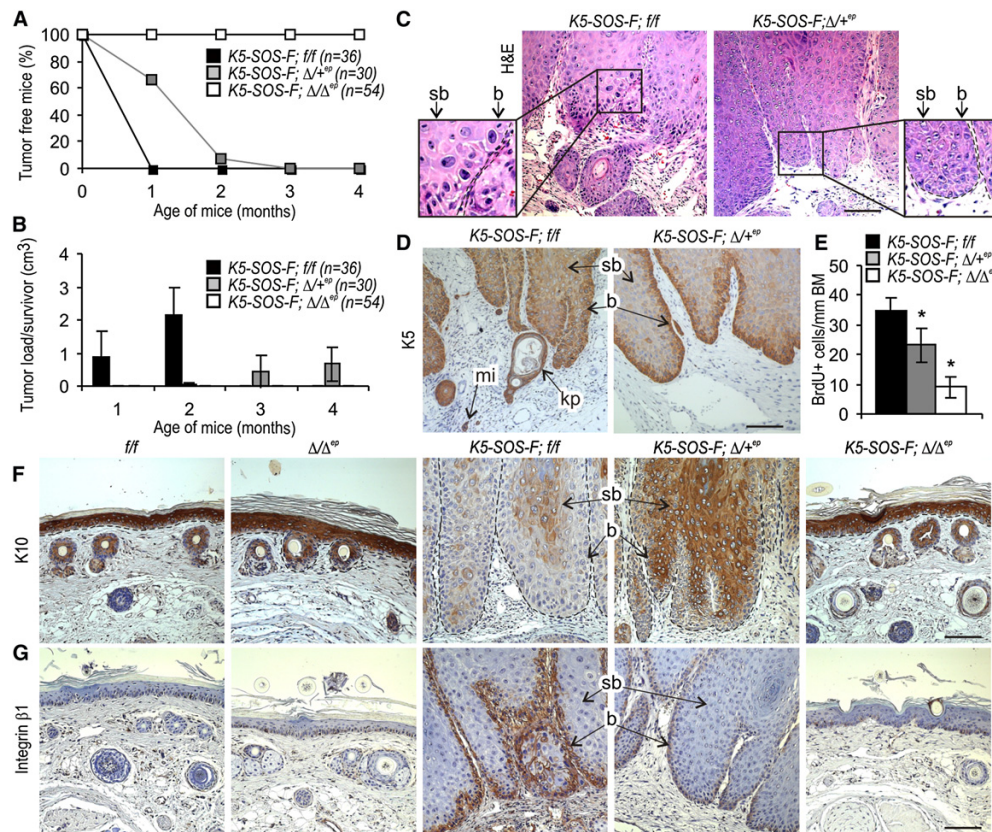
Figure 2. Raf-1 Ablation in Keratinocytes Prevents Tumor Formation and Tumor Progression in *K5-SOS-F+* Mice

(A and B) Tumor incidence and load in *K5-SOS-F;f/f*, *K5-SOS-F;Δ/+^{ep}* and *K5-SOS-F;Δ/Δ^{ep}* animals.

(C and D) Histochemical and immunohistochemical analysis of size-matched *f/f* and *Δ/+^{ep}* tumor sections stained with hematoxylin and eosin or with a K5 antibody for the basal layer visualization.

(E) Decreased mitotic index (BrdU+ cells/mm BM) in *K5-SOS-F;Δ/+^{ep}* versus *f/f* tumors. The mitotic index of *K5-SOS-F;Δ/Δ^{ep}* epidermis is indistinguishable from that of *f/f* epidermis and is shown as a reference. The plot shows the results of the analysis of at least three animals/genotype.

(F and G) Increased differentiation in *K5-SOS-F;Δ/+^{ep}* compared to *K5-SOS-F;f/f* tumors. Differentiation is shown as K10 positive layers (F). Undifferentiated integrin β1+ cells in *K5-SOS-F;Δ/+^{ep}* are reduced in number and confined to the basal layer compared to *K5-SOS-F;f/f* tumor sections (G). *K5-SOS-F;Δ/+^{ep}* epidermis is indistinguishable from that of *f/f* or *Δ/Δ* epidermis. Positive cells are stained in brown. The scale bar represents 100 μm. b, basal layer; sb, suprabasal layer; mi, microinvasions; kp, keratin pearls. The dashed line indicates the border between epidermis and dermis. Error bars indicate SD of the mean. *p < 0.01 according to Student's t test.

differentiate in vitro. To avoid measuring a combination of effects on proliferation, differentiation, and apoptosis, the impact of Raf-1 ablation on the proliferative ability of keratinocytes in vitro was determined by assessing the percentage of cells incorporating BrdU. Only few *K5-SOS-F+* keratinocytes, *f/f* or *Δ/Δ^{ep}* of the 129/Sv background, proliferated in complete media (Figure 4A), possibly because of oncogenic stress, which induces growth arrest in premalignant cells (Collado et al., 2005). Raf-1 ablation had no effect on the percentage of proliferating keratinocytes cultured in complete media (Figure 4A), which was reduced by chemical inhibition of the ERK but not of the Rok pathway (Figure 4A). We next induced keratinocyte differentiation by exposing cells of different genotypes to high concentrations of CaCl$_2$, a method widely used to recapitulate the biochemical events accompanying the transition from the basal to the upper

epidermal layers during differentiation in vivo. Differentiation was measured as the number of involucrin+ cells developing in the presence of 1.2 mM CaCl$_2$ (Figures 4B and 4C). *f/f* and *Δ/Δ^{ep}* keratinocytes differentiated efficiently under these conditions, whereas *K5-SOS-F+;f/f* keratinocytes failed to do so (Figure 4C; Sibilia et al., 2000). In contrast, *K5-SOS-F* expression did not prevent differentiation of Raf-1-deficient keratinocytes (Figure 4C). Thus, Raf-1 ablation counteracts the *K5-SOS-F*-mediated differentiation block in vivo and in vitro.

Raf-1 Is Required to Restrain Rok Signaling in *K5-SOS-F+* Cells and Epidermis

To gain insight into the mechanisms underlying the increased differentiation of *K5-SOS-F+;Δ/Δ^{ep}* cells, we monitored the activation of two signaling pathways connected to Ras/Raf and
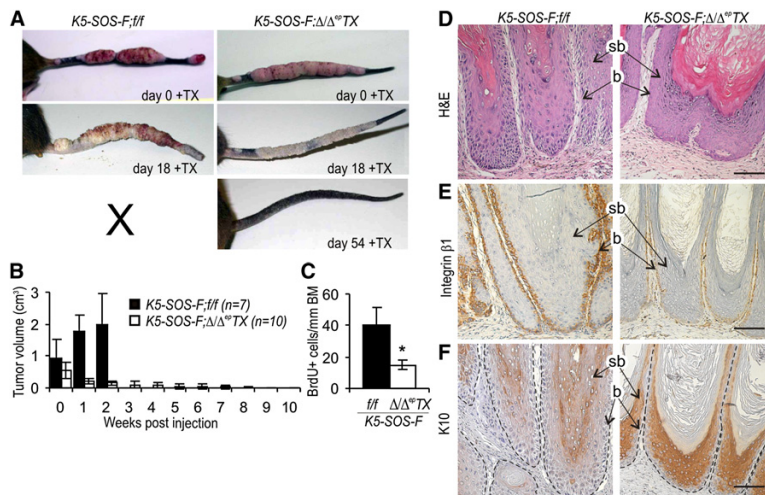
Ras Addicted to Raf-1

Figure 3. K5-SOS-F Tumors Are Addicted to Raf-1

Tumor-bearing *K5-SOS-F;Δ/Δ^{ep}TX* mice and *K5-SOS-F;f/f* were injected with tamoxifen for five consecutive days and tumor regression was monitored.

(A) Representative pictures of a *K5-SOS-F;f/f* and *K5-SOS-F;Δ/Δ^{ep}TX* mouse after tamoxifen treatment. Note the thick layer of squames on the surface of the regressing tumor. (X) Control mice had to be culled because of the increasing tumor load.

(B) Quantification of tumor regression.

(C) Decreased cell proliferation (BrdU+ cells/mm of BM) in *K5-SOS-F;Δ/Δ^{ep}TX* tumors 7 days after tamoxifen injection. Error bars indicate SD of the mean. *p < 0.01 according to Student's t test.

(D–F) Sections of *K5-SOS-F; f/f* and of *Δ/Δ^{ep}TX* tumors 7 days after tamoxifen injection. Note the thick layer of squames in the regressing tumors. (D) shows hematoxylin and eosin staining. Note the increased cell and tissue compaction in *K5-SOS-F;Δ/Δ^{ep}TX* tumors. (E) shows decreased numbers of integrin β1+ cells, and (F) shows increased differentiation (K10 expression) in *K5-SOS-F;Δ/Δ^{ep}TX* tumors compared to *K5-SOS-F;f/f* tumors. Positive cells are stained in brown. The scale bar represents 100 μm.

implicated in keratinocyte differentiation, namely ERK (Schmidt et al., 2000; Wakamatsu et al., 2007) and Rok (McMullan et al., 2003; Vaezi et al., 2002). Treatment of differentiating keratinocytes with chemical inhibitors of these pathways efficiently blocked differentiation of cells of all four genotypes (Figure 4C). Rok inhibition concomitantly increased proliferation in differentiating cultures, whereas MEK/ERK inhibition completely abrogated it (Figure 4D). Both pathways were activated during differentiation: ERK phosphorylation, however, increased only slightly and was essentially indistinguishable in *f/f* and *Δ/Δ^{ep}* cells (Figure 4E, left panel). *K5-SOS-F* expression resulted in a strong increase in ERK phosphorylation that was not affected by the lack of Raf-1 (Figure 4E, right panel). Activation of the Rok pathway was measured by the phosphorylation of the downstream targets myosin light chain 2 (MLC2) and cofilin. MLC2 phosphorylation is required for actin/myosin motor activation and enhances cell contractility (Zhao and Manser, 2005); cofilin is an actin-severing protein whose phosphorylation, mediated by the Rok effector LIMK, promotes actin polymerization. Cofilin phosphorylation increases during the differentiation of cultured human keratinocytes and has been implicated in the compaction of the granular layer of human epidermis in organotypic cultures (Honma et al., 2006). Phosphorylation of MLC2 and (more slightly) of cofilin increased during differentiation of wild-type and Raf-1-deficient keratinocytes, in which it was already present before the induction of differentiation (Figure 4E, left panel). *K5-SOS-F* expression suppressed phosphorylation, particularly of cofilin, but suppression was less severe in *Δ/Δ^{ep}* keratinocytes (Figure 4E, right panel). In addition, consistent with previous reports on the negative regulation of Rok by ERK (Mavria et al., 2006), the phosphorylation of Rok downstream targets was increased by treating the cells with a MEK/ERK inhibitor. In contrast, the Rok inhibitor reduced the phosphorylation of MLC2 and cofilin without affecting ERK phosphorylation (Figure 4E).

Thus, the increased differentiation of Raf-1-deficient keratinocytes in vitro was paralleled by the activation of Rok downstream targets, but not of the ERK pathway. To investigate whether this was the case in vivo, we performed immunohistochemistry on tumor sections from *K5-SOS-F+ f/f*, *Δ/+^{ep}* or *Δ/Δ^{ep}* mice. We found that ERK activation was if anything increased in *Δ/+^{ep}* tumors and in the lesions regressing after Raf-1 ablation. In both cases, phospho-ERK was localized mainly in the terminally differentiating cells of the suprabasal layers, in contrast to the *f/f* tumors in which phospho-ERK staining was observed in the basal layer (Figures 5A and 5B). The pattern of ERK phosphorylation in *K5-SOS-F;Δ/Δ^{ep}* epidermis was indistinguishable from that of *f/f* or *Δ/Δ^{ep}* epidermis not expressing the *K5-SOS-F* transgene (Figure 5A).

In contrast to ERK, cofilin phosphorylation was clearly suppressed in the *f/f* tumors compared to *Δ/+^{ep}* tumors and to *K5-SOS-F;Δ/Δ^{ep}* epidermis (Figure 5C). A similar increase in cofilin phosphorylation was noted in *Δ/+^{ep}* tumors induced by DMBA/TPA (Figure S2B). More importantly, cofilin phosphorylation was strongly induced in the regressing *Δ/Δ^{ep}TX* tumors, concomitantly with the cell compaction and with the massive differentiation caused by Raf-1 ablation (Figure 5D). These results indicate that the expression of the *K5-SOS-F* transgene restrains Rok signaling in keratinocytes in culture and in the epidermis and that *K5-SOS-F*-mediated Rok inhibition is disabled by chronic as well as acute Raf-1 ablation.

Raf-1 physically interacts with Rok-α (Ehrenreiter et al., 2005). To monitor whether K5-SOS-F increased Raf-1:Rok-α interaction in vivo, we prepared crude epidermal lysates and monitored complex formation by assessing the presence of Raf-1 in endogenous Rok-α immunoprecipitates. The crude *Δ/Δ^{ep}* lysates contained a residual Raf-1 band (Figure 5E, left panel), which was absent in pure keratinocyte cultures (Figure 4E) and therefore results from contamination by other tissues, most likely dermis
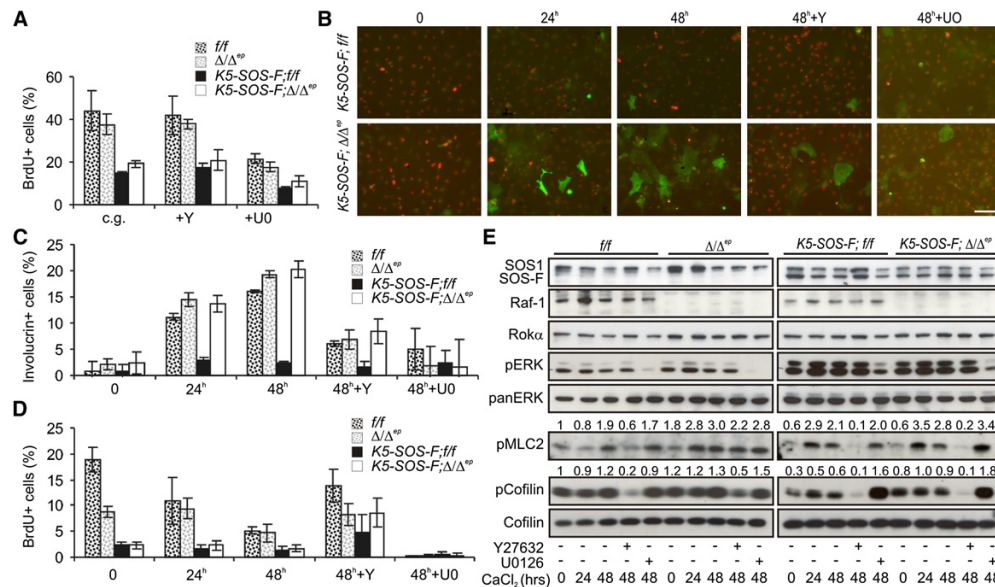
Figure 4. Raf-1 Ablation Enforces the Differentiation of *K5-SOS-F+* Keratinocytes by a Mechanism Involving Rok Activation

(A) Proliferation of primary keratinocytes isolated from *f/f*, *Δ/Δ^{ep}*, *K5-SOS-F;f/f*, and *K5-SOS-F;Δ/Δ^{ep}* mice. Cells of all genotypes were cultured in complete growth medium (c.g., continuously growing). Y-27632 (10 μM) or U0126 (10 μM) were added for inhibition of the Rok and the MEK/ERK pathway, respectively. The percentage of proliferating cells was determined by BrdU incorporation.

(B–D) Raf-1 ablation promotes the differentiation of *K5-SOS-F+* keratinocytes. The percentage of differentiating or proliferating keratinocytes was determined in cultures exposed to 1.2 mM CaCl₂ for the indicated time periods in the absence and presence of the inhibitors Y-27632 and U0126. Differentiating cells were defined by the expression of involucrin+ (B and C; green; the scale bar represents 100 μm) and proliferating cells by BrdU+ incorporation (D). The plots in (A), (C), and (D) show a quantification of the results obtained in three different experiments. Error bars indicate SD of the mean.

(E) Increased Rok pathway, but not ERK activation, in *Δ/Δ^{ep}* keratinocytes. Immunoblot analysis of lysates prepared from keratinocytes differentiating in the presence or absence of the Rok or of the MEK/ERK inhibitor is shown. The figures on top of the pMLC2 and pCofilin panels represent a quantification of the intensity of the bands, normalized to loading controls. The value corresponding to wild-type keratinocytes at time point 0 was arbitrarily defined as 1.

and vessels. In *K5-SOS-F+;f/f* lysates, the Raf-1 band was stronger and showed a slower migration that has been correlated with Raf-1 phosphorylation and activation (Figure 5E, left panel). Since the *K5-SOS-F+;f/f* mice already bore tumors of different sizes, the data indicate that Raf-1 increased in tumors, in line with previous observations in human SCC (Riva et al., 1995; Leicht et al., 2007), and that SOS-F expression drove Raf-1 hyperphosphorylation. A Raf-1:Rok-α complex was detectable only in *K5-SOS-F+;f/f* lysates, and its amount was proportional to Raf-1 expression and to the size of the tumor affecting the epidermis (Figure 5E, right panel). Importantly, Rok-α kinase activity was significantly higher in crude lysates of *K5-SOS-F+;Δ/Δ^{ep}* epidermis than in *K5-SOS-F+;f/f* lysates (Figure 5F).

Together, the data indicate that inhibition of Rok signaling by Raf-1 is one of the strategies by which SOS and active Ras inhibit keratinocyte differentiation.

Raf-1 Is Required for STAT3 Activation and Myc Expression in *K5-SOS-F* Tumors

Besides its effects on the actin cytoskeleton, active (unphosphorylated) cofilin enhances the phosphorylation of the transcription factor STAT3 and the expression of its target gene c-*myc* in human psoriatic epidermis (Honma et al., 2006). This mechanism had never been associated with tumorigenesis.

Both STAT3 phosphorylation and Myc expression, however, are increased in human SCC (Chen et al., 2008; Seethala et al., 2008; Watt et al., 2008) and promote the development of epidermal hyperplasia and/or malignant tumors in mice (Chan et al., 2007, 2004; Sano et al., 1999; Watt et al., 2008). Therefore, we next determined whether Raf-1 ablation had an impact on STAT3 phosphorylation and Myc expression. pSTAT3+ and Myc+ cells were present at very low levels in *f/f* and *Δ/+^{ep}* epidermis (data not shown) and in *K5-SOS-F+;Δ/Δ^{ep}* epidermis, in which they were essentially confined to the basal layer (Figure 6). A substantial increase in pSTAT3+ and Myc+ cells was detectable in the basal and suprabasal layers of *K5-SOS-F;f/f* and *Δ/+^{ep}* tumors, although the number of pSTAT3+ and Myc+ cells remained significantly lower in the latter (Figure 6A). More importantly, acute ablation of Raf-1 in established tumors caused a dramatic decrease in both STAT3 phosphorylation and Myc expression, and suprabasal staining was no longer observed (Figure 6B).

Topical Application of a Rok Inhibitor Induces Proliferation and Dedifferentiation in *K5-SOS-F;Δ/Δ^{ep}* Epidermis

The data above indicate that Raf-1 ablation limits cofilin activation, STAT3 phosphorylation, and Myc expression during
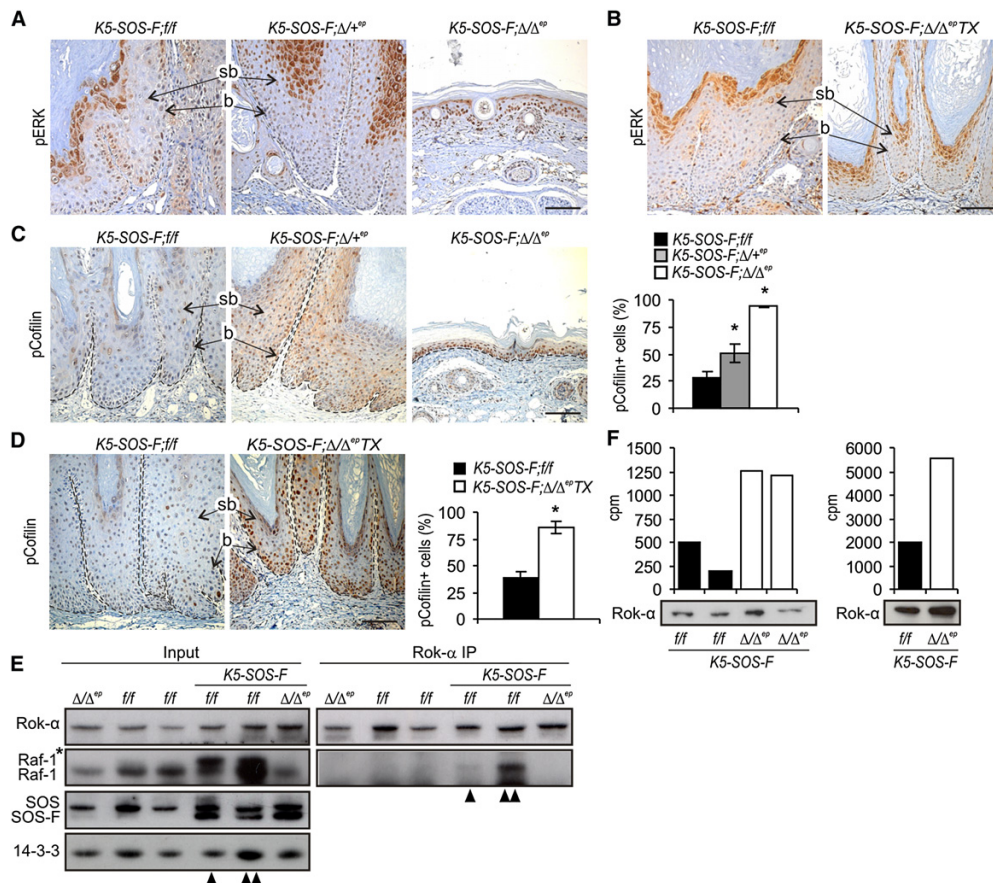
Figure 5. Chronic and Acute Raf-1 Ablation Induces the Phosphorylation of the Rok Downstream Target Cofilin in *K5-SOS-F* Tumors

(A and B) Raf-1 ablation does not affect ERK phosphorylation in *K5-SOS-F* tumors.

(C) Raf-1 ablation increases the phosphorylation (and inactivation) of cofilin in *K5-SOS-F;Δ/+ep* versus *K5-SOS-F;f/f* tumors. *K5-SOS-F;Δ/Δep* epidermis is indistinguishable from that of *f/f* or *Δ/Δep* epidermis not expressing the *K5-SOS-F* transgene and is shown as a reference.

(D) Regressing *K5-SOS-F;Δ/Δep*TX tumors contain high amounts of pCofilin+ cells (day 7 after tamoxifen treatment). ERK and cofilin phosphorylation were determined by immunohistochemistry of skin and tumor sections of the different genotypes as indicated. Positive cells are stained in brown. The scale bar represents 100 μm. The plots represent the results of the analysis of at least three animals/genotype, evaluating ≥600 cells/mouse.

(E) Raf-1 interacts with Rok-α in *K5-SOS-F*+ epidermis. Rok-α was immunoprecipitated from crude epidermis lysates. The presence of Raf-1 and Rok-α was detected by immunoblotting in whole-cell lysates (Input) and Rok-α immunoprecipitates (IP). In addition, SOS and SOS-F expression were determined in the crude lysates. 14-3-3 is shown as a loading control. Note that in *K5-SOS-F*+ lysates Raf-1 is present as a doublet; the slower migrating form is associated with phosphorylation and possibly activation. The Raf-1 band in the *Δ/Δep* lysates is probably due to contamination by other tissues (dermis or vessels). Arrowheads denote tumor-bearing mice. Tumor volume: 6, 98 mm³; 66, 236 mm³. Control tail volume: 78.5 mm³.

(F) Increased Rok-α activity in crude lysates of *K-SOS-F;Δ/Δep* epidermis. The kinase activity of Rok-α immunoprecipitates from 200 μg (left panel) or 400 μg of crude epidermis lysates from *K-SOS-F*+ *f/f* or *Δ/Δep* mice was assessed using the long S6 peptide as a substrate. The amount of Rok-α in the immunoprecipitates is shown below the graphs. Error bars indicate SD of the mean. *p < 0.01 according to Student's t test.

Ras-induced tumor development. This is probably due to Rok-α hyperactivation. To determine whether Rok-α hyperactivation limits activation of the cofilin/STAT3/Myc pathway and tumor development in vivo, we applied the Rok inhibitor Y-27632 on the right ear of *K5-SOS-F;Δ/+ep* or *K5-SOS-F;Δ/Δep* mice. The left ear was treated with DMSO as a vehicle and as skin permeation enhancer. We chose the ears for this treatment because the epidermis is thinner than that of other body sites (Porter et al., 1998). A thinner epidermis increases the chances of the inhibitor to reach the basal layer and therefore the target cells.

DMSO itself caused skin irritation and some proliferation (3- to 4-fold increase) of the epidermis, as previously described (Lashmar et al., 1989). Y-27632, however, induced a significant increase in the proliferation of *K5-SOS-F;Δ/+ep* and *K5-SOS-F;Δ/Δep* epidermis (Figure 7A), measured both as epidermal thickness and as a percentage of BrdU+ cells. Conversely, differentiation, defined by the percentage of K10+ epidermal layers, was strongly reduced (Figure 7B). The inhibitor also caused a reduction in the percentage of pCofilin+ cells as well as a decrease in the intensity of pCofilin staining. The latter aspect
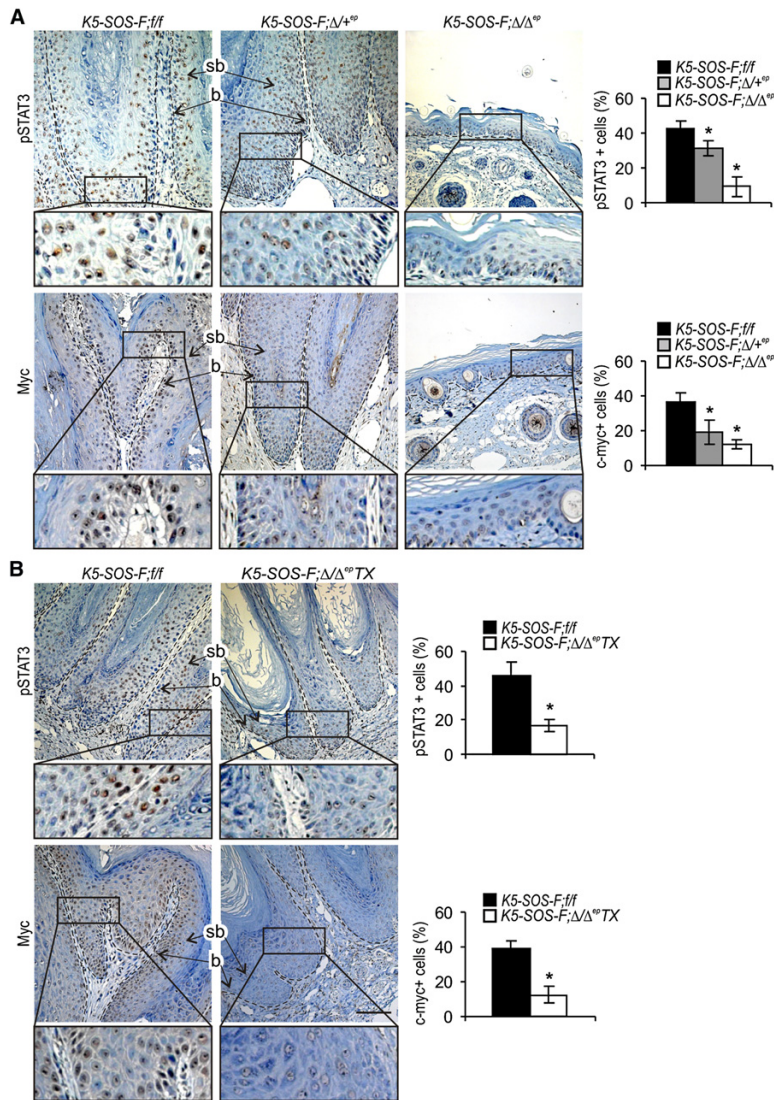
Figure 6. Chronic and Acute Raf-1 Ablation Decreases the Phosphorylation of STAT3 and the Expression of Myc in *K5-SOS-F* Tumors

(A) Raf-1 ablation decreases the phosphorylation of STAT3 (upper panel) and the expression of the STAT3 target Myc (lower panel) in *K5-SOS-F;Δ/+ep* versus *K5-SOS-F;f/f* tumors. *K5-SOS-F;Δ/Δep* epidermis is indistinguishable from epidermis not expressing the *K5-SOS-F* transgene. The scale bar represents 100 μm.

(B) STAT3 phosphorylation (upper panel) and Myc expression (lower panel) are dramatically reduced in regressing *K5-SOS-F;Δ/ΔepTX* tumors (day 7 after tamoxifen treatment). STAT3 phosphorylation and Myc expression were determined by immunohistochemistry of skin and tumor sections of the different genotypes as indicated. Positive cells are stained in brown. The scale bar represents 100 μm. The plots represent the results of the analysis of at least three animals/genotype, evaluating ≥600 cells/mouse. Error bars indicate SD of the mean. *p < 0.01 according to Student's t tests.

Together, the data link Raf-1 ablation with the activation of Rok, the inhibition of the cofilin/STAT3/Myc pathway, and the increased differentiation of Ras-induced tumors in vivo (Figure 7F).

DISCUSSION

The data above prove that in the mouse Raf-1 is required for the establishment and maintenance of skin tumors driven by the activation of Ras, achieved either by somatic mutation (DMBA/TPA model) or, more similar to the situation in human SCC, by the constitutive activation of the endogenous Ras pathway. Raf-1 ablation completely precludes tumor formation in both models and Raf-1 heterozygosity reduces it. More importantly, Raf-1 ablation causes the complete regression of established tumors. In contrast to the results obtained by interfering with other Ras effectors (Gonzalez-Garcia et al., 2005; Gupta et al., 2007; Malliri et al., 2002), the requirement for Raf-1 in Ras-driven carcinogenesis is absolute and it extends to tumor maintenance.

Raf-1 is also the first Ras effector for which a cell-autonomous requirement has been clearly demonstrated by the concomitant activation of Ras and ablation of Raf-1 in the same cell, the K5+ keratinocyte, in the context of an otherwise intact host. This does not, per se, rule out the possibility that a defective interaction of the Raf-1-deficient tumor cells with the stroma may contribute to the block of tumor development and maintenance, as we have recently described for B-Raf-deficient insulinomas (Sobczak et al., 2008). Such defects, however, could not explain the lack of primary tumor development observed in the *Δ/Δep* epidermis

could not be easily quantified and taken into account in the plot (Figure 7C), which therefore understates the contribution of Rok to cofilin phosphorylation in vivo. Both STAT3 phosphorylation and Myc expression were strongly increased in the inhibitor-treated epidermis (Figures 7D and 7E), indicating that the cofilin/STAT3/Myc pathway is inhibited by Rok during the dedifferentiation of the keratinocytes required for tumor development. The *Δ/Δep* animals were more resistant to the Rok inhibitor than the *Δ/+ep* mice and had to be treated for a longer time period (6 weeks instead of 2) to achieve similar results. This is consistent with the idea that in *Δ/+ep* epidermis the residual inhibition of Rok by Raf-1 synergizes with Y-27632 to allow dedifferentiation/proliferation, whereas the complete absence of Raf-1 in the *Δ/Δep* epidermis renders it less permissive to the action of the inhibitor.

or the precipitous differentiation that follows Raf-1 ablation in established tumors. This accelerated differentiation can also be observed in cultured Raf-1-deficient keratinocytes, confirming the cell-autonomous nature of the defect (Figure 4).

In contrast to other Ras downstream targets such as RalGDS or PI-3K, whose main role is to support cell survival (Gonzalez-Garcia et al., 2005; Gupta et al., 2007), Raf-1 promotes tumor development by blocking differentiation. Surprisingly, this block in differentiation does not correlate with changes in the best-studied Raf downstream pathway MEK/ERK, whose activation was unchanged in Δ/Δ^{ep} epidermis and cultured keratinocytes. Instead, the Raf-1-dependent, SOS-F-induced differentiation block correlates with the reduced activation of Rok downstream targets, both in vivo in tumors and in keratinocytes differentiating in culture (Figures 4–6). In vivo treatment with a chemical Rok inhibitor induced dedifferentiation and increased proliferation in $K5\text{-}SOS\text{-}F;\Delta/\Delta^{ep}$ epidermis (Figure 7), establishing a causal relationship between Rok inhibition by Raf-1 and the SOS-F-induced differentiation block. Rok inhibition reduced cofilin phosphorylation and increased STAT3 phosphorylation and Myc expression. Activation of the cofilin/STAT3/Myc pathway had been previously reported in hyperproliferating psoriatic epidermis, in which it blocks cell compaction (Honma et al., 2006), but it had never been implicated in tumorigenesis. Our data show that activation of this pathway correlates with a block in keratinocyte differentiation and increased proliferation in Ras-induced tumors in vivo, but we do not interpret them to mean that the inhibition of the cofilin/STAT3/Myc pathway is the only relevant event downstream of Rok in epidermal carcinogenesis; other targets of Rok not tested here, like the transcription factor NF-κB, may be equally relevant in this context (Dajee et al., 2003; van Hogerlinden et al., 1999).

Together, the data support the hypothesis that Raf-1 is deployed by activated Ras to counteract the activity of Rok by direct binding as previously reported (Ehrenreiter et al., 2005). Consistent with this theory, the interaction between Raf-1 and Rok-α was increased, and Rok-α activity decreased, in the $K5\text{-}SOS\text{-}F+$ epidermis. Thus, one of the crucial functions of activated Ras in tumorigenesis is to prevent keratinocyte differentiation by restraining Rok activity, and Raf-1 is essential in this process (Figure 7F).

A role of Rok in cell differentiation and in the determination of cell fate has been recently emerging in other systems. Rok inhibition promotes the survival of human dissociated stem cells (Watanabe et al., 2007), perturbs epidermal stratification (Vaezi et al., 2002), and counteracts keratinocyte differentiation (Figures 4B and 7B; Honma et al., 2006; McMullan et al., 2003), whereas active Rok-α promotes it (McMullan et al., 2003). These observations are in line with a negative effect of Rok activation on tumorigenesis. In contrast, Rok is often upregulated in tumors (Sahai, 2005) and its activation can promote proliferation, invasion, and angiogenesis in xenograft models using human tumor cells (Croft et al., 2004; Itoh et al., 1999; Lefort et al., 2007). It is possible that the role of Rok in tumorigenesis is highly context dependent and that Rok activation may promote tumorigenesis when combined with mutations other than Ras activation. Alternatively, oncogenes are known to induce opposing signals, such as mitogenic and antiproliferative stress responses, the best known of which is senescence.

Indeed, some of the genes synergistically upregulated by the combination of mutant p53 and Ras proteins in tumor cell lines have recently been proven antitumorigenic (McMurray et al., 2008). It is conceivable that the Rok overexpression observed in tumors may have originally been part of such an antiproliferative program. Be that as it may, the fact that Rok inhibition allows dedifferentiation and proliferation of $SOS\text{-}F+$ epidermis, even in the absence of Raf-1, sounds a note of caution for the use of Rok inhibitors in the treatment of tumors, particularly of those relying on Ras activation.

Ras-driven skin tumors are addicted to Raf-1 in its role of endogenous Rok inhibitor, whereas Raf-1 signaling is not essential for epidermal development and homeostasis (Ehrenreiter et al., 2005). This discovery paves the way for the design of molecule-targeted therapies, which may include Raf-1 interference or allosteric inhibitors capable of disrupting the Raf-1:Rok complex. The treatment of cancer by inducing tumor cell differentiation in combination with chemotherapy has revolutionized the treatment of leukemia (Wang and Chen, 2008), but solid tumors have so far proven resistant. The complete differentiation induced by Raf-1 ablation in vivo raises hopes that combinations of Raf-1-targeted and conventional therapies may be successful at least in the treatment of Ras-driven skin epidermis tumors.

EXPERIMENTAL PROCEDURES

Mouse Strains, Genotyping, and Tumor Models

$c\text{-}raf\text{-}1\ \Delta/\Delta^{ep}$ or $\Delta/+^{ep}$, $K5\text{-}SOS\text{-}F$, and $K5\text{-}Cre\text{-}er(T)$ mice and the respective genotyping have been described (Ehrenreiter et al., 2005; Indra et al., 1999; Sibilia et al., 2000). All strains were maintained on a 129Sv background. For chemical two-stage carcinogenesis, mice were shaved 3 days before initiation with DMBA (25 μg/200μl acetone; Sigma) applied to the dorsal skin. Beginning 3 days later, TPA (6 μg/100μl acetone; Sigma) was applied twice per week for 20 weeks. Control mice were treated with acetone (Hsieh et al., 2006). Onset, number, and size of tumors were monitored at least twice a week. Tumors developing in Δ/Δ^{ep} mice or relapsing after TX treatment were genotyped isolating the DNA from paraffin section and extending the $c\text{-}raf\text{-}1$ PCR protocol by ten additional cycles to increase amplification. All animal experiments were performed in accordance with a protocol authorized by the Austrian Ministry of Science and Communications, following the approval by the national Ethical Committee for Animal Experimentation.

Histological Analysis

Hematoxylin/eosin staining and immunohistochemistry were performed on 3-μm-thick sections of 4% paraformaldehyde-fixed and paraffin-embedded tissues. Tail sections were decalcified by incubation of trimmed paraffin blocks for 10–15 min on paper towels soaked in 1 N HCl. Staining with the following antibodies was performed: α-BrdU (1:100; Zymed); α-c-myc (1:250; Milipore); α-E-cadherin (1:150; Santa Cruz); α-integrin β1 (1:50; BD Biosciences); α-K10 (1:500; BabCo); α-Ki67 (1:1000; Novocastra); α-pCofilin (Ser3, 1:50; Santa Cruz); α-pERK (Thr202/Tyr204, 1:50; Cell Signaling); and α-pSTAT3 (Tyr705, 1:100; Cell Signaling). For detection, we used the DAKO EnVision peroxidase system, followed by incubation with 0.01% diaminobenzidine (Sigma), in conjunction with avidin-biotinylated enzyme complex (Vector Laboratories) for biotinylated antibodies. Sections were counterstained with hematoxylin. BrdU incorporation was determined in mice injected with BrdU (12.5 mg/g body weight) 1 hr prior to tissue isolation.

Keratinocyte Isolation and Culture

Primary mouse keratinocytes were isolated from 18- to 21-day-old mice as previously described (Sibilia et al., 2000), plated at a density of $\sim 6 \times 10^6$ cells/100 mm plate, and cultured in MEM (Sigma) containing 1 μg/ml insulin (Sigma), 5 ng/ml EGF (Roche), 5 μg/ml transferrin (Sigma), 10 μM phosphoethanolamine (Sigma), 10 μM ethanolamine (Sigma), 0.36 μg/ml hydrocortisone
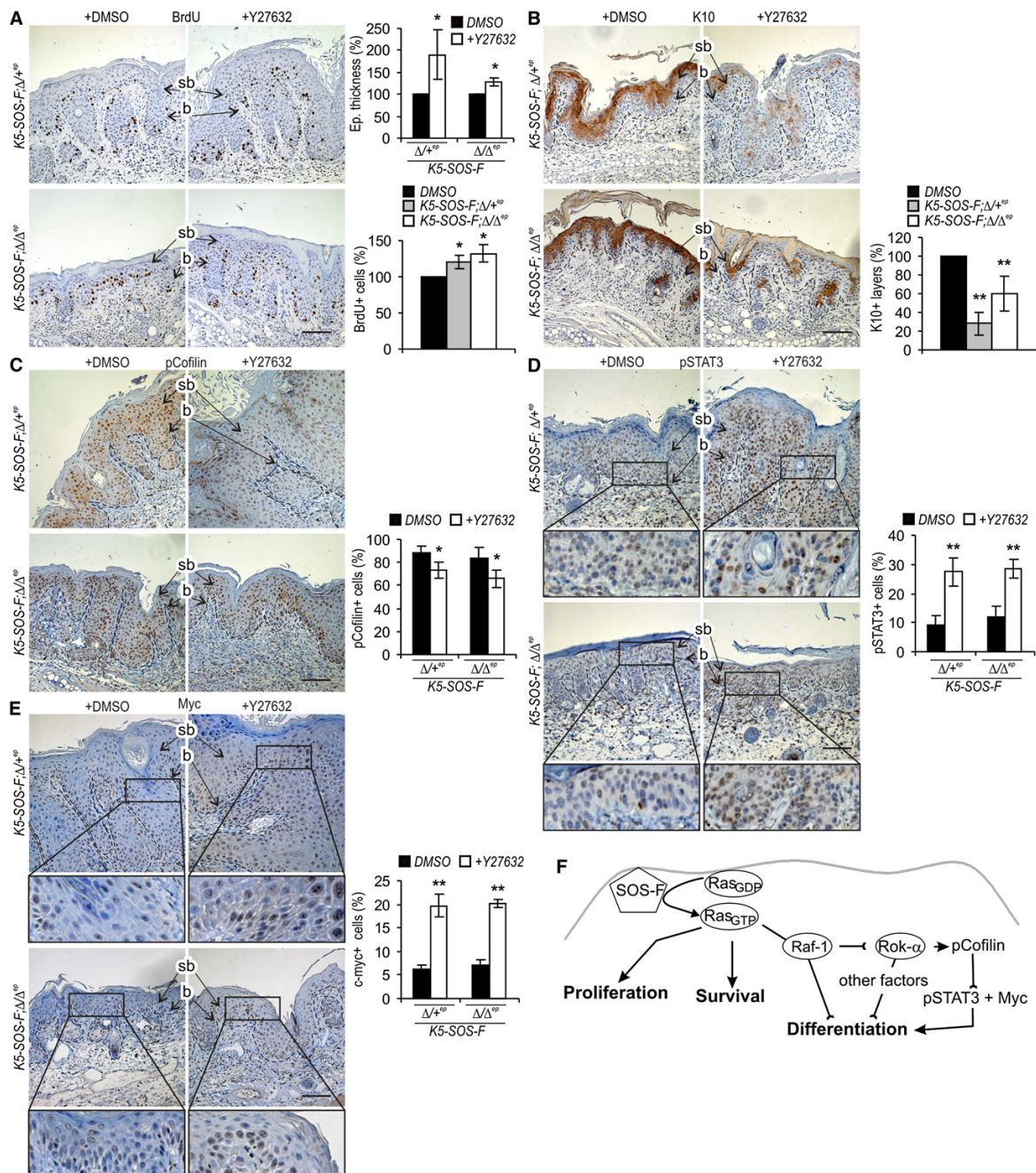
Figure 7. A Rok Inhibitor Induces Proliferation, Dedifferentiation, and Activation of the Cofilin/STAT3/Myc Pathway in the Epidermis of K5-SOS-F;Δ/+ᵉᵖ and K5-SOS-F;Δ/Δᵉᵖ Mice

Mice were treated with DMSO as a vehicle (left ear) or with Y-27632 (40 μM in DMSO; right ear) twice a day for 2 (*K5-SOS-F;Δ/+ᵉᵖ*) or 6 weeks (*K5-SOS-F;Δ/Δᵉᵖ*).
(A) Y-27632 causes proliferation of *K5-SOS-F;Δ/+ᵉᵖ* and *K5-SOS-F;Δ/Δᵉᵖ* epidermis. Proliferation was assessed both by counting the numbers of BrdU+ cells and by measuring epidermal thickness.
(B) Y-27632 causes dedifferentiation of *K5-SOS-F;Δ/+ᵉᵖ* and *K5-SOS-F;Δ/Δᵉᵖ* epidermis. Differentiation was assessed as the number of K10+ epidermal layers. In (A) and (B), proliferation and differentiation are expressed as a percentage of DMSO controls.

Cancer Cell

Ras Addicted to Raf-1

(Calbiochem), glutamine (Glutamax-I; Invitrogen), Pen/Strep (Invitrogen), and 6% chelated FCS (Chelex 100 Resin; Bio-Rad). The culture medium was exchanged every second day. For inducing differentiation, cells were transferred into starvation medium (containing only 2% chelated FCS and no growth factors) and treated with 1.2 mM $CaCl_2$ for different time periods. The Rok-α inhibitor Y-27632 (Calbiochem) and the MEK inhibitor U0126 (Cell Signaling) were added to the medium at a final concentration of 10 μM.

For the analysis of differentiation, cells were fixed in 4% PFA, permeabilized (0.2% Triton X-100), and blocked with 1% BSA before incubation with primary antibodies (α-Involucrin, 1:500; BabCo) followed by detection with the secondary FITC antibody (α-rabbit alexa 448 nm, 1:1500; Molecular Probes) and mounted with ProLong Antifade (Promega). Microscopical analysis was performed with an Axiovert 200 (Carl Zeiss MicroImaging, Inc.) equipped with an AxioCam. Images were acquired with the AxioVision Software (Carl Zeiss MicroImaging, Inc.) Proliferation was assessed by the In Situ Cell Proliferation Kit FLUOS (Roche) according to the manufacturer's recommendation. Cells were examined by light microscopy (Zeiss AxioVision; Carl Zeiss MicroImaging, Inc.), and the number of BrdU+ cells was quantified with the AutoMeasure software (Carl Zeiss MicroImaging, Inc.).

Rok-α Immunoprecipitation and Immunoprecipitation Kinase Assays

Crude epidermis lysates were prepared from the tail of 17-day-old mice. In brief, the skin was digested with trypsin to separate the epidermis from the dermis. The epidermis was placed in lysis buffer (200 mM Tris-HCl [pH 7.4], 2 mM EDTA, and 1% Triton X-100, supplemented with protease and phosphatase inhibitors) and homogenized with the PreCellys24 homogenizer (PeqLab). Rok-α immunoprecipitates were prepared from 1200 μg of protein with a Rok-α antibody (Upstate) and analyzed by immunoblotting or assayed for Rok-α kinase activity with the long S6 kinase (Upstate) as a substrate according to the manufacturer's instructions. The Rho kinase inhibitor Y-27632 (20 μM final) was used for assessment of Rok-α-specific kinase activity.

Immunoblotting

Membranes were probed with α-Cofilin (Abcam); α-panERK, α-Raf-1, α-Rok-α (Transduction Labs); α-panRasV12 (Calbiochem); α-pCofilin, α-pMLC2 (Santa Cruz); α-pERK (Cell Signaling); and α-SOS (BD Biosciences). After incubation with the appropriate secondary antibody, the antigens were visualized by ECL (Pierce).

Statistical Analysis

All values are expressed as mean (±SD) of at least three independent experiments. p values were calculated with the two-tailed Student's t test. A p value ≤ 0.05 is considered statistically significant.

SUPPLEMENTAL DATA

Supplemental Data contain four figures and can be found with this article online at http://www.cell.com/cancer-cell/supplemental/S1535-6108(09)00183-4.

REFERENCES

Bailleul, B., Surani, M.A., White, S., Barton, S.C., Brown, K., Blessing, M., Jorcano, J., and Balmain, A. (1990). Skin hyperkeratosis and papilloma formation in transgenic mice expressing a ras oncogene from a suprabasal keratin promoter. Cell *62*, 697–708.

Benitah, S.A., Frye, M., Glogauer, M., and Watt, F.M. (2005). Stem cell depletion through epidermal deletion of Rac1. Science *309*, 933–935.

Chan, K.S., Sano, S., Kiguchi, K., Anders, J., Komazawa, N., Takeda, J., and DiGiovanni, J. (2004). Disruption of Stat3 reveals a critical role in both the initiation and the promotion stages of epithelial carcinogenesis. J. Clin. Invest. *114*, 720–728.

Chan, K.S., Sano, S., Kataoka, K., Abel, E., Carbajal, S., Beltran, L., Clifford, J., Peavey, M., Shen, J., and DiGiovanni, J. (2007). Forced expression of a constitutively active form of Stat3 in mouse epidermis enhances malignant progression of skin tumors induced by two-stage carcinogenesis. Oncogene *27*, 1087–1094.

Chen, S.-Y., Takeuchi, S., Moroi, Y., Hayashida, S., Kido, M., Chen, S.-J., Tomoeda, H., Uenotsuchi, T., Tu, Y.-T., Furue, M., et al. (2008). Overexpression of phosphorylated-ATF2 and STAT3 in cutaneous squamous cell carcinoma, Bowen's disease and basal cell carcinoma. J. Dermatol. Sci. *51*, 210–215.

Collado, M., Gil, J., Efeyan, A., Guerra, C., Schuhmacher, A.J., Barradas, M., Benguria, A., Zaballos, A., Flores, J.M., Barbacid, M., et al. (2005). Tumour biology: senescence in premalignant tumours. Nature *436*, 642.

Croft, D.R., Sahai, E., Mavria, G., Li, S., Tsai, J., Lee, W.M., Marshall, C.J., and Olson, M.F. (2004). Conditional ROCK activation in vivo induces tumor cell dissemination and angiogenesis. Cancer Res. *64*, 8994–9001.

Dajee, M., Tarutani, M., Deng, H., Cai, T., and Khavari, P.A. (2002). Epidermal Ras blockade demonstrates spatially localized Ras promotion of proliferation and inhibition of differentiation. Oncogene *21*, 1527–1538.

Dajee, M., Lazarov, M., Zhang, J.Y., Cai, T., Green, C.L., Russell, A.J., Marinkovich, M.P., Tao, S., Lin, Q., Kubo, Y., et al. (2003). NF-kappaB blockade and oncogenic Ras trigger invasive human epidermal neoplasia. Nature *421*, 639–643.

Ehrenreiter, K., Piazzolla, D., Velamoor, V., Sobczak, I., Small, J.V., Takeda, J., Leung, T., and Baccarini, M. (2005). Raf-1 regulates Rho signaling and cell migration. J. Cell Biol. *168*, 955–964.

Gonzalez-Garcia, A., Pritchard, C.A., Paterson, H.F., Mavria, G., Stamp, G., and Marshall, C.J. (2005). RalGDS is required for tumor formation in a model of skin carcinogenesis. Cancer Cell *7*, 219–226.

Green, C.L., and Khavari, P.A. (2004). Targets for molecular therapy of skin cancer. Semin. Cancer Biol. *14*, 63–69.

Grossi, M., Hiou-Feige, A., Tommasi Di Vignano, A., Calautti, E., Ostano, P., Lee, S., Chiorino, G., and Dotto, G.P. (2005). Negative control of keratinocyte differentiation by Rho/CRIK signaling coupled with up-regulation of KyoT1/2 (FHL1) expression. Proc. Natl. Acad. Sci. USA *102*, 11313–11318.

Gupta, S., Ramjaun, A.R., Haiko, P., Wang, Y., Warne, P.H., Nicke, B., Nye, E., Stamp, G., Alitalo, K., and Downward, J. (2007). Binding of ras to

(C) Y-27632 reduces cofilin phosphorylation in *K5-SOS-F;Δ/+ᵉᵖ* and *K5-SOS-F;Δ/Δᵉᵖ* epidermis. Both the number of pCofilin+ cells and the intensity of the staining are reduced. Only the first parameter, however, can be reliably quantified and is represented by the plot on the right, which therefore understates the result. (D and E) Y-27632 increases STAT3 phosphorylation (D) and Myc expression (E) in *K5-SOS-F;Δ/+ᵉᵖ* and *K5-SOS-F;Δ/Δᵉᵖ* epidermis. The plots in (C)–(E) show the percentage of positive cells in DMSO- versus Y-27632-treated epidermis. Positive cells are stained in brown. The scale bar represents 100 μm. The plots represent the results of the analysis of at least three animals/genotype, evaluating ≥600 cells/mouse. Error bars indicate SD of the mean. *p < 0.05 and **p < 0.01 according to Student's t tests.

(F) Role of Raf-1 in SOS-F-driven tumorigenesis. Our data are consistent with a working model in which Raf-1 is essential to inhibit Rok-α activity. Rok-α activates downstream pathways, including the phosphorylation of cofilin and a decrease in STAT3 phosphorylation and Myc expression, which induce keratinocyte differentiation.

phosphoinositide 3-kinase p110alpha is required for ras-driven tumorigenesis in mice. Cell *129*, 957–968.

Haase, I., Hobbs, R.M., Romero, M.R., Broad, S., and Watt, F.M. (2001). A role for mitogen-activated protein kinase activation by integrins in the pathogenesis of psoriasis. J. Clin. Invest. *108*, 527–536.

Honma, M., Benitah, S.A., and Watt, F.M. (2006). Role of LIM kinases in normal and psoriatic human epidermis. Mol. Biol. Cell *17*, 1888–1896.

Hsieh, Y.H., Juliana, M.M., Hicks, P.H., Feng, G., Elmets, C., Liaw, L., and Chang, P.L. (2006). Papilloma development is delayed in osteopontin-null mice: implicating an antiapoptosis role for osteopontin. Cancer Res. *66*, 7119–7127.

Indra, A.K., Warot, X., Brocard, J., Bornert, J.M., Xiao, J.H., Chambon, P., and Metzger, D. (1999). Temporally-controlled site-specific mutagenesis in the basal layer of the epidermis: comparison of the recombinase activity of the tamoxifen-inducible Cre-ER(T) and Cre-ER(T2) recombinases. Nucleic Acids Res. *27*, 4324–4327.

Ise, K., Nakamura, K., Nakao, K., Shimizu, S., Harada, H., Ichise, T., Miyoshi, J., Gondo, Y., Ishikawa, T., Aiba, A., et al. (2000). Targeted deletion of the H-ras gene decreases tumor formation in mouse skin carcinogenesis. Oncogene *19*, 2951–2956.

Itoh, K., Yoshioka, K., Akedo, H., Uehata, M., Ishizaki, T., and Narumiya, S. (1999). An essential part for Rho-associated kinase in the transcellular invasion of tumor cells. Nat. Med. *5*, 221–225.

Lashmar, U.T., Hadgraft, J., and Thomas, N. (1989). Topical application of penetration enhancers to the skin of nude mice: a histopathological study. J. Pharm. Pharmacol. *41*, 118–122.

Lefort, K., Mandinova, A., Ostano, P., Kolev, V., Calpini, V., Kolfschoten, I., Devgan, V., Lieb, J., Raffoul, W., Hohl, D., et al. (2007). Notch1 is a p53 target gene involved in human keratinocyte tumor suppression through negative regulation of ROCK1/2 and MRCKalpha kinases. Genes Dev. *21*, 562–577.

Leicht, D.T., Balan, V., Kaplun, A., Singh-Gupta, V., Kaplun, L., Dobson, M., and Tzivion, G. (2007). Raf kinases: Function, regulation and role in human cancer. Biochim. Biophys. Acta *1773*, 1196–1212.

Levy, L., Broad, S., Diekmann, D., Evans, R.D., and Watt, F.M. (2000). beta1 integrins regulate keratinocyte adhesion and differentiation by distinct mechanisms. Mol. Biol. Cell *11*, 453–466.

Lim, K.-H., and Counter, C.M. (2005). Reduction in the requirement of oncogenic Ras signaling to activation of PI3K/AKT pathway during tumor maintenance. Cancer Cell *8*, 381–392.

Lin, A.W., and Lowe, S.W. (2001). Oncogenic ras activates the ARF-p53 pathway to suppress epithelial cell transformation. Proc. Natl. Acad. Sci. USA *98*, 5025–5030.

Malliri, A., van der Kammen, R.A., Clark, K., van der Valk, M., Michiels, F., and Collard, J.G. (2002). Mice deficient in the Rac activator Tiam1 are resistant to Ras-induced skin tumours. Nature *417*, 867–871.

Mavria, G., Vercoulen, Y., Yeo, M., Paterson, H., Karasarides, M., Marais, R., Bird, D., and Marshall, C.J. (2006). ERK-MAPK signaling opposes Rho-kinase to promote endothelial cell survival and sprouting during angiogenesis. Cancer Cell *9*, 33–44.

McMullan, R., Lax, S., Robertson, V.H., Radford, D.J., Broad, S., Watt, F.M., Rowles, A., Croft, D.R., Olson, M.F., and Hotchin, N.A. (2003). Keratinocyte differentiation is regulated by the Rho and ROCK signaling pathway. Curr. Biol. *13*, 2185–2189.

McMurray, H.R., Sampson, E.R., Compitello, G., Kinsey, C., Newman, L., Smith, B., Chen, S.-R., Klebanov, L., Salzman, P., Yakovlev, A., et al. (2008). Synergistic response to oncogenic mutations defines gene class critical to cancer phenotype. Nature *453*, 1112–1116.

Mueller, M.M. (2006). Inflammation in epithelial skin tumours: Old stories and new ideas. Eur. J. Cancer *42*, 735–744.

Porter, R.M., Reichelt, J., Lunny, D.P., Magin, T.M., and Lane, E.B. (1998). The relationship between hyperproliferation and epidermal thickening in a mouse model for BCIE. J. Invest. Dermatol. *110*, 951–957.

Quintanilla, M., Brown, K., Ramsden, M., and Balmain, A. (1986). Carcinogen-specific mutation and amplification of Ha-ras during mouse skin carcinogenesis. Nature *322*, 78–80.

Repasky, G.A., Chenette, E.J., and Der, C.J. (2004). Renewing the conspiracy theory debate: does Raf function alone to mediate Ras oncogenesis? Trends Cell Biol. *14*, 639–647.

Ridky, T.W., and Khavari, P.A. (2004). Pathways sufficient to induce epidermal carcinogenesis. Cell Cycle *3*, 621–624.

Riva, C., Lavieille, J.P., Reyt, E., Brambilla, E., Lunardi, J., and Brambilla, C. (1995). Differential c-myc, c-jun, c-raf and p53 expression in squamous cell carcinoma of the head and neck: Implication in drug and radioresistance. Eur. J. Cancer B Oral Oncol. *31B*, 384–391.

Roper, E., Weinberg, W., Watt, F.M., and Land, H. (2001). p19ARF-independent induction of p53 and cell cycle arrest by Raf in murine keratinocytes. EMBO Rep. *2*, 145–150.

Sahai, E. (2005). Mechanisms of cancer cell invasion. Curr. Opin. Genet. Dev. *15*, 87–96.

Sano, S., Itami, S., Takeda, K., Tarutani, M., Yamaguchi, Y., Miura, H., Yoshikawa, K., Akira, S., and Takeda, J. (1999). Keratinocyte-specific ablation of stat3 exhibits impaired skin remodeling, but does not affect skin morphogenesis. EMBO J. *18*, 4657–4668.

Schmidt, M., Goebeler, M., Posern, G., Feller, S.M., Seitz, C.S., Brocker, E.-B., Rapp, U.R., and Ludwig, S. (2000). Ras-independent activation of the Raf/MEK/ERK pathway upon calcium-induced differentiation of keratinocytes. J. Biol. Chem. *275*, 41011–41017.

Scholl, F.A., Dumesic, P.A., and Khavari, P.A. (2004). Mek1 alters epidermal growth and differentiation. Cancer Res. *64*, 6035–6040.

Seethala, R.R., Gooding, W.E., Handler, P.N., Collins, B., Zhang, Q., Siegfried, J.M., and Grandis, J.R. (2008). Immunohistochemical analysis of phosphotyrosine signal transducer and activator of transcription 3 and epidermal growth factor receptor autocrine signaling pathways in head and neck cancers and metastatic lymph nodes. Clin. Cancer Res. *14*, 1303–1309.

Sibilia, M., Fleischmann, A., Behrens, A., Stingl, L., Carroll, J., Watt, F.M., Schlessinger, J., and Wagner, E.F. (2000). The EGF receptor provides an essential survival signal for SOS-dependent skin tumor development. Cell *102*, 211–220.

Sobczak, I., Galabova-Kovacs, G., Sadzak, I., Kren, A., Christofori, G., and Baccarini, M. (2008). B-Raf is required for ERK activation and tumor progression in a mouse model of pancreatic [beta]-cell carcinogenesis. Oncogene *27*, 4779–4787.

Solit, D.B., Garraway, L.A., Pratilas, C.A., Sawai, A., Getz, G., Basso, A., Ye, Q., Lobo, J.M., She, Y., Osman, I., et al. (2006). BRAF mutation predicts sensitivity to MEK inhibition. Nature *439*, 358–362.

Tarutani, M., Cai, T., Dajee, M., and Khavari, P.A. (2003). Inducible activation of Ras and Raf in adult epidermis. Cancer Res. *63*, 319–323.

Vaezi, A., Bauer, C., Vasioukhin, V., and Fuchs, E. (2002). Actin cable dynamics and Rho/Rock orchestrate a polarized cytoskeletal architecture in the early steps of assembling a stratified epithelium. Dev. Cell *3*, 367–381.

van Hogerlinden, M., Rozell, B.L., Ahrlund-Richter, L., and Toftgard, R. (1999). Squamous cell carcinomas and increased apoptosis in skin with inhibited Rel/nuclear factor-kappaB signaling. Cancer Res. *59*, 3299–3303.

Wakamatsu, K., Ogita, H., Okabe, N., Irie, K., Tanaka-Okamoto, M., Ishizaki, H., Ishida-Yamamoto, A., Iizuka, H., Miyoshi, J., and Takai, Y. (2007). Up-regulation of loricrin expression by cell adhesion molecule nectin-1 through Rap1-ERK signaling in keratinocytes. J. Biol. Chem. *282*, 18173–18181.

Wang, Z.Y., and Chen, Z. (2008). Acute promyelocytic leukemia: from highly fatal to highly curable. Blood *111*, 2505–2515.

Watanabe, K., Ueno, M., Kamiya, D., Nishiyama, A., Matsumura, M., Wataya, T., Takahashi, J.B., Nishikawa, S., Nishikawa, S.-i., Muguruma, K., et al. (2007). A ROCK inhibitor permits survival of dissociated human embryonic stem cells. Nat. Biotechnol. *25*, 681–686.

Watt, F.M., Frye, M., and Benitah, S.A. (2008). MYC in mammalian epidermis: how can an oncogene stimulate differentiation? Nat. Rev. Cancer *8*, 234–242.

Wu, X., Quondamatteo, F., Lefever, T., Czuchra, A., Meyer, H., Chrostek, A., Paus, R., Langbein, L., and Brakebusch, C. (2006). Cdc42 controls progenitor cell differentiation and beta-catenin turnover in skin. Genes Dev. *20*, 571–585.

Zhao, Z.S., and Manser, E. (2005). PAK and other Rho-associated kinases–effectors with surprisingly diverse mechanisms of regulation. Biochem. J. *386*, 201–214.

9   Keratinocyte-specific Stat3 heterozygosity impairs development of skin tumors in human papillomavirus 8 transgenic mice

Marco De Andrea[1,2], Massimo Rittà[1,2], Manuela M. Landini[2], Cinzia Borgogna[2], Michele Mondini[2], Florian Kern[3], Karin Ehrenreiter[3], Manuela Baccarini[3], Gian Paolo Marcuzzi[4], Sigrun Smola[4,5], Herbert Pfister[4], Santo Landolfo[1], and Marisa Gariglio[2]

[1]Department of Public Health and Microbiology, Medical School of Turin, Turin, Italy;

[2]Department of Clinical and Experimental Medicine, Medical School of Novara, Novara, Italy;

[3]Max F. Perutz Laboratories, University of Vienna, Vienna, Austria;

[4]Institute of Virology, Center of Molecular Medicine, University of Cologne, Cologne, Germany; and

[5]Institute of Virology, Saarland University, Homburg/Saar, Germany

[*]Correspondence: Marisa Gariglio; gariglio@med.unipmn.it

Relevance & Contribution: This article shows the importance of accurate STAT3 signaling in human papillomavirus mediated skin carcinogenesis. Moreover, the STAT3 signaling pathway might play a more general role in skin tumorigenesis as it is as well affected in Ras-driven tumorigenesis through the above mentioned Raf-1/Rok-α/LIMK/Cofilin/STAT3 link. Most of the histological part of the publication was done in a collaboration of E.K. and F.K. with M. A. Moreover E.K. and F.K. provided technical and scientific support on the analysis.

Cancer Research

Keratinocyte-Specific Stat3 Heterozygosity Impairs Development of Skin Tumors in Human Papillomavirus 8 Transgenic Mice

Marco De Andrea, Massimo Rittà, Manuela M. Landini, et al.

Updated Version	Access the most recent version of this article at: doi:10.1158/0008-5472.CAN-10-1128

Cited Articles	This article cites 34 articles, 12 of which you can access for free at: http://cancerres.aacrjournals.org/content/70/20/7938.full.html#ref-list-1

E-mail alerts	Sign up to receive free email-alerts related to this article or journal.
Reprints and Subscriptions	To order reprints of this article or to subscribe to the journal, contact the AACR Publications Department at pubs@aacr.org.
Permissions	To request permission to re-use all or part of this article, contact the AACR Publications Department at permissions@aacr.org.

Molecular and Cellular Pathobiology

Cancer Research

Keratinocyte-Specific Stat3 Heterozygosity Impairs Development of Skin Tumors in Human Papillomavirus 8 Transgenic Mice

Marco De Andrea[1,2], Massimo Rittà[1,2], Manuela M. Landini[2], Cinzia Borgogna[2], Michele Mondini[2], Florian Kern[3], Karin Ehrenreiter[3], Manuela Baccarini[3], Gian Paolo Marcuzzi[4], Sigrun Smola[4,5], Herbert Pfister[4], Santo Landolfo[1], and Marisa Gariglio[2]

Abstract

Human papillomaviruses (HPV) of the genus β are thought to play a role in human skin cancers, but this has been difficult to establish using epidemiologic approaches. To gain insight into the transforming activities of β-HPV, transgenic mouse models have been generated that develop skin tumors. Recent evidence suggests a central role of signal transducer and activator of transcription 3 (Stat3) as a transcriptional node for cancer cell–autonomous initiation of a tumor-promoting gene signature associated with cell proliferation, cell survival, and angiogenesis. Moreover, high levels of phospho-Stat3 have been detected in tumors arising in HPV8-CER transgenic mice. In this study, we investigate the *in vivo* role of Stat3 in HPV8-induced skin carcinogenesis by combining our established experimental model of HPV8-induced skin cancer with epidermis-restricted Stat3 ablation. Stat3 heterozygous epidermis was less prone to tumorigenesis than wild-type epidermis. Three of the 23 (13%) Stat3$^{+/-}$:HPV8 animals developed tumors within 12 weeks of life, whereas 54.3% of Stat3$^{+/+}$:HPV8 mice already exhibited tumors in the same observation period (median age for tumor appearance, 10 weeks). The few tumors that arose in the Stat3$^{+/-}$:HPV8 mice were benign and never progressed to a more malignant phenotype. Collectively, these results offer direct evidence of a critical role for Stat3 in HPV8-driven epithelial carcinogenesis. Our findings imply that targeting Stat3 activity in keratinocytes may be a viable strategy to prevent and treat HPV-induced skin cancer. *Cancer Res; 70(20); 7938–48. ©2010 AACR.*

Introduction

Human papillomaviruses (HPV) are small DNA tumor viruses that are strictly epitheliotropic and infect keratinocytes at a wide range of body sites. More than 120 different types of HPV have been identified to date, classified into several phylogenetic groups (1). Of these, the α-genus HPVs, associated with infections of mucosal epithelia, are the best characterized and can be grouped into "low-risk" and "high-risk" types depending on the relative tendency of the virus-induced neoplasm to undergo malignant progression (2, 3).

β-HPVs are associated with infections of the skin and comprise a similarly large group of HPVs (4, 5). They cause widespread inapparent or asymptomatic infections in the general population, and children become infected at an early age. In immunosuppressed patients and individuals suffering from epidermodysplasia verruciformis (6, 7), a rare inherited skin disease, these viruses can spread unchecked and have been implicated in the development of nonmelanoma skin cancer (NMSC), particularly in sun-exposed areas (8).

The causal relationship between HPV infection and squamous cell carcinoma (SCC) of the genital tract is well established. HPV β-genotypes are suspected of playing a role in skin cancers, but this has been difficult to establish using epidemiologic approaches due to the ubiquitous prevalence of these viruses in the general population and their absence in some cancers (4, 9).

Transgenic mouse models have been used to gain insight into the transforming activities of β-HPV. Expression of the complete early genome region (CER) of HPV8 in transgenic mice was found to be sufficient for the spontaneous development of NMSC (10). In addition, our group has shown the intrinsic oncogenic potential of HPV8 E2 (11) and HPV8 E6 (12) using transgenic animals. Once more using transgenic technology, several mouse lines have been developed that express E6/E7 from other β-genotypes, such as HPV38 (13) and HPV20 (14), but HPV8 has thus far been the only cutaneous HPV type found to induce skin cancer completely on its own in the absence of any additional co-carcinogenic treatment.

Authors' Affiliations: [1]Department of Public Health and Microbiology, Medical School of Turin, Turin, Italy; [2]Department of Clinical and Experimental Medicine, Medical School of Novara, Novara, Italy; [3]Max F. Perutz Laboratories, University of Vienna, Vienna, Austria; [4]Institute of Virology, Center of Molecular Medicine, University of Cologne, Cologne, Germany; and [5]Institute of Virology, Saarland University, Homburg/Saar, Germany

Note: M. De Andrea and M. Rittà contributed equally to this work.

Corresponding Author: Marisa Gariglio, Department of Clinical and Experimental Medicine, Medical School of Novara, via Solaroli 17, 28100 Novara, Italy. Phone: 39-0321-660649; Fax: 39-0321-620421. E-mail: gariglio@med.unipmn.it.

doi: 10.1158/0008-5472.CAN-10-1128

©2010 American Association for Cancer Research.

American Association for *Cancer Research*

Signal transducer and activator of transcription 3 (Stat3) is a transcription factor that belongs to a family of cytoplasmic proteins that participate in normal cellular responses to cytokines and growth factors (15). Activation of a wide variety of cell surface receptors leads to the tyrosine phosphorylation of Stat3 (pStat3), which then dimerizes and translocates to the nucleus, where it modulates the expression of target genes that are involved in various physiologic functions, including cell cycle regulation, apoptosis, and cell differentiation (16, 17). Knocking Stat3 out of the germline results in embryonic lethality (18), implying that Stat3 has global and critical effects on development. Keratinocyte-specific Stat3-null mice show that Stat3 plays a pivotal role in skin remodeling because the hair cycle and wound-healing processes are found to be severely compromised in these mice (19). Chan and colleagues (20) went on to show that these knockouts are completely resistant to the two-stage carcinogenesis regimen using 7,12-dimethylbenz(a)anthracene as the initiator and 12-O-tetradecanoylphorbol-13-acetate as the promoter, thus indicating that Stat3 is essential for the development of chemically induced skin tumors in mice. In addition, they found that Stat3-deficient keratinocytes were highly sensitive to UVB-induced apoptosis, whereas overexpression of Stat3 or expression of a Stat3C transgene protected keratinocytes from UVB-induced apoptosis (21–24). All in all, these findings clearly show that Stat3 plays a critical role in both two-stage chemical-induced and physical UVB-mediated skin carcinogenesis.

In this study, we address the $in\ vivo$ role of Stat3 in HPV8-induced skin carcinogenesis using HPV8-CER transgenic mice crossed with keratinocyte-specific Stat3-disrupted mice, and report the remarkable observation that heterozygous mice, carrying only one Stat3 functional allele, respond poorly to proliferation induced by viral oncogenic proteins. The present study shows, for the first time, that the reduced expression of the Stat3 gene has a significant effect on skin tumor development in this mouse model of viral carcinogenesis, and provides a rationale for evaluating the potential use of Stat3 inhibitors in the prevention and treatment of tumors associated with β-HPV infection.

Materials and Methods

Generation of transgenic mice

K14-HPV8/FVB transgenic mice have been previously described (10). K5Cre-Stat3$^{wt/LoxP}$ mice were obtained by crossing K5Cre transgenic mice expressing Cre recombinase under the control of the keratinocyte-specific keratin 5 (K5) promoter (25, 26) with Stat3$^{LoxP/LoxP}$ animals previously described (kindly provided by Dr. David Levy, New York University; ref. 27). Mice were housed in accordance with The Guide for the Care and Use of Laboratory Animals.

Genotyping of progeny

Genomic DNA was isolated from tail biopsies of 7-day-old mice using the QIAamp Tissue kit (Qiagen) or from 0.5% dispase II (Roche)– and trypsin (Sigma)–treated full-thickness skin. PCR analysis to detect Stat3 wild-type (wt), floxed, or null alleles was performed using primers designed to amplify the DNA sequence between exons 15 and 22 (Fig. 1A). Briefly, DNA (~0.3 μg) was incubated with two forward primers ("A": 5′-CAGAACCAGGCGGCTCGTGTGC-G-3′, specific for intron 21; "C": 5′-GAAGGCAGGTCTCTCTGGT-GCTTC-3′, specific for intron 15) and one reverse primer ("B": 5′-GCTGCCAACAGCCACTGCCCCAG-3′, specific for intron 21; [final] = 0.25 μmol/L) in a final volume of 25 μL using REDTaq ReadyMix PCR Reaction Mix (Sigma). PCRs were performed on a MJ PTC-200 thermal cycler (Bio-Rad) using the following protocol: 94°C for 2 minutes; 35 cycles of 94°C for 45 seconds, 58°C for 40 seconds, and 72°C for 1 minute; and a final extension period at 72°C for 7 minutes. PCR products were separated by 2% agarose–TAE gel electrophoresis, and ethidium bromide staining was used to detect the separated bands. Stat3 band sizes were expected to be ~140 bp for the wt allele, ~240 bp for the floxed allele, and ~400 bp for the null allele. The PCR protocols used for the Cre and HPV8 transgenes were previously described (10, 25).

Preparation of epidermal cell lysates and Western blot analysis

Mice were sacrificed by cervical dislocation. The dorsal skin of the mice was shaved and depilated; the skin was then excised and the epidermis was peeled away from the dermis following overnight treatment with 0.5% dispase II (Roche) and then homogenized in lysis buffer containing 100 mmol/L Tris-HCl (pH 6.8), 1.25% β-mercaptoethanol, 4% SDS, 1% bromphenol blue, 10% glycerol, 25 μL/mL Protease Inhibitor Cocktail (Sigma), and 1 μL/100 μL Phosphatase Inhibitor Cocktail 2 (Sigma). Supernatants were analyzed for protein concentration using the QuantiPro BCA Assay kit (Sigma). Three whole-cell lysates were pooled, fractionated on 8% to 12% SDS-PAGE, and transferred to polyvinylidene difluoride membranes (Millipore). The following primary antibodies were used: Stat3 and pStat3 (clones 124H6 and D3A7; 1:1,000 and 1:2,000; Cell Signaling Technology), vimentin (clone V9; 1:3,000; Sigma), pan-epithelial keratin (clone Ks 5+8.22/C 22; 1:300; Progen Biotechnik), and actin (clone C4; 1:3,000; Chemicon).

Histologic and immunohistochemical analysis of the skin

Sections (4 μm thick) were cut from formalin-fixed and paraffin-embedded skin, deparaffinized, and rehydrated using standard procedures. Serial sections were either stained with H&E or used for immunostaining using primary antibodies raised against the following proteins: K5 (clone AF138; 1:500; Covance), K10 (1:1,000; Covance), proliferating cell nuclear antigen (PCNA; 1:4,000; Santa Cruz Biotechnology), Stat3 (1:100; Cell Signaling Technology), and pStat3 (clone D3A7; 1:50; Cell Signaling Technology). Endogenous peroxidase activity was blocked by treatment with 3% hydrogen peroxide in 1× PBS for 10 minutes. Antigen unmasking was performed by microwaving the sections for 10 minutes in 10 mmol/L citrate buffer (pH 6.0)
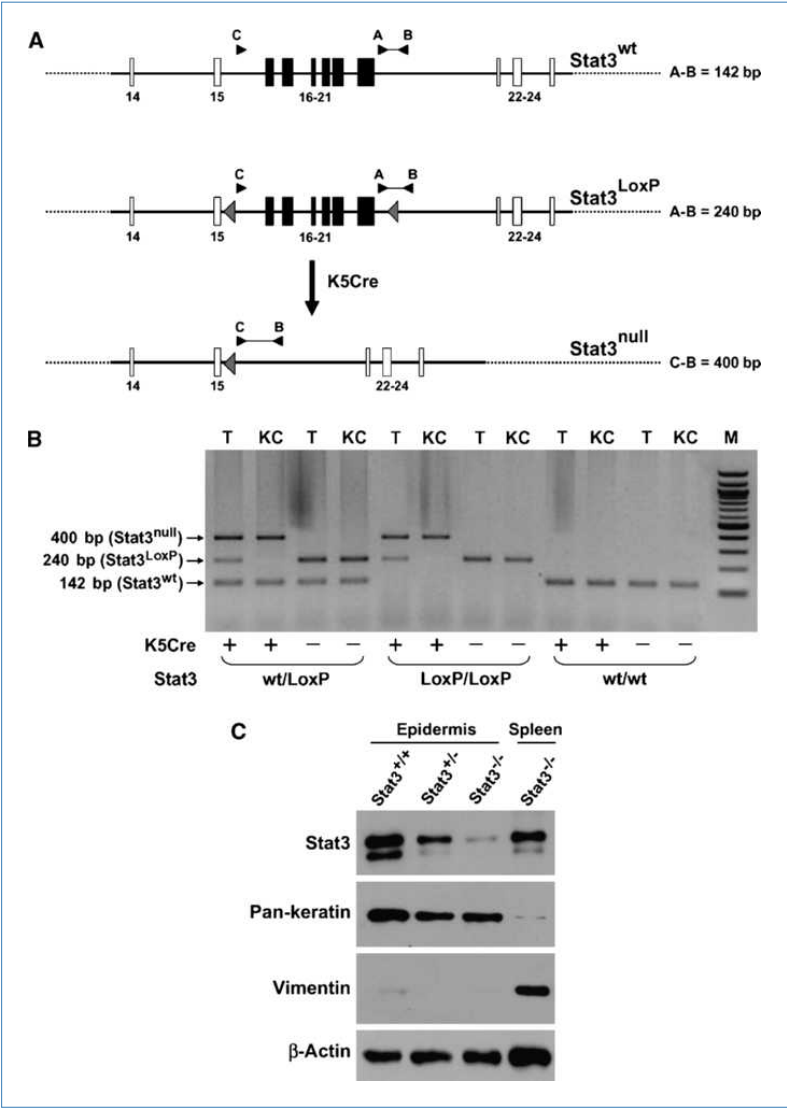
49

De Andrea et al.

Figure 1. Keratinocyte-specific disruption of the Stat3 gene by the Cre-LoxP system. A, a partial genomic map of the Stat3 gene before and after Cre-mediated disruption. The exons to be excised (16–21, solid boxes) were flanked by two identically oriented LoxP sites (dotted triangles). The three primers indicated (A, B, and C) were used for the detection of wt, floxed (LoxP), and disrupted (null) Stat3 alleles, respectively. B, allele-specific PCR analysis performed on tail (T) and keratinocyte (KC) genomic DNA preparations; the primers used are described in Materials and Methods (M; Quick-Load 100-bp DNA ladder). C, analysis of Stat3 protein levels in epidermal lysates (30 μg) pooled from three animals for each genotype. β-Actin was used to control for equal loading.

for K5, K10, Stat3, and PCNA antibodies, and for pStat3 in 1 mmol/L EDTA (pH 8.0) for 12 minutes. For K5, K10, Stat3, and PCNA antibodies, we used the biotinylated universal anti-rabbit/mouse secondary antibody followed by incubation with the streptavidin–horseradish peroxidase complex (Vector Laboratories). For revelation of pStat3, we used the DAKO EnVision Plus Detection System. Bound antibodies were visualized by 3,3′-diaminobenzidine, counterstained with Mayer's hematoxylin, and mounted with VectaMount permanent mounting medium (Vector Laboratories).

Evaluation of epidermal thickness, PCNA, and pStat3 staining

Paraffin sections were stained with H&E, and the epidermal thickness was measured by using Image-Pro Plus 6.0 software technology. For the quantification of PCNA- and pStat3-positive staining cells, 10 random areas were selected for each mouse. The number of cells showing positive labeling and the total number of cells counted (1,000) were recorded by using Image-Pro Plus 6.0 software technology. An average percentage was then calculated based on the total number of cells and the number of positive staining cells from each set of 10 fields counted.

50

Quantitative real-time reverse transcription-PCR

For the determination of E6 and E7 gene expression levels, RNA was extracted from 0.5% dispase II– and trypsin-treated full-thickness skin using the NucleoSpin RNA Extraction kit (Macherey-Nagel) and treated with DNase I (Sigma). Total RNA (1 μg) was retrotranscribed using the ImProm-II Reverse Transcription System (Promega). SYBR Green I quantitative real-time reverse transcription-PCR (qRT-PCR) was performed, and the housekeeping gene β-actin was used to normalize the variation in cDNA levels. Each standard curve was constructed using values from serially diluted HPV8-negative mouse cDNA mixed with plasmid encoding E6/E7 of HPV8. wt mouse cDNA was amplified to verify the absence of genomic contaminations. SYBR Green I amplifications were performed as previously described (10) using the GeneAmp 7000 Sequence Detection System (Applied Biosystems).

Statistical analysis

All statistical tests were performed using GraphPad Prism version 5.00 for Windows. Two-way ANOVA, followed by Bonferroni post tests, was used to analyze whether the differences in mean epidermal thickness and PCNA proliferating indices were affected by the Stat3 genotype. One-way ANOVA followed by the Bonferroni post test was used to analyze the differences in the pStat3 immunohistochemical score between genotypes. Finally, the Fisher's exact test was used to compare tumor incidences between mouse genotypes.

Results and Discussion

Phenotypes of skin-specific Stat3 knockout mice expressing HPV8 early genes

Mice with epidermis-restricted Stat3 deletion (K5Cre-Stat3$^{wt/LoxP}$ mice) were mated with animals in which HPV8 early gene expression was driven by the K14 promoter (K14-HPV8 mice). The resulting K5Cre-Stat3$^{wt/LoxP}$/K14-HPV8 mice were then backcrossed with parental K14-HPV8 mice for six generations to yield a pure FVB/N background and finally interbred to generate all the possible genotypes detailed in Table 1.

Table 1. Genotype of animals

Genotypes	Aliases
K5Cre:Stat3$^{LoxP/LoxP}$/K14-HPV8	Stat3$^{-/-}$:HPV8
K5Cre:Stat3$^{wt/LoxP}$/K14-HPV8	Stat3$^{+/-}$:HPV8
K5Cre:Stat3$^{wt/wt}$/K14-HPV8	
Stat3$^{LoxP/LoxP}$/K14-HPV8	Stat3$^{+/+}$:HPV8
Stat3$^{wt/LoxP}$/K14-HPV8	
Stat3$^{wt/wt}$/K14-HPV8	
K5Cre:Stat3$^{LoxP/LoxP}$	Stat3$^{-/-}$
K5Cre:Stat3$^{wt/LoxP}$	Stat3$^{+/-}$
K5Cre:Stat3$^{wt/wt}$	
Stat3$^{LoxP/LoxP}$	
Stat3$^{wt/LoxP}$	Stat3$^{+/+}$
Stat3$^{wt/wt}$	

Because K5 and K14 proteins are expressed in the same cell lineages (28), including the basal keratinocytes of the interfollicular epidermis and the outer root sheath (i.e., the follicular keratinocytes), the Stat3$^{-/-}$:HPV8 mice have a constitutive overexpression of the HPV8 early genes in the same cells as those carrying the Cre-mediated Stat3 ablation. Genotyping of the Stat3 gene for both alleles was carried out by genomic PCR (Fig. 1A and B), and the efficiency and specificity of the Cre-mediated Stat3 disruption were determined by Western blot analysis (Fig. 1C). Stat3 protein levels were dramatically reduced in homozygous mice as a consequence of the Cre-mediated Stat3 gene disruption, whereas levels were reduced by ∼50% in heterozygous mice compared with the parental mice. As expected, the epidermal lysates contained the epithelial-specific marker pan-keratin, but not the fibroblast-specific marker vimentin, confirming their purity.

Soon after birth, both Stat3$^{-/-}$ and Stat3$^{-/-}$:HPV8 mice started to fail (Fig. 2A). Within postnatal day 10 (PD10), they exhibited lethargy, retarded development, spontaneous wounds, and sparse hair development. By PD12 to PD15, they developed patches of rough skin with scales and crusts and invariably died prematurely. Most homozygous mice died between 20 and 30 days after birth irrespective of whether they possessed the HPV8 transgenes or not; a few survived longer, but for no more than 40 days. Previous reports have shown that the K5 gene is expressed not only in the epidermis but also in the esophagus and stomach (25, 29, 30); Stat3 disruption would therefore also occur in these tissues as a consequence of K5-driven Cre expression. Indeed, no food was found in the stomach of the dead mice, and the esophagus was smaller in mutant mice than in wt mice (data not shown), suggesting that death was primarily caused by a defect in food intake as a result of esophagus dysfunction. The fact that the Stat3$^{-/-}$ mice have a high morbidity rate and short life span meant that it was not possible to investigate the tumorigenic effects of HPV8 early genes in these mice. In contrast, mice carrying a single functional Stat3 allele did not show any overt phenotype or gross modifications of the skin and lived a normal average life span. These phenotype results are similar to those reported by Sano and colleagues (19), but in our mouse model, they appear earlier and with stronger severity. The Cre-LoxP system used by Sano and colleagues specifically removed the tyrosine residue essential for phosphorylation (Tyr^{705}) and the mitogen-activated protein kinase recognition site spanning exons 21 to 22 within the Stat3 gene, deleting full-length Stat3 but allowing the expression of truncated form with possible residual activity. In contrast, the gene disruption strategy used in our study, resulting in the total deletion of exons 16 to 21, completely abolished Stat3 expression, thus justifying the stronger phenotype observed in our mouse model.

Histologic analysis and measurement of the epidermal thickness of the skin obtained from healthy areas of the different genotypes (four mice for each genotype) at ∼1 month of age revealed marked differences between wt and Stat3-null mice. The epidermis in the null mice was so thin that it was not possible to measure it (Fig. 2B and E), and there was no increase in epidermal layer thickness as a consequence of viral oncoprotein expression. Severely distorted hair follicles
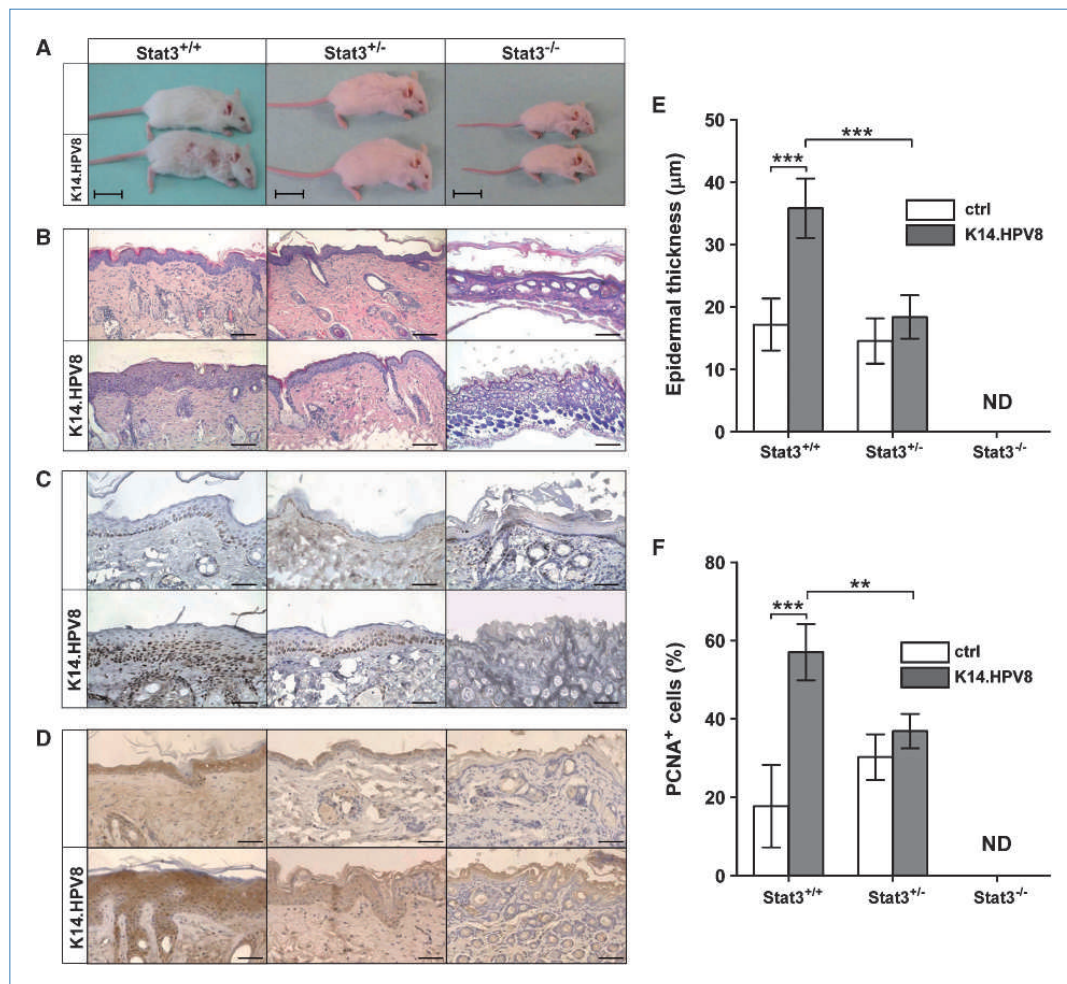
51

De Andrea et al.

Figure 2. Stat3 deletion in keratinocytes causes retarded development and epidermal defects. A, appearance of Stat3^{+/+}, Stat3^{+/−}, and Stat3^{−/−} mice not expressing (top part) or expressing (bottom part) HPV8 early genes at PD25. Scale bars, 1 cm. B, histology of mouse skin, stained with H&E, obtained from nonlesional areas of the mice shown in A. Scale bars, 50 μm. C, immunohistochemical staining of PCNA in serial sections obtained from the skin specimens shown in B. Dark brown, PCNA-positive cells; blue, nuclear counterstaining. Scale bars, 25 μm. D, immunohistochemistry of serial sections of the skin specimens shown in B stained for Stat3. Dark brown, positive cells; blue, nuclear counterstaining. Scale bars, 25 μm. E, quantification of epidermal thickness. Columns, mean of four mice; bars, SD. There were six skin sections per mouse. Two sections were scored for a total of at least six views. ***, $P < 0.001$, two-way ANOVA followed by Bonferroni post test. ND, not detectable. F, quantification of PCNA-positive cells. An average of at least four mice per genotype was used to calculate the percentage. Columns, mean; bars, SD. ***, $P < 0.001$; **, $P < 0.01$, two-way ANOVA followed by Bonferroni post test.

could be observed that formed cysts filled with lamellar and eosinophilic material in the upper dermis, particularly in the Stat3^{−/−}:HPV8 mice. This alteration of hair architecture has been previously reported and is related to the lack of Stat3 in the outer root sheath cells (19). In contrast, both stratification of the squamous epithelia of the skin and hair follicle development were normal in heterozygous mice. The epidermis of nontransgenic Stat3^{+/−} mice was slightly thinner than

that of Stat3^{+/+} and was not significantly thicker in Stat3^{+/−}: HPV8. In contrast, the total thickness of the epidermis of Stat3^{+/+}:HPV8 mice was approximately doubled compared with their nontransgenic wt counterparts and significantly thicker than that of Stat3^{+/−}:HPV8 mice. Proliferation was also evaluated by PCNA immunostaining. Consistent with the results observed by measuring epidermal thickness, PCNA staining was not detectable in the epidermis of Stat3-null
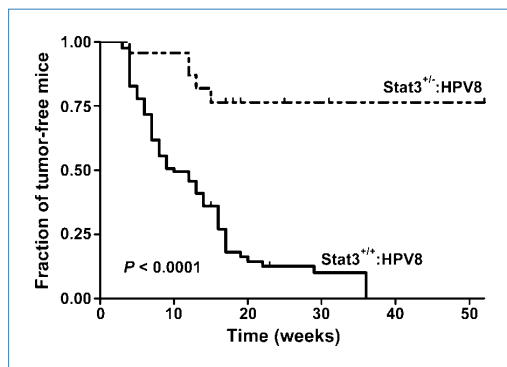
52

Stat3 Function in HPV8-Induced Skin Carcinogenesis

Figure 3. Kaplan-Meier plot of the tumor-free state as a function of time in Stat3$^{+/+}$:HPV8 and Stat3$^{+/-}$:HPV8 mice. Mice were monitored twice weekly over a period of 52 wk and for at least 12 wk after birth. The indicated P value refers to log-rank test.

mice, nor was it present in the Stat3$^{-/-}$:HPV8 transgenic mice (Fig. 2C). The number of PCNA-positive cells was significantly greater in the epidermis of Stat3$^{+/+}$:HPV8 compared with their nontransgenic counterparts, and no significant difference was found between Stat3$^{+/-}$:HPV8 mice and the nontransgenic Stat3$^{+/-}$ mice (Fig. 2F). Here, again, the number of PCNA-positive cells was significantly greater in Stat3$^{+/+}$:HPV8 mice compared with Stat3$^{+/-}$:HPV8 mice.

Keratinocyte-specific ablation of Stat3 expression was confirmed by immunohistochemistry. As shown in Fig. 2D, strong positive immunostaining was observed in all layers of the epithelium in both Stat3$^{+/+}$ and Stat3$^{+/+}$:HPV8 skin sections. According to the protein levels detected by

Western blotting (Fig. 1C), Stat3 expression was significantly reduced in heterozygous mice in comparison with wts, yet remained present in all layers of the epithelium. As expected, Stat3 staining was absent in the skin of Stat3$^{-/-}$ mice in both interfollicular epidermis and follicular keratinocytes. Collectively, these findings indicate that, even in nonlesional skin of heterozygous mice, the reduction of Stat3 protein levels significantly affects the degree of hyperplasia induced by HPV8 oncoproteins.

Stat3 heterozygosity significantly decreases HPV8-induced tumor formation

From our initial characterization of the different mouse genotypes, to our surprise, we noted that spontaneous skin lesions in a sample of Stat3$^{+/-}$:HPV8 mice did not occur during an observation period that spanned the first 3 months of life. On account of this finding, we monitored spontaneous tumor formation over a 52-week period in a larger cohort of Stat3$^{+/-}$:HPV8 mice ($n = 23$) and Stat3$^{+/+}$:HPV8 mice ($n = 81$). All animals were followed for a minimum of 12 weeks. The Kaplan-Meier plot of the tumor-free state as a function of time showed statistically significant differences between the two groups (Fig. 3), with a disease-free survival greatly enhanced in the Stat3 heterozygous mice. The median age for tumor appearance was 10 weeks in Stat3$^{+/+}$:HPV8 mice ($P < 0.0001$, log-rank test). Indeed, only 3 of the 23 Stat3$^{+/-}$:HPV8 mice (13%) displayed tumor formation within 12 weeks of life, whereas in the same period 44 of the 81 Stat3$^{+/+}$:HPV8 had already developed one or more tumors (54.3%; Table 2). No influence of gender on tumor development was detected. The macroscopic appearance and the localization of the skin lesions in Stat3$^{+/+}$:HPV8 were identical to the skin tumors previously described in HPV8-CER mice (10). These lesions progressed continuously (15.8% of tumors

Table 2. Summary of tumor characteristics in the skin

Genotypes	at 12 wk of age			at 52 wk of age			Average age of tumor onset
	No. mice	Mice with tumor	Mice with multiple tumors	No. mice	Mice with tumor	Mice with multiple tumors	
Stat3$^{+/+}$	125	0	0	110	0	0	NA
Stat3$^{+/-}$	44	0	0	37	0	0	NA
Stat3$^{-/-}$	19	NA	NA	13	NA	NA	NA
Stat3$^{+/+}$:HPV8	81	44	37	65	65	55	10.1
Stat3$^{+/-}$:HPV8	23	3*	3†	11	5*	4†	11.3‡
Stat3$^{-/-}$:HPV8	17	NA	NA	11	NA	NA	NA

Abbreviation: NA, data not applicable.
*Partial loss of Stat3 in the skin resulted in a significant reduction of tumor incidence in Stat3$^{+/-}$:HPV8 in comparison with Stat3$^{+/+}$:HPV8 transgenic mice, at both week 12 ($P = 0.0006$) and week 52 ($P < 0.0001$).
†In tumor-bearing mice, partial loss of Stat3 in the skin did not result in a significant change of multiple tumor incidence in Stat3$^{+/-}$:HPV8 in comparison with Stat3$^{+/+}$:HPV8 transgenic mice ($P > 0.05$, at both weeks 12 and 52).
‡Partial loss of Stat3 in the skin resulted in a not significant delayed time of tumor onset in Stat3$^{+/-}$:HPV8 in comparison with Stat3$^{+/+}$:HPV8 transgenic mice.

53

De Andrea et al.

progressed to malignancy) and never regressed. Interestingly, in Stat3 heterozygous mice, all the tumors were benign, as they did not exhibit any signs of ulceration, although they developed in the same location and with the same initial morphology as those in Stat3$^{+/+}$:HPV8 mice. Indeed, they remained circumscribed and reduced in size for the entire observation period, whereas lesions in the Stat3$^{+/+}$:HPV8 mice became more hyperkeratotic and spread diffusely. Overall, skin lesions in Stat3$^{+/-}$:HPV8 mice did not progress, neither did they show any signs of regression. Because three of the five Stat3$^{+/-}$:HPV8 mice that developed skin lesions were sacrificed for immunohistochemical analysis, sample numbers were too small to conclude with statistics that they would not have progressed to malignancy as occurred in the wt counterparts. It is worth noting, however, that the two Stat3$^{+/-}$:HPV8 mice that lived longer than the observation period (12 months) never developed any signs of malignant progression. Collectively, these observations show that the susceptibility to HPV8-induced skin tumor development is significantly reduced under conditions of Stat3 heterozygosity.

To verify that the results obtained were not related to different transgene expression levels between the wt and heterozygous mice, the levels of HPV8 E6 and HPV8 E7 mRNA in total RNA isolated from epidermal lysates of nonlesional skin in Stat3$^{+/+}$:HPV8 and Stat3$^{+/-}$:HPV8 animals (three of each genotype) were measured in duplicate by qRT-PCR. Epidermal expression levels of the HPV8 E6 and HPV8 E7 mRNAs did not differ between mice of the same genotype or between mice of different genotype and were highest for E7 as previously reported. The mean range values (±SE) were 0.22 ± 0.01 versus 0.16 ± 0.06 for E6 transcripts in Stat3$^{+/+}$:HPV8 versus Stat3$^{+/-}$:HPV8 mice, and 0.43 ± 0.12 versus 0.47 ± 0.24 for E7 transcripts in Stat3$^{+/+}$:HPV8 versus Stat3$^{+/-}$:HPV8, respectively. As a further control, the HPV8 transgene copy number was determined by qRT-PCR in tumor-bearing mice from either Stat3$^{+/+}$:HPV8 or Stat3$^{+/-}$:HPV8 and compared with tumor-free mice from both groups and Stat3$^{+/+}$:HPV8 mice showing SCC progression. The proportion of hemizygous (30%) or homozygous (70%) animals for the HPV8 transgene was equally distributed, excluding the possibility that the results obtained were due to accumulation of HPV8 homozygous mice in a specific group during interbreeding (data not shown).

Assessment of Stat3 status, tumor growth, and proliferation

As stated above and shown in the representative example reported in Fig. 4A, lesions in 15.8% of Stat3$^{+/+}$:HPV8 mice spontaneously progressed from papilloma to carcinoma over a time period of 8 to 24 weeks from their onset, at an average age of 17.3 weeks. Tumors arising in Stat3$^{+/+}$:HPV8 mice were mostly ulcerated and invasive, features of malignancy. This progression was never observed in Stat3$^{+/-}$:HPV8 mice where lesions were limited in size and self-contained, thus indicative of benign papillomas, even at older ages (e.g., 20 weeks), as reported in the example of Fig. 4 (right column). The histopathologic analysis confirmed they were all benign papillomas containing an endophytic component that grew toward

the dermis (Fig. 4A, middle right). They possessed concentrically keratinized structures, a common feature of β-HPV–induced hyperplasia. Even in older Stat3$^{+/-}$:HPV8 mice, these lesions never showed signs of early malignant transformation, such as hyperchromatic nuclei, loss of stratification, and mitotic figures in the upper cell layers; such features were commonly detected in the lesions obtained from the Stat3$^{+/+}$:HPV8 mice of the same age (data not shown). Papillomas arising in Stat3$^{+/+}$:HPV8 mice displayed the same histologic features described for Stat3$^{+/-}$:HPV8. In contrast, carcinomas arising in Stat3$^{+/+}$:HPV8 mice showed loss of epithelium stratification, with markedly atypical cells, and infiltrative growth of tumor cells into the underlying connective tissue (Fig. 4A, middle column). Collectively, these results show that a reduction in Stat3 protein levels strongly affects the progression of skin carcinogenesis.

Having established that Stat3 plays a crucial role in keratinocyte transformation induced by HPV8 early genes *in vivo*, we determined whether there had been any effect on the status of Stat3 phosphorylation. Following phosphorylation, Stat3 translocates to the nucleus, becomes transcriptionally active, and promotes the development of epidermal hyperplasia and/or malignant tumors in mice (22). Immunohistochemical analysis revealed keratinocyte-specific nuclear localization of the tyrosine-phosphorylated (activated) form of Stat3 (pStat3) in all the lesions analyzed from both Stat3$^{+/+}$:HPV8 and Stat3$^{+/-}$:HPV8 mice (Fig. 4A, bottom row) in the basal and suprabasal layers. In nonlesional skin of both genotypes, pStat3 nuclear localization was restricted to just a few cells in the basal proliferating layer of the epidermis (data not shown). The number of pStat3-positive cells was significantly higher in the papillomas arising in both the Stat3$^{+/+}$:HPV8 and Stat3$^{+/-}$:HPV8 mice compared with nonlesional epidermis from both genotypes, and moreover, the scores were similar in the papillomas (Fig. 4B). In Stat3$^{+/+}$:HPV8 mice, scores for pStat3 nuclear staining were higher for carcinomas than for papillomas. Upregulation of the Stat3 protein as well as its activation in the tumors that arose in both wt and heterozygous mice were also confirmed by immunoblotting (Fig. 4C). Thus, these results clearly indicate that Stat3 activation is associated with HPV8-induced hyperproliferation, and suggest that a requisite level of activated Stat3 must accumulate for a neoplasia to develop.

In addition, to analyze the proliferative status of the skin cells, nuclei were stained for the presence of PCNA (Fig. 5, top row). Expression of the viral oncoproteins increased the number of PCNA-positive cells in the suprabasal layers of papillomas from both Stat3$^{+/+}$:HPV8 and Stat3$^{+/-}$:HPV8 mice, although in heterozygous mice the staining was more disorganized with a higher number of positive cells in the inner suprabasal layers. As expected, PCNA expression in carcinomas from Stat3$^{+/+}$:HPV8 mice extended all the way through the dysplastic epidermis.

To assess whether the differences in HPV8-induced tumor progression in Stat3$^{+/+}$ versus Stat3$^{+/-}$ were associated with the degree of tumor cell differentiation, we evaluated the expression of a marker of suprabasal differentiated keratinocytes

Stat3 Function in HPV8-Induced Skin Carcinogenesis

Figure 4. HPV8-induced skin cancer progression is impaired in Stat3$^{+/-}$ transgenic mice. A, gross appearance of Stat3$^{+/+}$:HPV8 mice at 6 wk of age with benign papillomas that convert into carcinomas by 15 wk. Right, a Stat3$^{+/-}$:HPV8 mouse at 20 wk of age showing benign papillomas. Representative H&E-stained skin lesion sections derived from the photographed mice are shown. Scale bars, 100 μm. Immunohistochemistry for pStat3 of serial sections of the skin specimens stained by H&E. Dark brown, positive cells; blue, nuclear counterstaining. Scale bars, 25 μm. B, quantification of pStat3-positive cells. An average of at least three mice per group was used to calculate the percentage. Columns, mean; bars, SD. ***, $P < 0.001$; **, $P < 0.01$, one-way ANOVA followed by Bonferroni post test. C, analysis of Stat3 and pStat3 protein levels in nonlesional versus tumor epidermal lysates from Stat3$^{+/+}$ and Stat3$^{+/-}$ mice, transgenic or nontransgenic for HPV8 oncoproteins. Lysates (30 μg) were pooled from three animals for each genotype. β-Actin was used to control for equal loading.
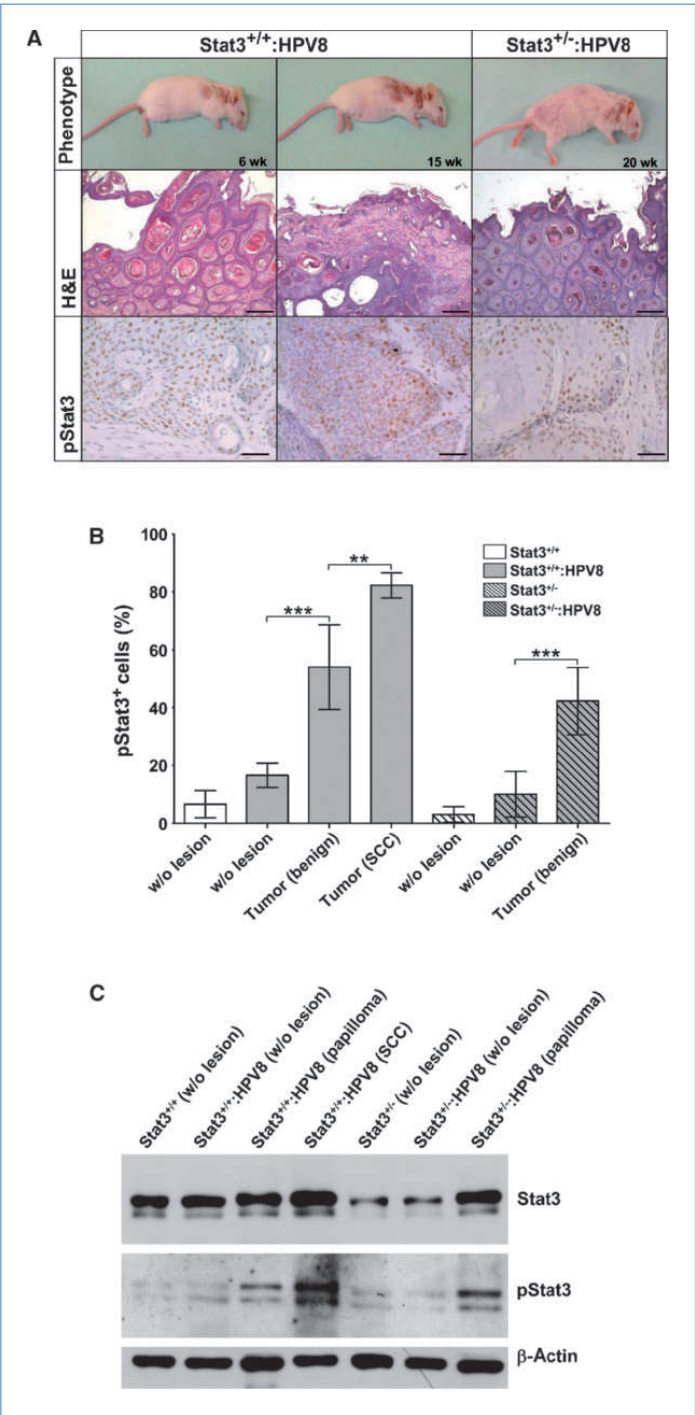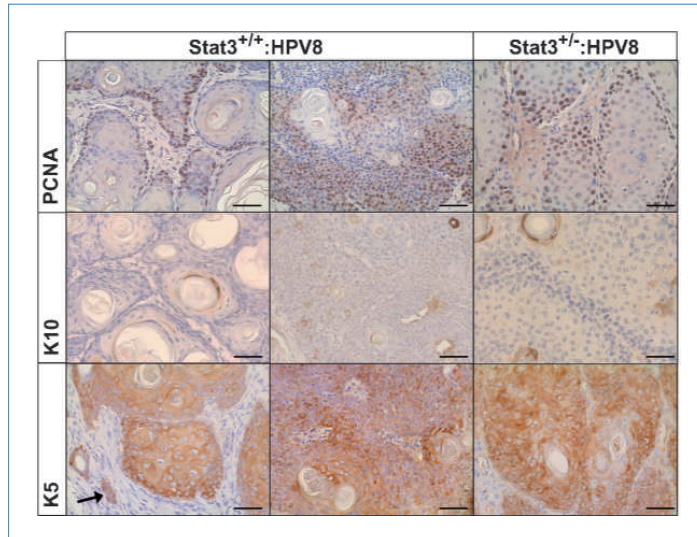
55

De Andrea et al.

Figure 5. Expression of PCNA, K10, and K5 in skin lesions from Stat3$^{+/-}$:HPV8 and Stat3$^{+/+}$:HPV8 mice. Immunohistochemistry of serial sections of the skin specimens shown in Fig. 4A stained for PCNA, K10, and K5. Dark brown, positive cells; blue, nuclear counterstaining. Scale bars, 25 μm. The arrow indicates an island of K5-positive keratinocytes in the dermis.

(K10) and of undifferentiated basal (K5) compartments of the epidermis. In control epidermis, K10 is expressed by postmitotic keratinocytes in the suprabasal layers during normal differentiation (data not shown). As shown in Fig. 5 (middle row), the hyperplasia of suprabasal keratinocytes induced by HPV8 oncoproteins in papillomas and carcinomas from Stat3$^{+/+}$:HPV8 mice was paralleled by a strong reduction of K10 expression in the inner suprabasal layers; expression was shifted outwards, sporadically observed in the flattened cells positioned just beneath the malformed corny layer. A similar pattern was observed in the papillomas from heterozygous mice, although clusters of K10-positive cells were still present in the more differentiated areas of the concentrically keratinized structures. The increased proliferation and hyperplasia of suprabasal keratinocytes induced by viral oncoprotein expression was accompanied by the accumulation of less differentiated suprabasal cells. This was indicated by the persistent expression of the basal marker K5 in the suprabasal layers and its retention throughout the hyperplastic epidermis (Fig. 5, bottom row). It is also worth mentioning that K5-positive invading keratinocytes were present in the dermal compartment of Stat3$^{+/+}$:HPV8 papillomas, confirming that these lesions are malignant, but never in Stat3$^{+/-}$:HPV8 papillomas.

The physiologic importance of Stat3 in the maintenance of skin integrity as well as the pathogenesis of skin diseases has been described in many experimental settings, including *in vitro* cell culture systems (19, 21, 31) and skin-specific Stat3-deficient mice obtained by conditional gene targeting (19). In the current study, by using a different Cre-LoxP strategy to that used by Sano and colleagues (19), we have confirmed the fundamental role of Stat3 in the maintenance of hair growth and epidermal homeostasis. Indeed, histology of

the skin from Stat3$^{-/-}$ mice revealed severe epidermal loss and alteration of hair architecture.

To comprehend further the biological functions of Stat3, we addressed the question of whether more subtle changes in Stat3 expression could also influence tumor development in our experimental setting. Stat3$^{+/-}$ mice appeared identical to their Stat3$^{+/+}$ littermates: They had no apparent abnormalities and lived a normal average life span. However, comparing tumor yields in Stat3$^{+/+}$:HPV8 versus Stat3$^{+/-}$:HPV8 mice revealed surprisingly highly significant effects of Stat3 heterozygosity on skin tumor susceptibility triggered by HPV8 early genes. Despite the rather modest effect on Stat3 expression, the effect on tumor development was considerable: Significantly fewer tumors were produced in Stat3$^{+/-}$:HPV8 mice compared with Stat3$^{+/+}$:HPV8 mice, a finding that provides genetic proof of the notion that even a relatively modest reduction in Stat3 expression can indeed affect tumor development in a rather profound manner. Moreover, all the tumors in the Stat3 heterozygous mice showed signs of being benign and never progressed to a more malignant phenotype. The rate and extent of keratinocyte proliferation, the delay in keratinocyte differentiation, and the level of pStat3 positively stained nuclei were similar between papillomas arising in Stat3$^{+/+}$:HPV8 and Stat3$^{+/-}$:HPV8 mice. These findings indicate that a certain amount of activated Stat3 is necessary to achieve uncontrolled proliferation, and therefore, only cells that display the appropriate levels of Stat3 will be capable of proliferating in response to the viral oncoproteins. Our findings support the emerging concept that differences in tissue expression levels of proteins involved in cell cycle control, resulting from either overexpression or reductions, can affect tumor susceptibility (32). Furthermore, a surprising number of complicated clinical manifestations associated with genetic

56

Stat3 Function in HPV8-Induced Skin Carcinogenesis

syndromes are due to mutations in genes encoding transcription factors (33). The mechanism through which transcription factor defects cause disease is often heterozygosity, indicating that half-normal levels of many transcription factors are simply not enough to provide normal function (34).

A causal link between Stat3 ablation and reduction in tumor yield was also shown by Bollrath and colleagues (35) in their Stat3$^{\Delta IEC}$, mice where Stat3 was selectively knocked out in all the epithelial cell lineages of the intestine. The Stat3$^{\Delta IEC}$ mice were generated by a Cre-LoxP strategy expressing Cre recombinase under the control of the intestine-specific villin gene promoter. Exposure of these Stat3$^{\Delta IEC}$ mice to the colitis-associated cancer challenge revealed that they were almost completely protected from the development of tubular adenomas induced by the colonotropic mutagen azoxymethane. Consistent with our findings, the few polypoid lesions protruding into the lumen that developed in a small proportion of Stat3$^{\Delta IEC}$ mice were markedly reduced in size.

Collectively, these studies provide for the first time evidence of a critical role of Stat3 in the experimental mouse model of HPV8-induced epithelial carcinogenesis and suggest that targeting Stat3 in keratinocytes may be a viable strategy for the prevention and treatment of HPV-induced skin cancer.

Disclosure of Potential Conflicts of Interest

No potential conflicts of interest were disclosed.

References

1. de Villiers EM, Fauquet C, Broker TR, Bernard HU, zur Hausen H. Classification of papillomaviruses. Virology 2004;324:17–27.
2. Snijders PJ, Steenbergen RD, Heideman DA, Meijer CJ. HPV-mediated cervical carcinogenesis: concepts and clinical implications. J Pathol 2006;208:152–64.
3. zur Hausen H. Papillomaviruses in the causation of human cancers—a brief historical account. Virology 2009;384:260–5.
4. Akgul B, Cooke JC, Storey A. HPV-associated skin disease. J Pathol 2006;208:165–75.
5. Nindl I, Gottschling M, Stockfleth E. Human papillomaviruses and non-melanoma skin cancer: basic virology and clinical manifestations. Dis Markers 2007;23:247–59.
6. Zavattaro E, Azzimonti B, Mondini M, et al. Identification of defective Fas function and variation of the perforin gene in an epidermodysplasia verruciformis patient lacking EVER1 and EVER2 mutations. J Invest Dermatol 2008;128:732–5.
7. Dell'oste V, Azzimonti B, De Andrea M, et al. High β-HPV DNA loads and strong seroreactivity are present in epidermodysplasia verruciformis. J Invest Dermatol 2009;129:1026–34.
8. Bouwes Bavinck JN, Plasmeijer EI, Feltkamp MC. β-Papillomavirus infection and skin cancer. J Invest Dermatol 2008;128:1355–8.
9. Pfister H. Chapter 8: Human papillomavirus and skin cancer. J Natl Cancer Inst Monogr 2003:52–6.
10. Schaper ID, Marcuzzi GP, Weissenborn SJ, et al. Development of skin tumors in mice transgenic for early genes of human papillomavirus type 8. Cancer Res 2005;65:1394–400.
11. Pfefferle R, Marcuzzi GP, Akgul B, et al. The human papillomavirus type 8 E2 protein induces skin tumors in transgenic mice. J Invest Dermatol 2008;128:2310–5.
12. Marcuzzi GP, Hufbauer M, Kasper HU, Weissenborn SJ, Smola S, Pfister H. Spontaneous tumour development in human papillomavirus type 8 E6 transgenic mice and rapid induction by UV-light exposure and wounding. J Gen Virol 2009;90:2855–64.
13. Dong W, Kloz U, Accardi R, et al. Skin hyperproliferation and susceptibility to chemical carcinogenesis in transgenic mice expressing E6 and E7 of human papillomavirus type 38. J Virol 2005;79:14899–908.
14. Michel A, Kopp-Schneider A, Zentgraf H, Gruber AD, de Villiers EM. E6/E7 expression of human papillomavirus type 20 (HPV-20) and HPV-27 influences proliferation and differentiation of the skin in UV-irradiated SKH-hr1 transgenic mice. J Virol 2006;80:11153–64.
15. Zhong Z, Wen Z, Darnell JE, Jr. Stat3: a STAT family member activated by tyrosine phosphorylation in response to epidermal growth factor and interleukin-6. Science 1994;264:95–8.
16. Levy DE, Darnell JE, Jr. Stats: transcriptional control and biological impact. Nat Rev Mol Cell Biol 2002;3:651–62.
17. Aggarwal BB, Kunnumakkara AB, Harikumar KB, et al. Signal transducer and activator of transcription-3, inflammation, and cancer: how intimate is the relationship? Ann N Y Acad Sci 2009;1171:59–76.
18. Takeda K, Noguchi K, Shi W, et al. Targeted disruption of the mouse Stat3 gene leads to early embryonic lethality. Proc Natl Acad Sci U S A 1997;94:3801–4.
19. Sano S, Itami S, Takeda K, et al. Keratinocyte-specific ablation of Stat3 exhibits impaired skin remodeling, but does not affect skin morphogenesis. EMBO J 1999;18:4657–68.
20. Chan KS, Sano S, Kiguchi K, et al. Disruption of Stat3 reveals a critical role in both the initiation and the promotion stages of epithelial carcinogenesis. J Clin Invest 2004;114:720–8.
21. Sano S, Chan KS, Kira M, et al. Signal transducer and activator of transcription 3 is a key regulator of keratinocyte survival and proliferation following UV irradiation. Cancer Res 2005;65:5720–9.
22. Chan KS, Sano S, Kataoka K, et al. Forced expression of a constitutively active form of Stat3 in mouse epidermis enhances malignant progression of skin tumors induced by two-stage carcinogenesis. Oncogene 2008;27:1087–94.
23. Kataoka K, Kim DJ, Carbajal S, Clifford JL, DiGiovanni J. Stage-specific disruption of Stat3 demonstrates a direct requirement during both the initiation and promotion stages of mouse skin tumorigenesis. Carcinogenesis 2008;29:1108–14.
24. Kim DJ, Angel JM, Sano S, DiGiovanni J. Constitutive activation and targeted disruption of signal transducer and activator of transcription 3 (Stat3) in mouse epidermis reveal its critical role in UVB-induced skin carcinogenesis. Oncogene 2009;28:950–60.
25. Tarutani M, Itami S, Okabe M, et al. Tissue-specific knockout of the mouse Pig-a gene reveals important roles for GPI-anchored proteins in skin development. Proc Natl Acad Sci U S A 1997;94:7400–5.

57

De Andrea et al.

26. Ehrenreiter K, Piazzolla D, Velamoor V, et al. Raf-1 regulates Rho signaling and cell migration. J Cell Biol 2005;168:955–64.
27. Chiarle R, Simmons WJ, Cai H, et al. Stat3 is required for ALK-mediated lymphomagenesis and provides a possible therapeutic target. Nat Med 2005;11:623–9.
28. Fuchs E. Keratins and the skin. Annu Rev Cell Dev Biol 1995;11: 123–53.
29. Byrne C, Fuchs E. Probing keratinocyte and differentiation specificity of the human K5 promoter in vitro and in transgenic mice. Mol Cell Biol 1993;13:3176–90.
30. Ramirez A, Bravo A, Jorcano JL, Vidal M. Sequences 5′ of the bovine keratin 5 gene direct tissue- and cell-type-specific expression of a lacZ gene in the adult and during development. Differentiation 1994;58:53–64.
31. Yin W, Cheepala S, Roberts JN, Syson-Chan K, DiGiovanni J, Clifford JL. Active Stat3 is required for survival of human squamous cell carcinoma cells in serum-free conditions. Mol Cancer 2006;5:15.
32. Santarosa M, Ashworth A. Haploinsufficiency for tumour suppressor genes: when you don't need to go all the way. Biochim Biophys Acta 2004;1654:105–22.
33. McKusick VA. OMIM™: Online Mendelian Inheritance in Man. Available from: http://www.ncbi.nlm.nih.gov/Omim/.
34. Seidman JG, Seidman C. Transcription factor haploinsufficiency: when half a loaf is not enough. J Clin Invest 2002;109:451–5.
35. Bollrath J, Phesse TJ, von Burstin VA, et al. gp130-mediated Stat3 activation in enterocytes regulates cell survival and cell-cycle progression during colitis-associated tumorigenesis. Cancer Cell 2009; 15:91–102.

58

10   Essential ERK-dependent and -independent roles of Raf in Ras-driven skin carcinogenesis

Florian Kern[1], Eszter Doma[1], Christian Rupp[1], Theodora Niault[1], and Manuela Baccarini[*,1]

[1]Max F. Perutz Laboratories, Department of Microbiology and Immunobiology, University of Vienna, 1030 Vienna, Austria

[*]Correspondence: Professor M. Baccarini; E-mail: manuela.baccarini@univie.ac.at

Relevance & Contribution: Using the same mouse and tumor models as in "Raf-1 Addiction in Ras-Induced Skin Carcinogenesis" this manuscript demonstrates an unprecedented essential role of B-Raf in Ras-driven tumorigenesis. In stark contrast to Raf-1 this crucial role of B-Raf is manifested through its kinase function to activate downstream MEK and ERK and the resulting implication on proliferation. Moreover, the concomitant ablation of B-Raf and Raf-1 in this system revealed that the involved processes are independent but act synergistic in tumor regression. The manuscript was written by M.B. and F.K., T.N. initiated the project and started the early experiments, the majority of the experiments were carried out by F.K..

Essential ERK-dependent and –independent roles of Raf in Ras-driven skin carcinogenesis

Florian Kern, Eszter Doma, Christian Rupp, Theodora Niault, and Manuela Baccarini

Department of Microbiology and Immunobiology, University of Vienna, Max F. Perutz Laboratories, Doktor-Bohr-Gasse 9, 1030 Vienna, Austria

Corresponding author: Manuela Baccarini; phone ++431 4277 54607; fax: ++431 4277 9546; email: manuela.baccarini@univie.ac.at

Running title: Roles of Raf in Ras-driven carcinogenesis

Summary

Ras carcinogenesis is assumed to depend on Raf for ERK activation and proliferation, yet a requirement for Raf as MEK/ERK activator could not yet be demonstrated. Here, we show that epidermis-restricted B-Raf ablation restrains the onset and stops the progression of established Ras-driven tumors by limiting MEK/ERK activation and proliferation. Concomitant elimination of B-Raf and Raf-1 enforces the abrupt regression of established tumors due to the decrease in ERK activation and proliferation caused by B-Raf ablation combined with the increase in Rok signaling and differentiation triggered by Raf-1 inactivation. Thus, B-Raf and Raf-1 have non-redundant functions in Ras-driven tumorigenesis, and the concomitant disruption of B-Raf- and Raf-1-dependent pathways would be an optimal strategy for the therapy of Ras-dependent epidermal tumors.

1

Significance

As the activator of the MEK/ERK pathway, Raf has long been considered the most promising druggable Ras effector. Potent Raf inhibitors have been developed which achieve impressive results in melanomas harboring oncogenic BRAF, but are ineffective against Ras-driven tumors; moreover, alarming side-effects (paradox ERK activation driving therapy-related skin tumors) as well as primary and acquired resistance have been reported. In our system, B-Raf ablation reduces ERK activation and stops tumor growth, but sudden and complete regression is only achieved by the concomitant ablation of Raf-1 and the ensuing reactivation of a differentiation program. These results suggest that therapies targeting both Raf-dependent pathways may be effective against a broader range of malignancies and reduce the risks of adverse effects and/or resistance.

Highlights:

- B-Raf is necessary for the initiation and progression of Ras-driven epidermal tumors.

- B-Raf is required for full-fledged ERK activation and proliferation.

- B-Raf and Raf-1 have non-redundant roles in Ras-driven tumorigenesis.

- Compound B-Raf/Raf-1 ablation leads to abrupt tumor regression.

2

Introduction

The epidermis constantly turns over to preserve its function as a barrier between the body and the environment. Changes in this self-renewal process, such as keratinocyte proliferation/differentiation defects can induce skin barrier defects or lead to tumor formation. Squamous cell carcinoma (SCC), a prevalent human skin cancer, is an example of a condition caused by an imbalance between keratinocyte proliferation, differentiation, and apoptosis. Activation of the small GTPase Ras is observed in the majority of human SCC and is considered a pivotal event in its development (Kern et al., 2011; Khavari and Rinn, 2007). In animal models, activation of Ras by the transgenic expression of Ras mutant or by the expression of Ras activating guanine nucleotide exchange factors (GEFs) in the basal layer of mouse epidermis induces proliferation, promotes survival, and inhibits differentiation (Khavari and Rinn, 2007; Oki-Idouchi and Lorenzo, 2007; Sibilia et al., 2000; Vitale-Cross et al., 2004).

Ras activation stimulates multiple effector molecules, several of which have been implicated in distinct aspects of skin tumorigenesis by gain- and loss-of-function experiments in the mouse. They include the phosphoinositide-3 kinases (PI-3K)/Akt and the Tiam-1/Rac1 pathway, implicated in both proliferation (Malliri et al., 2002; Murayama et al., 2007; Wang et al., 2010) and survival (Gupta et al., 2007; Malliri et al., 2002; Sibilia et al., 2000); and the Ral-GDS pathway, which protect the cells from apoptosis (Gonzalez-Garcia et al., 2005).

Undoubtedly however, the Ras effector branch most directly connected with proliferation is the Raf/MEK/ERK pathway (Kern et al., 2011; Khavari and Rinn, 2007), a three-tiered kinase cascade in which each tier is represented by more than one enzyme. In mammals, there are three Raf isoforms (A-Raf, B-Raf, and Raf-1, also known as C-Raf), all of which bind to Ras and phosphorylate MEK; two MEK isoforms, both of which are phosphorylated by Raf and have a single common target, ERK; and two ERK isoforms, for which more than 100 substrates have

3

been described. In mouse models, epidermis-restricted, inducible activation of Raf or MEK causes cutaneous hyperplasia and reduced differentiation (Khavari and Rinn, 2007). While the ablation of B-Raf (Galabova-Kovacs et al., 2006), Raf-1 (Ehrenreiter et al., 2005), MEK1, MEK2 (Scholl et al., 2007), ERK1 or ERK2 (Dumesic et al., 2009) does not impair epidermal homeostasis, simultaneous MEK1/MEK2 ablation results in hypoplasia and perinatal death (Scholl et al., 2007), and compound ERK1/ERK2 ablation inhibits keratinocyte division (Dumesic et al., 2009); in addition, reducing the expression of MEK impairs Ras-induced epidermic hyperplasia (Scholl et al., 2009a), and MEK1 or ERK1 ablation decreases chemical carcinogenesis (Bourcier et al., 2006; Scholl et al., 2009b).

More recently, we have shown that one of the Raf kinases, Raf-1, is essential for both development and maintenance of Ras-driven tumors *in vivo* (Ehrenreiter et al., 2009). Surprisingly, Raf-1 was not required for the activation of the ERK pathway, but for the inhibition of the Rho-dependent kinase Rok-α, which drives keratinocyte differentiation (Ehrenreiter et al., 2009; Kern et al., 2011). Consistent with this crucial role, RAF1 is overexpressed in human SCC (Riva et al., 1995).

Within the Raf/MEK/ERK pathway, BRAF is the only member frequently found mutated in human tumors, particularly in melanoma. The most common mutation, V600E, activates the kinase, resulting in sustained MEK/ERK signaling; less frequently, BRAF mutations reduce catalytic activity but induce the formation of BRAF/RAF1 heterodimers in which BRAF stimulates wild-type RAF1 in trans [reviewed in (Niault and Baccarini, 2010; Wimmer and Baccarini, 2010)]. Recently, selective BRAFV600E inhibitors have shown exceptional response rates in metastatic melanoma trials, a major breakthrough in the therapy of this incurable disease (Bollag et al., 2010; Flaherty et al., 2010). The side effects are mild, but they include the rapid appearance of Keratoacanthomas and SCC in situ (Brower, 2010; Cichowski and Janne, 2010;

4

Wimmer and Baccarini, 2010). The molecular mechanism underlying this phenomenon are unknown, but it has been postulated that they may be connected to the ability of the inhibitors to promote the formation of BRAF/RAF1 dimers and activate the ERK pathway in wild-type cells and in cells expressing Ras mutations (Hatzivassiliou et al., 2010; Poulikakos et al., 2010).

Together, the results above confirm the role of Raf and of the ERK pathway in promoting proliferation and inhibiting differentiation in the epidermis.

Against this background, we have generated an epidermis-restricted B-Raf knock-out (*K5Cre;b-raf*$^{flox/flox}$ mice; hereafter referred to as *Δ/Δ*^{ep}) as well as mouse strains allowing tamoxifen-inducible, epidermis-restricted ablation (Indra et al., 1999) of B-Raf, alone or in combination with Raf-1, to investigate the role of Raf in Ras-driven epidermis carcinogenesis, using either the DMBA/TPA chemical carcinogenesis protocol (Ise et al., 2000) or a genetic model in which a membrane-tethered form of the Ras activator SOS expressed in basal keratinocytes (Sibilia et al., 2000) results in the constitutive activation of endogenous Ras, observed more frequently than Ras mutations in human SCC (Dajee et al., 2003).

5

Results

B-Raf ablation restrains Ras-dependent tumor formation. To investigate the role of B-Raf in Ras-dependent tumor formation, we combined epidermis-restricted B-Raf ablation (Δ/Δ^{ep}, deleted in epidermis) with the DMBA/TPA chemical carcinogenesis protocol, driven by an activating mutation in codon 61 of the *ras* gene (Quintanilla et al., 1986); or with a genetic model in which the expression of a membrane-tethered form of the Ras-GEF son of sevenless (SOS) expressed under the control of the K5 promoter [K5-SOS-F (Sibilia et al., 2000)] mimics the activation of endogenous, wild-type Ras observed in the majority of human SCCs (Dajee et al., 2003). Application of DMBA/TPA to the dorsal skin of wild-type (*f/f*) mice induced visible tumors within 6 weeks, with a 50% penetrance by week 13 (Figure 1A-B). 100% of the *K5-SOS-F+;f/f* mice developed visible, fast-growing tumors, mostly papillomas, predominantly on the tail, ears, and at sites subjected to scratching and biting (Sibilia et al., 2000) by the 6th week of life (Figure 1H). B-Raf ablation significantly delayed the onset of both DMBA/TPA tumors (from week 6 to 13, Figure 1A), and of K5-SOS-F-driven tumors (from week 3 to week 11, Figure 1H). While most Δ/Δ^{ep} animals developed chemically induced tumors (90% penetrance, Figure 1B), only 35% *K5-SOS-F+;Δ/Δ^{ep}* mice were affected (Figure 1E); in both cases, the tumors grew very slowly, were much smaller than the *f/f* tumors (Figure 1C and 1G), and didn't affect the general health of the mice.

Chemically induced *f/f* and Δ/Δ^{ep} tumors examined at week 20 were papillomas of different sizes but similar in structure, projecting above the surrounding tissue (Figure 1A, C-D). Similarly, the analysis of size-matched *K5-SOS-F+;f/f* and *K5-SOS-F+;Δ/Δ^{ep}* did not reveal any structural differences between genotypes (Figure 1H). In the latter case, since Δ/Δ^{ep} tumors never reached the size of *f/f* tumors, only small and medium-sized tumors, all papillomas, were analyzed; and

6

due to their slow growth rate, the Δ/Δ^{ep} samples were taken from animals much older than the *f/f* tumors. Although the numbers of proliferating cells in the tumors varied, chemically induced and *K5-SOS-F+* Δ/Δ^{ep} tumors contained about 50% less BrdU+ cells than *f/f* tumors (Figure 1D-E, and H-I). *f/f* tumors expressed the differentiation marker K10 only in 24-28% of the cells confined to the uppermost layer of the epidermis (Grade 3-4 according to Broder's classification). In contrast, Δ/Δ^{ep} papillomas contained around between 72% and 79% K10^{+} cells (Grade 1-2; Figure 1D-E and H-I).

Apoptotic cells were rarely found in *f/f* and Δ/Δ^{ep} tumors (Supplementary Figure 1A-B). Thus, B-Raf ablation reduced proliferation and increased differentiation in both chemically induced and SOS-F-driven tumors. Consistent with this, SOS-F expression failed to induce proliferation and to prevent differentiation in B-Raf-deficient epidermis (Figure 2A-D).

Together, these data indicate a requirement for B-Raf in the development of Ras-driven epidermal tumors.

B-Raf is necessary for the growth of established *K5-SOS-F*-induced tumors. We have recently shown that Raf-1 is absolutely required for the maintenance of SOS-F-induced tumors (Ehrenreiter et al., 2009). We used the same system to investigate whether a similar requirement exists for B-Raf, namely *K5-SOS-F;K5-Cre-ER(T);b-raf$^{f/f}$* mice, in which the Cre recombinase is expressed from the K5 promoter as a fusion protein that can be activated by 4-hydroxy-tamoxifen (TX) binding (Indra et al., 1999). To induce *b-raf* ablation, *K5-SOS-F;K5-Cre-ER(T);b-raf$^{f/f}$* and their *K5-SOS-F;b-raf$^{f/f}$* littermates bearing tumors of 0.3-0.7 cm in diameter were injected with TX (1mg/day intraperitoneally, 5 consecutive injections). *f/f* tumors progressed, doubling or tripling in size in the 2 weeks after the last TX injection, whereas the lesions from conditional knock-out mice ($\Delta/\Delta^{ep}TX$) stopped growing and partially regressed, without ever resolving

7

completely (Figure 3A and 3B). The *f/f* allele was efficiently converted to *Δ/Δ* in these lesions, indicating that their persistence was not due to incomplete recombination (Supplementary Figure 2). Of note, TX injection does not slow down tumor progression in *K5-SOS-F;K5-Cre-ER(T)* mice (Lichtenberger et al., 2010). The standstill of the *Δ/Δ^{ep}TX* tumors was accompanied by a 50% decrease in the number of proliferating cells, all restricted to the basal level (Figure 3C); importantly, however, the number of proliferating cells did not decrease further with time and remained constantly above the 3-5% BrdU+ cells detected in normal epidermis. The number of differentiating cells increased and suprabasal K10 staining was restored (Figure 3D). The compaction and thickness of the suprabasal layer, however, never reached control levels. *Δ/Δ^{ep}TX* tumors contained hardly any apoptotic cells (Supplementary Figure 1C). Together, the data indicate that the progression of B-Raf KO tumors is brought to a halt by a decrease in proliferation accompanied by a gradual increase in differentiation of the tumor cells (Figure 3C-D).

B-Raf-deficiency alters the proliferation and increases the differentiation of *K5-SOS-F*+ keratinocytes in vitro. To determine the relationship between decreased proliferation and increased differentiation in B-Raf-deficient tumors, we isolated primary keratinocytes and monitored their ability to proliferate and differentiate in vitro. The consequences of B-Raf ablation on keratinocyte proliferation were determined by assessing the percentage of cells incorporating BrdU, to avoid taking into account the reduction of cell numbers due to increased differentiation or decreased survival. In vitro, *K5-SOS-F*+ keratinocytes proliferate very poorly (Figure 3E) (Ehrenreiter et al., 2009), in agreement with the many observations showing that both cultured cells and premalignant tumors react to the hyperactivation of the Ras/Raf/MEK/ERK pathway with growth arrest (Maurer et al., 2011). B-Raf ablation, which lowered the level of MEK/ERK activation (Figure 4 A-B), relieved this growth arrest and allowed the proliferation of

8

cultured *K5-SOS-F+* keratinocytes. We next exposed cells of different genotypes to high $CaCl_2$

concentrations to induce keratinocyte differentiation, determined as the number of Involucrin+

cells developing in the cultures. The number of BrdU+ cells decreased, and that of Involucrin+

cells increased, in *f/f* and Δ/Δ^{ep} keratinocytes cultured in the presence of 1.2mM $CaCl_2$. Under

these conditions, *K5-SOS-F* expression maintained proliferation and prevented the differentiation

of *f/f* keratinocytes; B-Raf ablation reduced SOS-F-driven proliferation and partially restored

differentiation (Figure 3F-G). These results are entirely consistent with those obtained in vivo

(Figure 1-3).

B-Raf ablation correlates with reduced ERK activation in vitro and in vivo. To gain insight

in the mechanisms underlying the Δ/Δ^{ep} phenotype, we monitored the activation of the classical

Raf effectors MEK/ERK. MEK/ERK phosphorylation was reduced in B-Raf-deficient

keratinocytes deprived of growth factors for 12 hrs; the pathway still reacted to growth factor

stimulation and was induced by *K5-SOS-F* expression, but less efficiently than in *f/f* cells (Figure

4A-B). ERK phosphorylation was also reduced in B-Raf-deficient keratinocytes during $CacCl_2$-

induced differentiation (Figure 4C). Activation of the Rok pathway, which plays a crucial role in

keratinocyte differentiation (Ehrenreiter et al., 2009; Lock and Hotchin, 2009; McMullan et al.,

2003) was measured by the phosphorylation of the downstream target cofilin. SOS-F inhibited

cofilin phosphorylation; in agreement with our previous data showing that pharmacological

MEK/ERK inhibition induces cofilin phosphorylation in wild-type and *K5-SOS-F+*

keratinocytes (Ehrenreiter et al., 2009), reduced ERK phosphorylation in B-Raf deficient cells

correlated with a partial rescue of cofilin phosphorylation. In vivo, B-Raf ablation completely

prevented ERK phosphorylation in *K5-SOS-F+* epidermis at the time of tumor onset (Figure 4D)

and strongly reduced it in established tumors (Figure 4E, upper panel). Consistent with the

increased differentiation observed in the B-Raf-deficient tumors (Figure 3D), cofilin

9

phosphorylation was also increased; however, close examination revealed that the staining was mostly confined to the suprabasal layers, while basal keratinocytes were typically negative (Figure 4E, lower panel).

Concomitant ablation of B-Raf and Raf-1 causes the abrupt regression of Ras-driven tumors. The signaling alterations described above are clearly distinct from those caused by Raf-1 ablation, in which ERK activation was maintained but cofilin phosphorylation was induced in cells of the basal layer (Ehrenreiter et al., 2009). To investigate the genetic interaction between B-Raf and Raf-1-dependent pathways in Ras-driven epidermal tumors, we generated *K5-SOS-F*-expressing conditional double knockout mice (*Δ/Δ^{ep2}TX*) and induced the deletion of both alleles in tumors of approximately 0.3-0.7 cm of diameter. Double knockout tumors stopped growing virtually immediately and the tissue returned to normal within 18 days of ablation (Figure 5A-B), indicating that B-Raf and Raf-1 act synergistically to sustain Ras-driven tumorigenesis. The regressing tumors showed a profound decrease in proliferation and a strong increase in differentiation, but again no increase in apoptotic cells (Figure 5C; and Supplementary Figure 1C). Mechanistically, ERK phosphorylation was strongly decreased, while cofilin phosphorylation was increased in the regressing tumors, including the basal layer (Figure 5D). Consistent with this, phosphorylation of STAT3 and expression of c-myc, downstream effectors of cofilin (Ehrenreiter et al., 2009; Honma et al., 2006), was abrogated in the regressing tumors (Supplementary Figure 3). In line with the in vivo phenotype, continuously growing and differentiating double knockout keratinocytes proliferated poorly in culture (Figure 5E), and differentiated even more efficiently than wild-type cells despite the presence of SOS-F (Figure 5F). Continuously growing double knockout cells showed both the decrease in pERK typical of the B-Raf-deficient keratinocytes and the robust increase in pCofilin characteristic of Raf-1-deficient cells (Figure 5G). Double knockout cells simply combined the effects on ERK and

10

71

Cofilin phosphorylation observed in the single knockout cells, implying distinct essential

functions of B-Raf and Raf-1 in Ras-driven ERK activation and cross-talk with the Rho pathway.

11

Discussion

Our data provide evidence that B-Raf ablation in keratinocytes strongly reduces carcinogenesis driven by mutational activation of Ras (DMBA/TPA model) or by the constitutive activation of endogenous Ras (K5-SOS-F model). Thus, B-Raf joins Raf-1 (Ehrenreiter et al., 2009) and Rac1 (Wang et al., 2010) in the list of Ras effectors required in a cell-autonomous manner for this process. These data represent the first in vivo demonstration that B-Raf is essential for Ras-driven tumorigenesis; indeed, B-Raf is dispensable for the development of non-small cell lung carcinoma downstream of oncogenic K-Ras, while Raf-1 is absolutely required (Blasco et al., 2011; Karreth et al., 2011).

In the epidermis, B-Raf ablation stops the growth of established tumors and causes their slow regression, indicating a requirement that extends to tumor progression. Among the Ras effectors, a requirement for tumor maintenance has so far been demonstrated only for Raf-1 (Ehrenreiter et al., 2009). The two Raf kinases, however, act on distinct signaling pathways and processes downstream of Ras in the epidermis. Consistent with the observation that inducible activation of Raf or MEK in the epidermis induces cutaneous hyperplasia and reduces differentiation (Ridky and Khavari, 2004), B-Raf is necessary for full-fledged MEK/ERK activation and supports cell proliferation at the expense of differentiation in *K5-SOS-F+* tumors in vivo and in CaCl$_2$-treated keratinocytes in vitro (Figures 1-3). Residual MEK/ERK activation in B-Raf cells, mediated either by the other Raf kinases or by alternative kinases such as PAK (Wang et al., 2010), is not sufficient to induce growth arrest in premalignant, *K5-SOS-F+* keratinocytes (Figure 3E) and to sustain tumorigenesis. These data are in agreement with previous results showing that MEK gene dosage, and therefore strength of ERK activation, is rate-limiting for the hyperplastic response of mouse epidermis to activated Ras (Scholl et al., 2009a).

12

In contrast to B-Raf, Raf-1 is dispensable for ERK activation (Figure 5G), and its ablation does relieve the growth arrest induced by *K5-SOS-F+* in cultured premalignant keratinocytes (Ehrenreiter et al., 2009). Instead, Raf-1 works as an endogenous Rok-α inhibitor to counteract differentiation in keratinocyte cultures and in vivo, where Raf-1 ablation induces the synchronous activation of Rok-α (measured as the phosphorylation of the downstream target Cofilin) in all layers of the epidermis, enforces differentiation, and causes complete tumor regression (Ehrenreiter et al., 2009).

Together, these data suggest that B-Raf alters the balance between proliferation and differentiation primarily by acting as a MEK/ERK activator and thereby sustaining SOS-F-induced proliferation in tumors; Raf-1, in contrast, acts primarily as a Rok-α inhibitor preventing differentiation and thereby allowing sustained proliferation.

The effects of the two Raf proteins are independent from one another, and double knockout keratinocytes recapitulate the biochemical alterations observed in the single knockouts without evidence for synergism at the level of the ERK and Cofilin pathway; alterations in both pathways, however, engender the synergistic regression of SOS-F-induced tumors upon concomitant ablation of B-Raf and Raf-1. Interestingly, the Raf proteins, alone or in combination, do not play essential role in apoptosis (Supplementary Figure 1) (Ehrenreiter et al., 2009). This function appears to be effected in vivo by other Ras downstream targets such as RalGDS or PI-3K (Gonzalez-Garcia et al., 2005; Gupta et al., 2007).

The data above indicate that the concomitant disruption of both Raf-1 and B-Raf-dependent signaling pathways would be an optimal strategy for the therapy of Ras-dependent skin tumors, and possibly of other malignancies. In melanoma expressing activating B-Raf mutations, for instance, RAF inhibitors achieve spectacular clinical success, but only in doses causing ≥80% inhibition of the ERK pathway (Bollag et al., 2010); such levels of ERK inhibition, however,

13

might have considerable side effects, as suggested by the lethal outcome of compound MEK1/2
or ERK1/2 ablation in adult mice, while the compound knockout of B-Raf and Raf-1 is well
tolerated (Blasco et al., 2011). In addition, both primary insensitivity and acquired resistance to
RAF inhibitors have been reported (Downward, 2011; Solit and Rosen, 2011), and in a subset of
melanoma cells they correlate with elevated RAF1 protein levels (Montagut et al., 2008). Finally,
B-Raf mutations that do not increase intrinsic kinase activity appear to signal through Raf-1
downstream of Ras in melanoma (Heidorn et al., 2010); and about 30% metastatic melanoma
patients benefiting from the treatment with currently available Raf inhibitors develop squamous
cell carcinomas (Bollag et al., 2010; Flaherty et al., 2010), tentatively attributed to the activation
of the MEK/ERK pathway by drug-induced B-Raf-Raf-1 dimers (Hatzivassiliou et al., 2010;
Poulikakos et al., 2010; Wimmer and Baccarini, 2010). Taken together, the evidence that Raf-1
operates via direct protein-protein interaction with B-Raf, Rok-α, or other targets in the epidermis
(Ehrenreiter et al., 2009; Hatzivassiliou et al., 2010), and possibly in other tissues (Blasco et al.,
2011; Karreth et al., 2011) makes therapeutic strategies silencing Raf-1 and B-Raf expression or
small molecule inhibitors disrupting protein-protein interactions appear preferable to those aimed
at blocking enzymatic activity; by simultaneously targeting both kinase-dependent and-
independent Raf signaling pathways, these therapies might reduce the risk of adverse effects as
well as the incidence of primary or acquired resistance.

14

Experimental procedures

Mouse Strains, Genotyping, and Tumor Models. b-raf $^{f/f}$, c-raf-1$^{f/f}$, K5-SOS-F, *K5-Cre,* and *K5-Cre-er(T)* mice and the respective genotyping have been described (Chen et al., 2006; Ehrenreiter et al., 2009; Indra et al., 1999; Sano et al., 1999; Sibilia et al., 2000). *K5-Cre;b-raf $^{f/f}$(b-raf$^{Δ/Δep}$)* and *K5-Cre-er(T); b-raf $^{f/f}$(Δ/Δ^{ep}TX)* and *K5-Cre-er(T); b-raf $^{f/f}$;c-raf-1$^{f/f}$ (doubleΔ/Δ^{ep}TX)*, plus or minus the *K5-SOS-F+* trangenes were bred by crossing the appropriate genotypes. All strains were maintained on a 129Sv background. Genotyping was performed as described previously (Ehrenreiter et al., 2009; Galabova-Kovacs et al., 2006). All animal experiments were performed in accordance with a protocol authorized by the Austrian Ministry of Science and Communications, following the approval by the national Ethical Committee for Animal Experimentation.

Laser Capture Microdissection

To confirm the efficient conversion of the *b-raf f/f* to *Δ/Δ* alleles in tamoxifen-injected animals a Leica LMD6500-Laser Capture Microdissection / Imaging Unit was used to dissect 50.000 - 100.000 µm^2 from rehydrated 7 µm thick tumor sections from PEN-MembranSlides. The collected tissue was digested and genotyped using the standard PCR protocol with extended cycle numbers.

Statistical Analysis

All values plotted represent the mean (±SD) of at least three independent experiments. *p* values were calculated with the two-tailed Student's t test. A p value <0.05 is considered statistically significant.

Histological Analysis

Hematoxylin/eosin staining and immunohistochemistry were performed on 3-µm-thick sections of 4% paraformaldehyde-fixed and paraffin-embedded tissues (Ehrenreiter et al., 2009). Staining

15

with the following antibodies was performed: α-BrdU (1:100; abcam); α-c-myc (1:250; Milipore); α-K5 and a-K10 (1:500; BabCo); α-pCofilin (Ser3, 1:50; Santa Cruz); α-pERK (Thr202/Tyr204, 1:50; Cell Signaling); and α-pSTAT3 (Tyr705, 1:100; Cell Signaling). For detection, we used the DAKO EnVision peroxidase system, followed by incubation with 0.01% diaminobenzidine (Sigma), in conjunction with avidin-biotinylated enzyme complex (Vector Laboratories) for biotinylated antibodies. Sections were counterstained with hematoxylin. BrdU incorporation was determined in mice injected with BrdU (12.5 mg/g body weight) 1 hr prior to tissue isolation.

Keratinocyte Isolation and Culture

Primary mouse keratinocytes were isolated from 18- to 21-day-old mice as previously described (Ehrenreiter et al., 2009). Differentiation was induced by transferring the cells into starvation medium (containing only 2% chelated FCS and no growth factors) and treating them with 1.2 mM CaCl2 for different time periods. Differentiated cells were detected by immunofluorescence using α-Involucrin antibodies (1:500; BabCo) followed by a secondary FITC antibody (α-rabbit Alexa 448 nm, 1:1500; Molecular Probes). Microscopical analysis was performed with an Axiovert 200 (Carl Zeiss MicroImaging, Inc.) equipped with an AxioCam. Images were acquired with the AxioVision Software (Carl Zeiss MicroImaging, Inc.) Proliferation was assessed by the In Situ Cell Proliferation Kit FLUOS (Roche) according to the manufacturer's recommendation. Cells were examined by light microscopy (Zeiss AxioVision; Carl Zeiss MicroImaging, Inc.), and the number of BrdU+ cells was quantified.

Immunoblotting

Membranes were probed with α-Cofilin (Abcam); α-panERK, α-Raf-1, α-Rok-a (Transduction Labs); α-B-Raf, α-pCofilin, α-14-3-3 (Santa Cruz); α-pERK (Cell Signaling); and α-SOS (BD

16

Biosciences). After incubation with the appropriate secondary antibody, the antigens were visualized by ECL (Pierce).

References

Blasco, R. B., Francoz, S., Santamaria, D., Canamero, M., Dubus, P., Charron, J., Baccarini, M., and Barbacid, M. (2011). c-Raf, but Not B-Raf, Is Essential for Development of K-Ras Oncogene-Driven Non-Small Cell Lung Carcinoma. Cancer Cell *19*, 652-663.

Bollag, G., Hirth, P., Tsai, J., Zhang, J., Ibrahim, P. N., Cho, H., Spevak, W., Zhang, C., Zhang, Y., Habets, G.*, et al.* (2010). Clinical efficacy of a RAF inhibitor needs broad target blockade in BRAF-mutant melanoma. Nature *467*, 596-599.

Bourcier, C., Jacquel, A., Hess, J., Peyrottes, I., Angel, P., Hofman, P., Auberger, P., Pouyssegur, J., and Pages, G. (2006). p44 mitogen-activated protein kinase (extracellular signal-regulated kinase 1)-dependent signaling contributes to epithelial skin carcinogenesis. Cancer Res *66*, 2700-2707.

Brower, V. (2010). BRAF inhibitors: research accelerates in wake of positive findings. J Natl Cancer Inst *102*, 214-215.

17

Chen, A. P., Ohno, M., Giese, K. P., Kuhn, R., Chen, R. L., and Silva, A. J. (2006). Forebrain-specific knockout of B-raf kinase leads to deficits in hippocampal long-term potentiation, learning, and memory. J Neurosci Res *83*, 28-38.

Cichowski, K., and Janne, P. A. (2010). Drug discovery: Inhibitors that activate. Nature *464*, 358-359.

Dajee, M., Lazarov, M., Zhang, J. Y., Cai, T., Green, C. L., Russell, A. J., Marinkovich, M. P., Tao, S., Lin, Q., Kubo, Y., and Khavari, P. A. (2003). NF-kappaB blockade and oncogenic Ras trigger invasive human epidermal neoplasia. Nature *421*, 639-643.

Downward, J. (2011). Targeting RAF: trials and tribulations. Nat Med *17*, 286-288.

Dumesic, P. A., Scholl, F. A., Barragan, D. I., and Khavari, P. A. (2009). Erk1/2 MAP kinases are required for epidermal G2/M progression. J Cell Biol *185*, 409-422.

Ehrenreiter, K., Kern, F., Velamoor, V., Meissl, K., Galabova-Kovacs, G., Sibilia, M., and Baccarini, M. (2009). Raf-1 addiction in Ras-induced skin carcinogenesis. Cancer Cell *16*, 149-160.

Ehrenreiter, K., Piazzolla, D., Velamoor, V., Sobczak, I., Small, J. V., Takeda, J., Leung, T., and Baccarini, M. (2005). Raf-1 regulates Rho signaling and cell migration. J Cell Biol *168*, 955-964.

Flaherty, K. T., Puzanov, I., Kim, K. B., Ribas, A., McArthur, G. A., Sosman, J. A., O'Dwyer, P. J., Lee, R. J., Grippo, J. F., Nolop, K., and Chapman, P. B. (2010). Inhibition of mutated, activated BRAF in metastatic melanoma. N Engl J Med *363*, 809-819.

Galabova-Kovacs, G., Matzen, D., Piazzolla, D., Meissl, K., Plyushch, T., Chen, A. P., Silva, A., and Baccarini, M. (2006). Essential role of B-Raf in ERK activation during extraembryonic development. Proc Natl Acad Sci U S A *103*, 1325-1330.

18

Gonzalez-Garcia, A., Pritchard, C. A., Paterson, H. F., Mavria, G., Stamp, G., and Marshall, C. J. (2005). RalGDS is required for tumor formation in a model of skin carcinogenesis. Cancer Cell *7*, 219-226.

Gupta, S., Ramjaun, A. R., Haiko, P., Wang, Y., Warne, P. H., Nicke, B., Nye, E., Stamp, G., Alitalo, K., and Downward, J. (2007). Binding of ras to phosphoinositide 3-kinase p110alpha is required for ras-driven tumorigenesis in mice. Cell *129*, 957-968.

Hatzivassiliou, G., Song, K., Yen, I., Brandhuber, B. J., Anderson, D. J., Alvarado, R., Ludlam, M. J., Stokoe, D., Gloor, S. L., Vigers, G.*, et al.* (2010). RAF inhibitors prime wild-type RAF to activate the MAPK pathway and enhance growth. Nature *464*, 431-435.

Heidorn, S. J., Milagre, C., Whittaker, S., Nourry, A., Niculescu-Duvas, I., Dhomen, N., Hussain, J., Reis-Filho, J. S., Springer, C. J., Pritchard, C., and Marais, R. (2010). Kinase-Dead BRAF and Oncogenic RAS Cooperate to Drive Tumor Progression through CRAF. Cell *140*, 209-221.

Honma, M., Benitah, S. A., and Watt, F. M. (2006). Role of LIM kinases in normal and psoriatic human epidermis. Mol Biol Cell *17*, 1888-1896.

Indra, A. K., Warot, X., Brocard, J., Bornert, J. M., Xiao, J. H., Chambon, P., and Metzger, D. (1999). Temporally-controlled site-specific mutagenesis in the basal layer of the epidermis: comparison of the recombinase activity of the tamoxifen-inducible Cre-ER(T) and Cre-ER(T2) recombinases. Nucleic Acids Res *27*, 4324-4327.

Ise, K., Nakamura, K., Nakao, K., Shimizu, S., Harada, H., Ichise, T., Miyoshi, J., Gondo, Y., Ishikawa, T., Aiba, A., and Katsuki, M. (2000). Targeted deletion of the H-ras gene decreases tumor formation in mouse skin carcinogenesis. Oncogene *19*, 2951-2956.

Karreth, F. A., Frese, K. K., DeNicola, G. M., Baccarini, M., and Tuveson, D. A. (2011). C-Raf Is Required for the Initiation of Lung Cancer by K-RasG12D Cancer Discovery *in press*.

19

Kern, F., Niault, T., and Baccarini, M. (2011). Ras and Raf pathways in epidermis development
and carcinogenesis. Br J Cancer *104*, 229-234.

Khavari, T. A., and Rinn, J. (2007). Ras/Erk MAPK signaling in epidermal homeostasis and
neoplasia. Cell Cycle *6*, 2928-2931.

Lichtenberger, B. M., Tan, P. K., Niederleithner, H., Ferrara, N., Petzelbauer, P., and Sibilia, M.
(2010). Autocrine VEGF signaling synergizes with EGFR in tumor cells to promote epithelial
cancer development. Cell *140*, 268-279.

Lock, F. E., and Hotchin, N. A. (2009). Distinct roles for ROCK1 and ROCK2 in the regulation
of keratinocyte differentiation. PLoS ONE *4*, e8190.

Malliri, A., van der Kammen, R. A., Clark, K., van der Valk, M., Michiels, F., and Collard, J. G.
(2002). Mice deficient in the Rac activator Tiam1 are resistant to Ras-induced skin tumours.
Nature *417*, 867-871.

Maurer, G., Tarkowski, B., and Baccarini, M. (2011). Raf kinases in cancer-roles and therapeutic
opportunities. Oncogene.

McMullan, R., Lax, S., Robertson, V. H., Radford, D. J., Broad, S., Watt, F. M., Rowles, A.,
Croft, D. R., Olson, M. F., and Hotchin, N. A. (2003). Keratinocyte differentiation is regulated by
the Rho and ROCK signaling pathway. Curr Biol *13*, 2185-2189.

Montagut, C., Sharma, S. V., Shioda, T., McDermott, U., Ulman, M., Ulkus, L. E., Dias-
Santagata, D., Stubbs, H., Lee, D. Y., Singh, A*., et al.* (2008). Elevated CRAF as a potential
mechanism of acquired resistance to BRAF inhibition in melanoma. Cancer Res *68*, 4853-4861.

Murayama, K., Kimura, T., Tarutani, M., Tomooka, M., Hayashi, R., Okabe, M., Nishida, K.,
Itami, S., Katayama, I., and Nakano, T. (2007). Akt activation induces epidermal hyperplasia and
proliferation of epidermal progenitors. Oncogene *26*, 4882-4888.

20

Niault, T. S., and Baccarini, M. (2010). Targets of Raf in tumorigenesis. Carcinogenesis *31*, 1165-1174.

Oki-Idouchi, C. E., and Lorenzo, P. S. (2007). Transgenic overexpression of RasGRP1 in mouse epidermis results in spontaneous tumors of the skin. Cancer Res *67*, 276-280.

Poulikakos, P. I., Zhang, C., Bollag, G., Shokat, K. M., and Rosen, N. (2010). RAF inhibitors transactivate RAF dimers and ERK signalling in cells with wild-type BRAF. Nature *464*, 427-430.

Quintanilla, M., Brown, K., Ramsden, M., and Balmain, A. (1986). Carcinogen-specific mutation and amplification of Ha-ras during mouse skin carcinogenesis. Nature *322*, 78-80.

Ridky, T. W., and Khavari, P. A. (2004). Pathways sufficient to induce epidermal carcinogenesis. Cell Cycle *3*, 621-624.

Riva, C., Lavieille, J. P., Reyt, E., Brambilla, E., Lunardi, J., and Brambilla, C. (1995). Differential c-myc, c-jun, c-raf and p53 expression in squamous cell carcinoma of the head and neck: Implication in drug and radioresistance. European Journal of Cancer Part B: Oral Oncology *31*, 384-391.

Sano, S., Itami, S., Takeda, K., Tarutani, M., Yamaguchi, Y., Miura, H., Yoshikawa, K., Akira, S., and Takeda, J. (1999). Keratinocyte-specific ablation of stat3 exhibits impaired skin remodeling, but does not affect skin morphogenesis. Embo J *18*, 4657-4668.

Scholl, F. A., Dumesic, P. A., Barragan, D. I., Charron, J., and Khavari, P. A. (2009a). Mek1/2 gene dosage determines tissue response to oncogenic Ras signaling in the skin. Oncogene *28*, 1485-1495.

Scholl, F. A., Dumesic, P. A., Barragan, D. I., Harada, K., Bissonauth, V., Charron, J., and Khavari, P. A. (2007). Mek1/2 MAPK kinases are essential for Mammalian development, homeostasis, and Raf-induced hyperplasia. Dev Cell *12*, 615-629.

21

Scholl, F. A., Dumesic, P. A., Barragan, D. I., Harada, K., Charron, J., and Khavari, P. A. (2009b). Selective role for Mek1 but not Mek2 in the induction of epidermal neoplasia. Cancer Res *69*, 3772-3778.

Sibilia, M., Fleischmann, A., Behrens, A., Stingl, L., Carroll, J., Watt, F. M., Schlessinger, J., and Wagner, E. F. (2000). The EGF receptor provides an essential survival signal for SOS- dependent skin tumor development. Cell *102*, 211-220.

Solit, D. B., and Rosen, N. (2011). Resistance to BRAF inhibition in melanomas. N Engl J Med *364*, 772-774.

Vitale-Cross, L., Amornphimoltham, P., Fisher, G., Molinolo, A. A., and Gutkind, J. S. (2004). Conditional expression of K-ras in an epithelial compartment that includes the stem cells is sufficient to promote squamous cell carcinogenesis. Cancer Res *64*, 8804-8807.

Wang, Z., Pedersen, E., Basse, A., Lefever, T., Peyrollier, K., Kapoor, S., Mei, Q., Karlsson, R., Chrostek-Grashoff, A., and Brakebusch, C. (2010). Rac1 is crucial for Ras-dependent skin tumor formation by controlling Pak1-Mek-Erk hyperactivation and hyperproliferation in vivo. Oncogene.

Wimmer, R., and Baccarini, M. (2010). Partner exchange: protein-protein interactions in the Raf pathway. Trends in Biochemical Sciences *35*, 660-668.

22

Figure Legends

Figure 1 - B-Raf ablation in keratinocytes restrains Ras-driven tumor formation.

(A-E) Eight to twelve week-old B-Raf *f/f* and *Δ/Δ^{ep}* mice were subjected to the chemical two-stage carcinogenesis using DMBA/TPA. (A-D) *Δ/Δep* mice show an impressive reduction in tumor development, growth and size. (A) shows representative pictures of *f/f* and *Δ/Δep* animals after 20 weeks of promotion. (B) shows tumor incidence and (C) shows average tumor volume/mouse. (D) Strongly reduced size, decreased proliferation and increased differentiation in *Δ/Δep* compared to *f/f* tumors. Sections were stained with hematoxylin and eosin (H&E) to visualize tumor structure. Proliferation was determined as the number of BrdU positive cells per mm basal membrane (BM). At least 5 mm BM per mouse were analyzed. A K5 antibody was used to label basal keratinocytes and a K10 antibody to detect differentiating, suprabasal keratinocytes. (E) The plots show % of K10+ layers and the mitotic index of chemically induced *f/f* and *Δ/Δep* tumors of similar size (at least three animals/genotype).

(F-I) B-Raf ablation substantially delays tumor onset (F) and dramatically reduces the tumor load (G) in *K5SOS-F;Δ/Δep* animals. (H) Size-matched *K5SOS-F;f/f* and *K5SOS-F;Δ/Δep* tumors are structurally similar. Note the drastic age difference between the genotypes. Basal and suprabasal keratinocytes and BrdU+ cells were visualized as in (D). Positive cells are stained in brown, scale bars represent 100µm. (I), the plots represent the results of the analysis of at least three animals/genotype. Error bars indicate SD of the mean.*p<0.03 or ** p<0.01 according to Student's t-test.

23

Figure 2 - SOS-F expression fails to induce proliferation in B-Raf-deficient epidermis (A) representative pictures of 3 week old littermates. Tumor development is beginning in *K5SOS-F; f/f* animals. (B) Increased numbers of epidermal layers are visible in H&E-stained sections (top row) and correlate with increased numbers of BrdU+ cells (second row from the top). K5+ cells are evident in the suprabasal layers of *K5SOS-F+;f/f* epidermis but are confined to the basal layer in *f/f*, *Δ/Δep*, and *K5SOS-F+; Δ/Δep* epidermis. Conversely, hardly any K10+ cells were found in the suprabasal layers of *K5SOS-F+;f/f* epidermis. Scale bars represent 100μm, positive cells are stained in brown.   (C-D) The plots represent the results of the analysis of at least three animals/genotype (± SD). *p<0.001 according to Student's t-test.

Figure 3 –B-Raf ablation stalls the growth of established *K5-SOS-F*-induced tumors and affects the proliferation and differentiation of *K5-SOS-F*+ keratinocytes in vitro. Tumor-bearing *K5-SOS-F;Δ/Δ^{ep}TX* and *K5-SOS-F;f/f* mice were injected with tamoxifen for five consecutive days and tumor regression was monitored. (A) Representative pictures of a *K5-SOS-F;Δ/Δ^{ep}TX* mouse after tamoxifen treatment. (B) Quantification of tumor regression. 100% represents the starting size of the tumor. (C) Decreased cell proliferation (% BrdU+ cells) and (D) normalization of the distribution of K10+ cells to the suprabasal layer of the epidermis in *K5-SOS-F;Δ/Δ^{ep}TX* tumors 6 weeks after tamoxifen injection. Positive cells are stained in brown, scale bars represent 100μm. The plots represent the results of the analysis of three animals/genotype (± SD). (E-G) B-Raf ablation neutralizes the effects of *K5SOS-F* on keratinocyte proliferation (F-G) and partially restores the differentiation of K5SOS-F+ keratinocytes. Cells isolated from *f/f*, *Δ/Δep*, *K5SOS-F;f/f*, and *K5SOS-F;Δ/Δep* mice were cultured in complete growth medium (cg, continuously growing) or exposed to 1.2 mM CaCl$_2$ to induce differentiation. The percentage of proliferating cells was determined by BrdU

24

incorporation, differentiating cells were defined by the expression of involucrin. The plots show a quantification of the results obtained in three individual experiments. Error bars indicate SD of the mean. *p < 0.03, ** p < 0.01 and ***p < 0.001 according to Student's t test.

Figure 4 - B-Raf ablation correlates with reduced ERK activation in vitro and in vivo. (A-B) Immunoblot analysis of lysates prepared from primary *f/f* and *Δ/Δep* (A) or *K5SOS-F;f/f,* and *K5SOS-F;Δ/Δep* (B) keratinocytes cultured in complete growth medium (cg) or stimulated with 10 ng/ml EGF for the indicated time periods. U0126 was added 1h prior EGF stimulation to inhibit the MEK/ERK pathway. (C) Primary keratinocytes were cultured in vitro and exposed to 1.2mM CaCl$_2$ to induce differentiation for the indicated time periods. The presence of pERK and pCofilin was detected by immunoblotting with phosphospecific antibodies. A 14-3-3 immunoblot is shown as a loading control. * short and **long exposures are shown for pERK and pCofilin. (D-E) Chronic and acute B-Raf ablation abrogates K5SOSF-induced ERK phosphorylation in vivo. Immunohistochemical analysis of 3 week old *K5SOS-F;f/f,* and *K5SOS-F;Δ/Δep* littermates (D) and of *K5SOS-F;Δ/ΔepTX* tumors (E)*. The pCofilin staining in *K5SOS-F;Δ/ΔepTX* tumors was mostly confined to the suprabasal layers. ERK and cofilin phosphorylation were determined by immunohistochemistry of skin and tumor sections of the different genotypes as indicated. Positive cells are stained in brown, scale bars represent 100μm. The plots represent the results of the analysis of three animals/genotype (± SD). *p < 0.01 and **p < 0.001 according to Student's t test.

Figure 5 - Concomitant ablation of B-Raf and Raf-1 causes the abrupt regression of Ras-driven tumors accompanied by decreased ERK and increased Cofilin phosphorylation. Tumor-bearing *K5-SOS-F;Δ/Δep2TX* and *K5-SOS-F;f/f* mice were injected with tamoxifen for

25

five consecutive days and tumor regression was monitored. (A) Representative pictures of a *K5-SOS-F;Δ/Δep2TX* mouse after tamoxifen treatment showing complete and rapid regression within 18 days. (B) Quantification of tumor regression. 100% represents the starting size of the tumor. (C) Abrupt decrease in cell proliferation (% BrdU+ cells) and increase in differentiation (K10+ cell layers) in *K5-SOS-F;Δ/Δep2TX* tumors only 6 days after tamoxifen injection. (D) ERK phosphorylation is abrogated and Cofilin phosphorylation is massively increased in all epidermal layers of regressing *K5-SOS-F;Δ/Δep2TX* tumors. Positive cells are stained in brown, scale bars represent 100µm. (E) Compound B-Raf-Raf-1 ablation does not affect the proliferation of continuously growing (cg) *K5SOS-F+* keratinocytes, but reduces the proliferation of cells exposed to 1.2 mM $CaCl_2$ to induce differentiation. (F) Compound B-Raf-Raf-1 ablation enforces the differentiation of *K5SOS-F+* keratinocytes. Cells isolated from *f/f, Δ/Δep2TX, K5SOS-F;f/f, and K5SOS-F;Δ/Δep2TX* mice were treated as described in the legend to Figure 3. (G) B-Raf ablation reduces ERK phosphorylation and Raf-1 ablation induces Cofilin phosphorylation in continuously growing keratinocytes; *Δ/Δep2* keratinocytes show a decrease in pERK comparable to that of B-Raf-deficient cells and an increase in pCofilin comparable to that of Raf-1-deficient cells. The plots show a quantification of the results obtained in three individual experiments. Error bars indicate SD of the mean. *p < 0.04 and **p < 0.001 according to Student's t test.
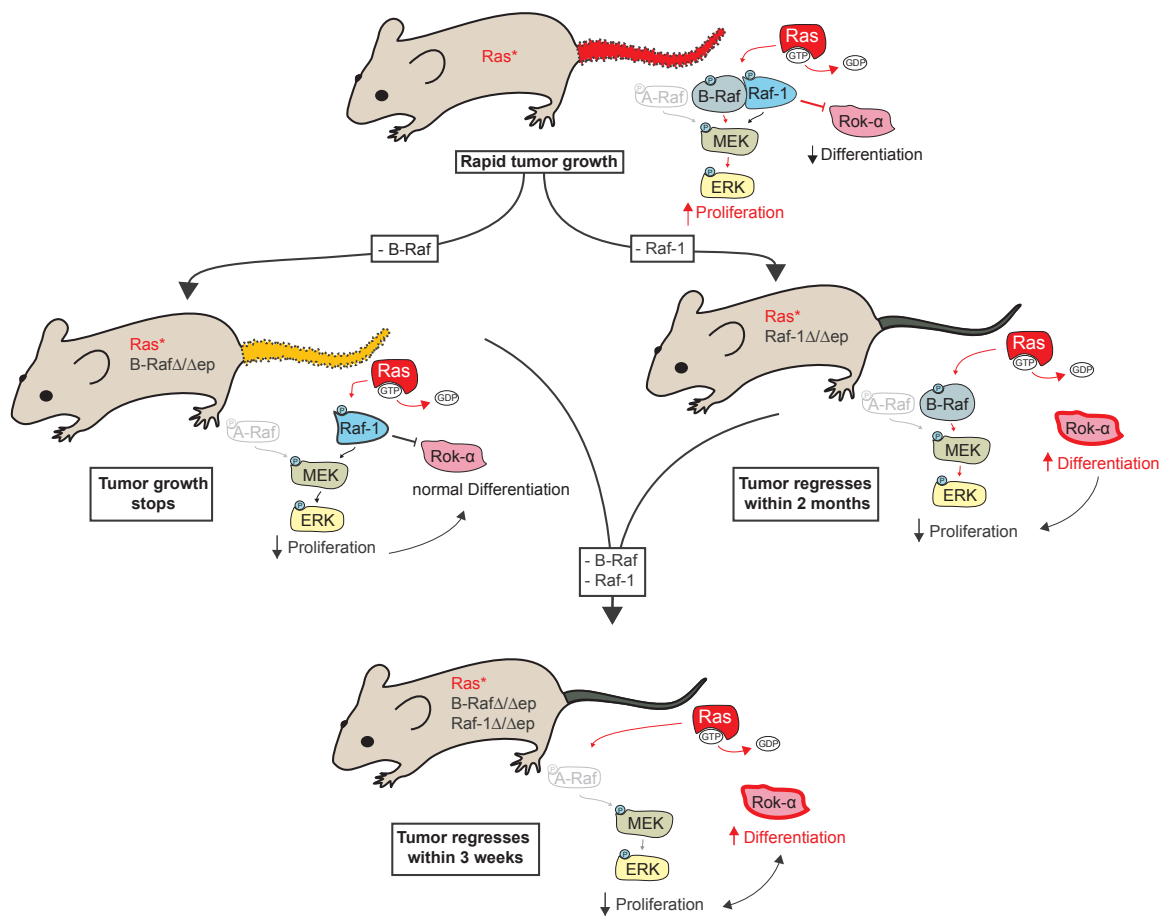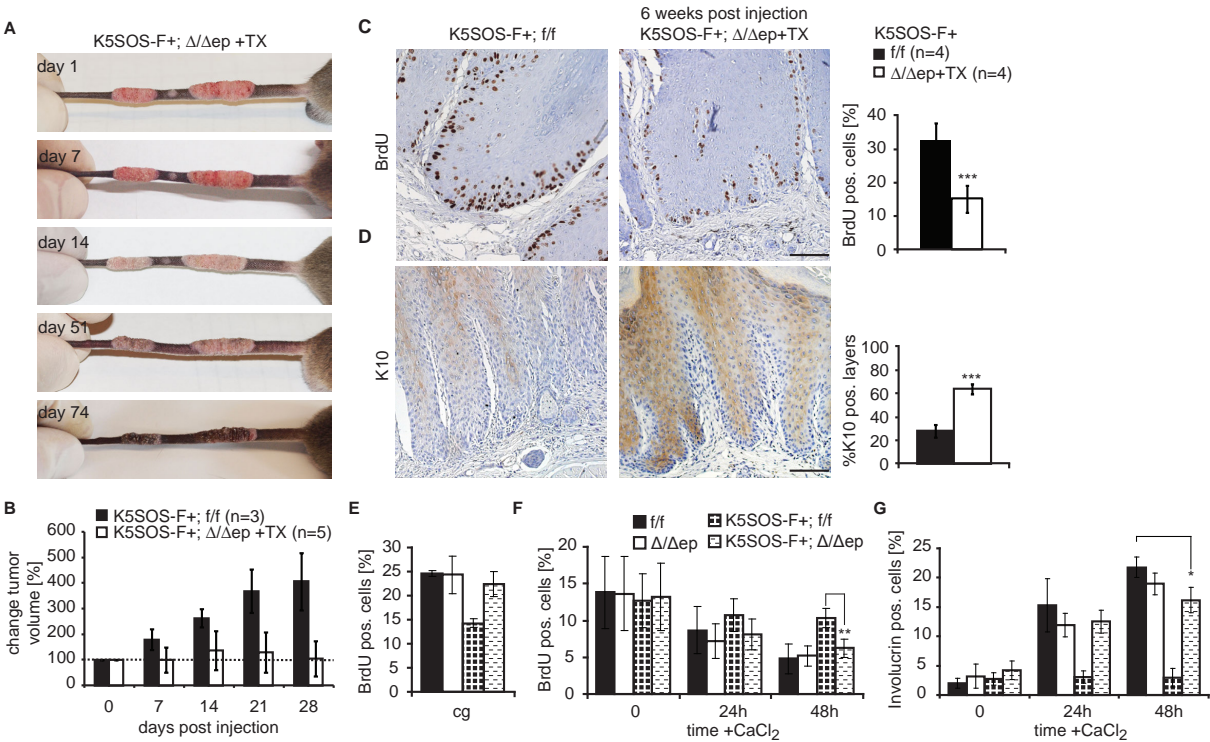
26
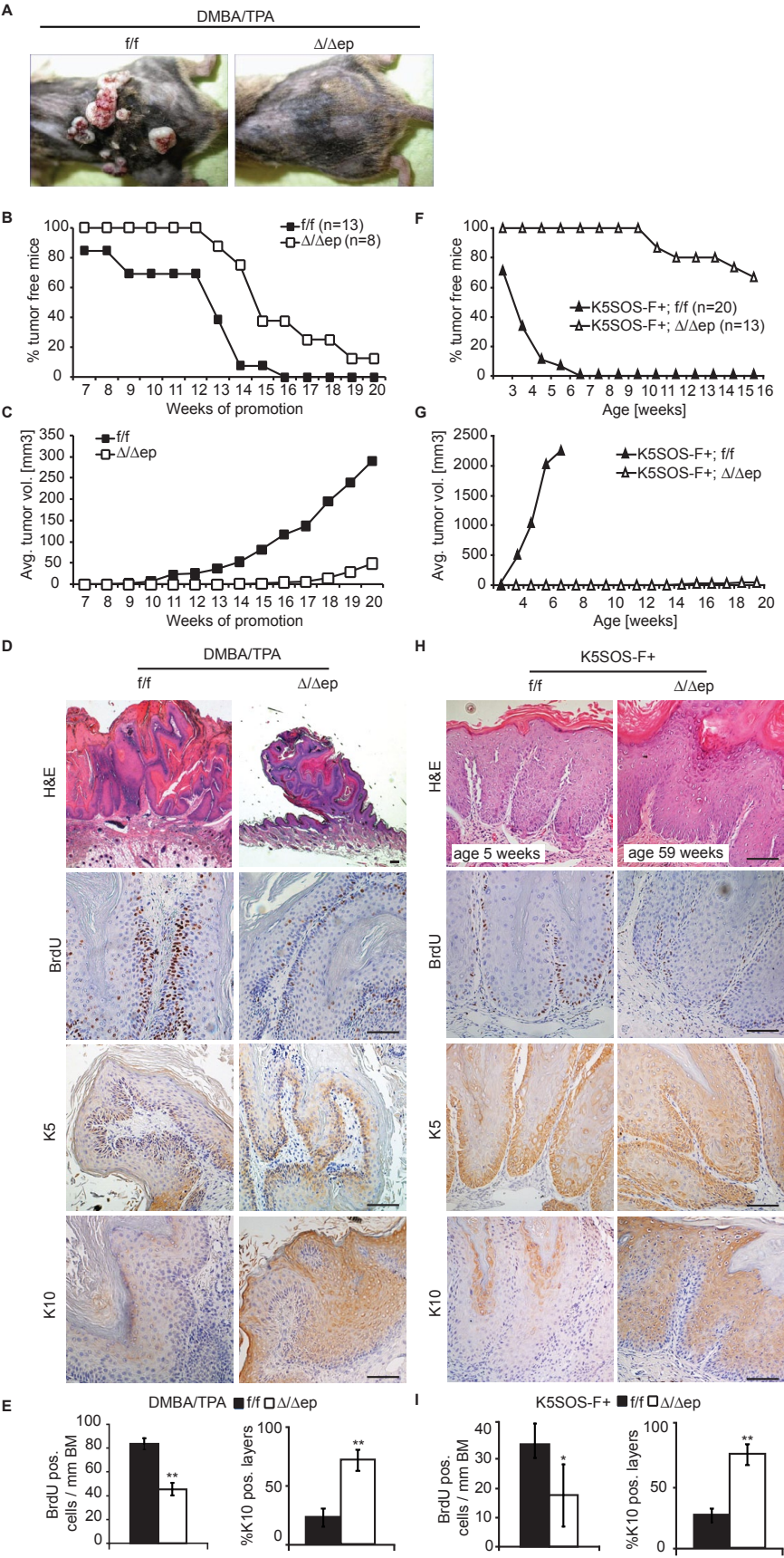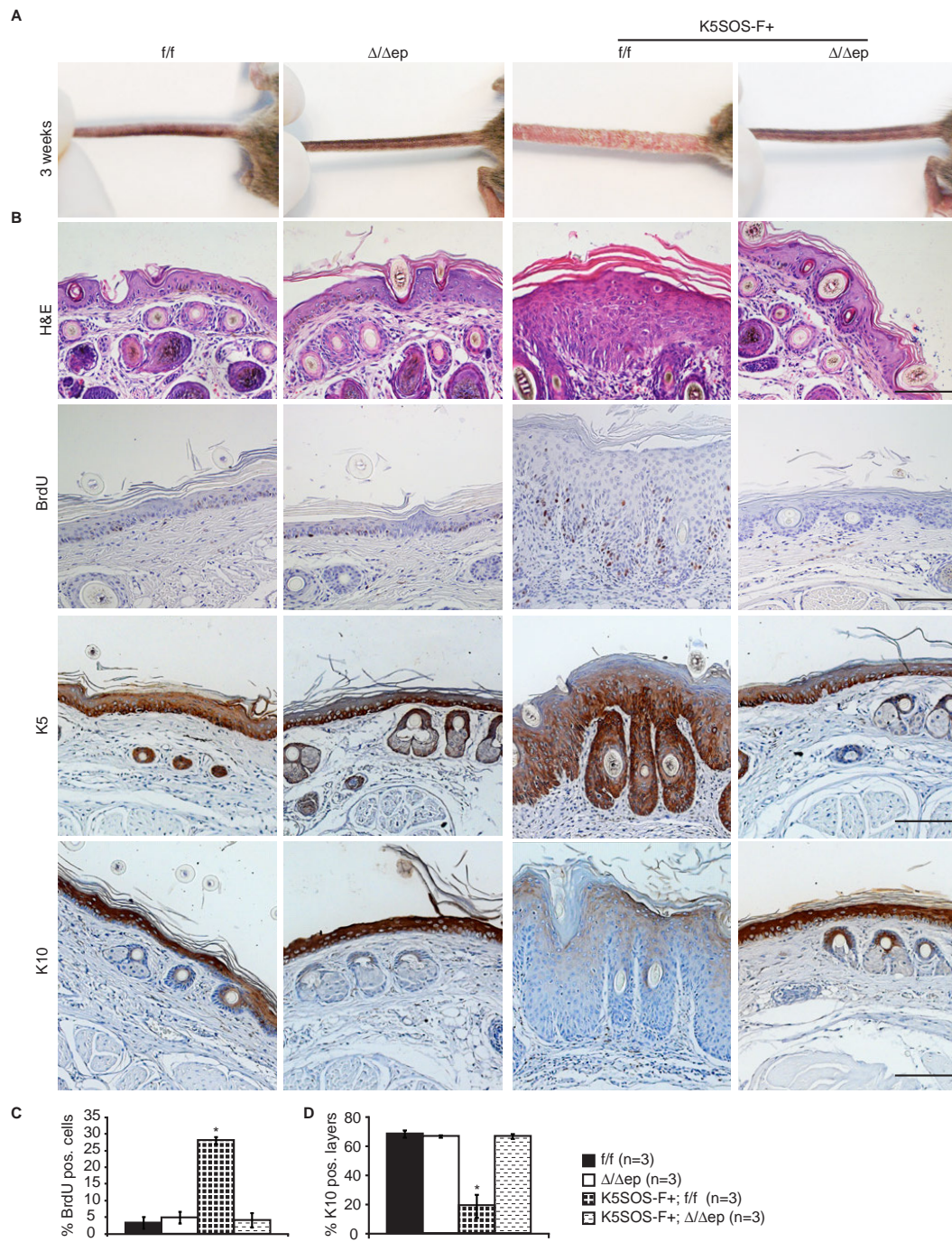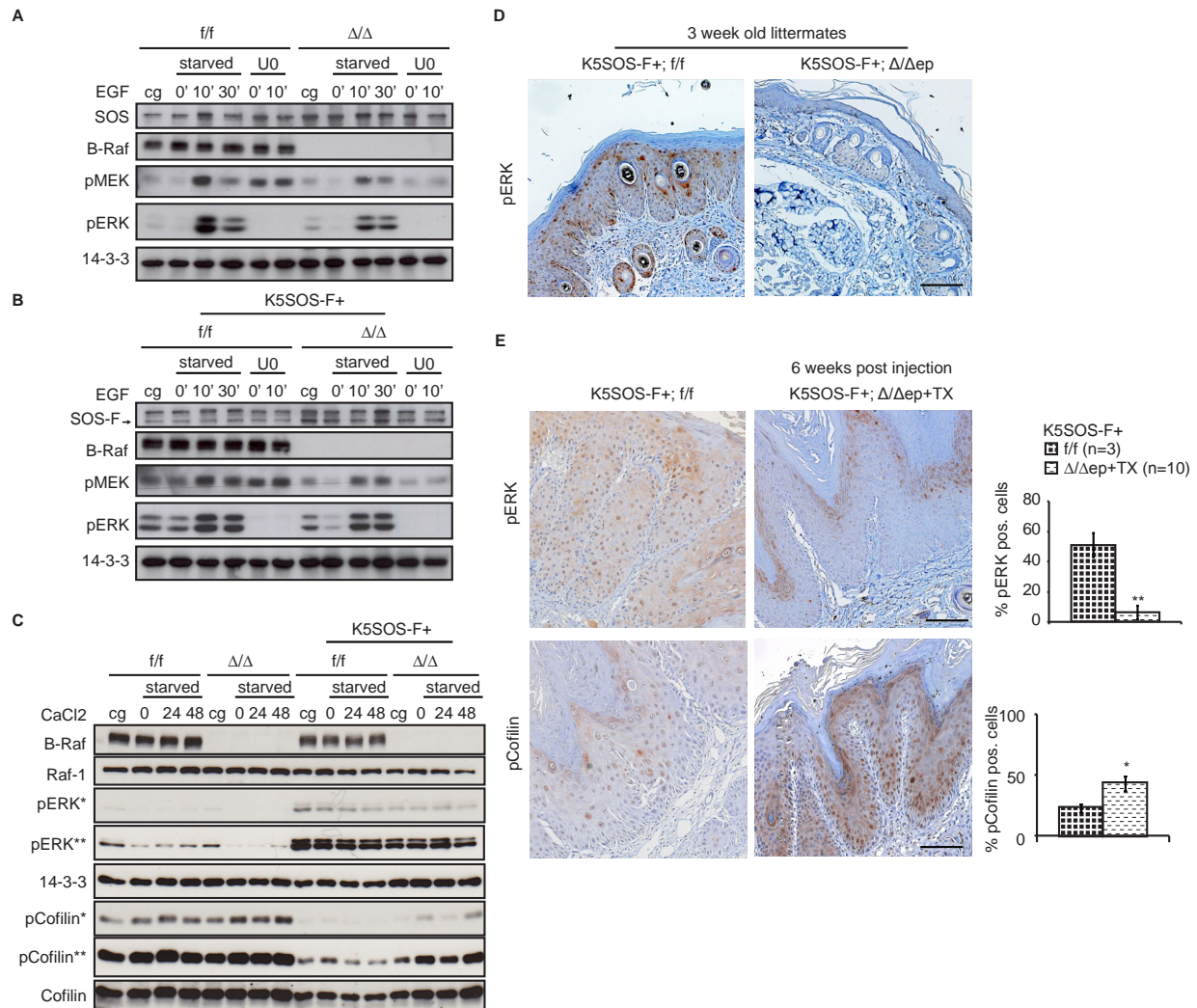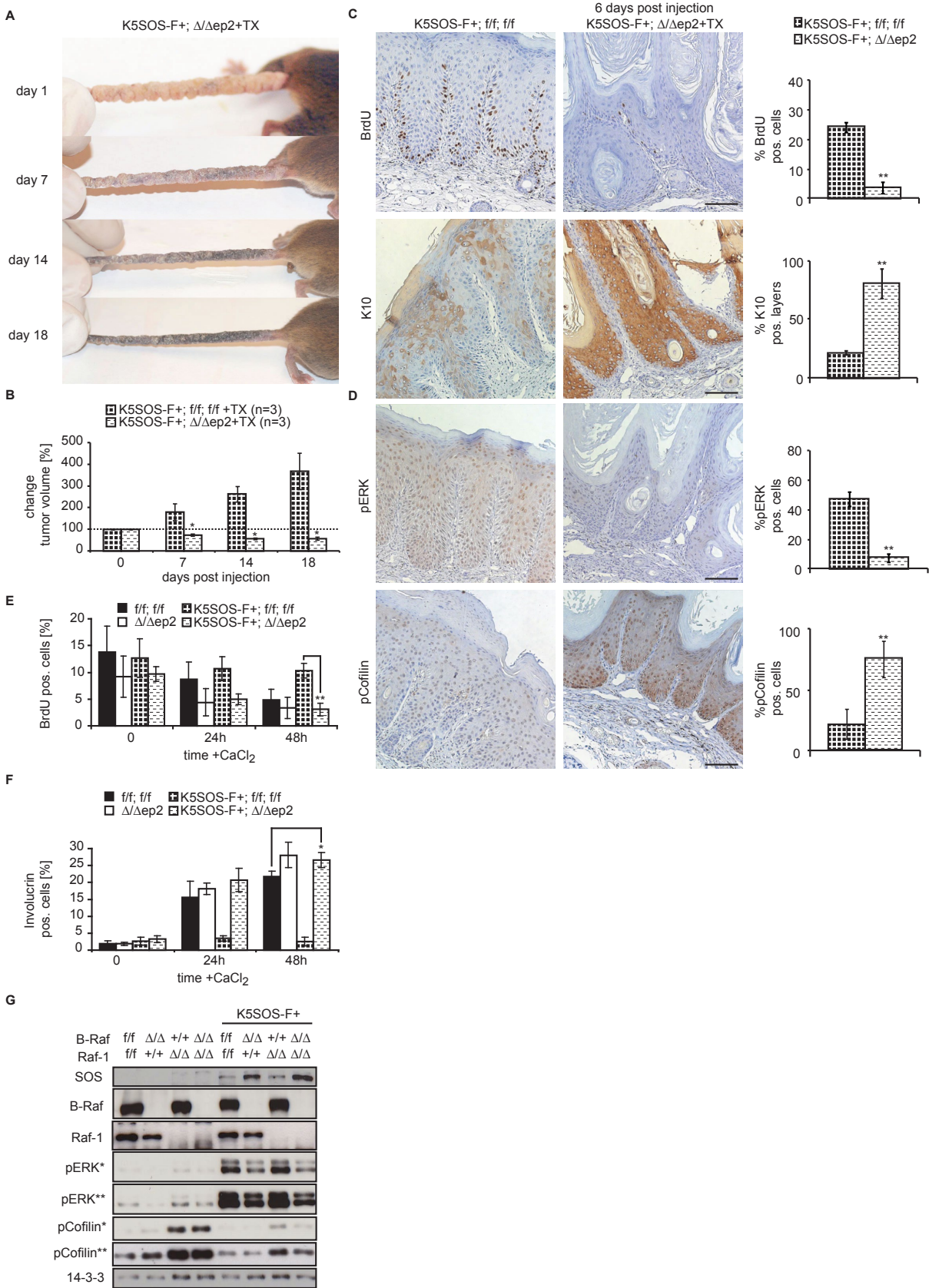
Supplemental Data

Essential ERK-dependent and –independent roles of Raf in Ras-driven skin carcinogenesis

Florian Kern, Eszter Doma, Christian Rupp, Theodora Niault, and Manuela Baccarini

Figure S1- Raf ablation does not induce apoptosis (linked to Figures 1, 3, and 5)

Figure S2- Efficient conversion of B-Raf *f/f* alleles to *Δ/Δep* in tamoxifen injected animals (linked to Figure 3)

Figure S3 - Concomitant ablation of B-Raf and Raf-1 decreases the phosphorylation of STAT3 and the expression of Myc in *K5-SOS-F*-driven tumors (linked to Figure 5)

1
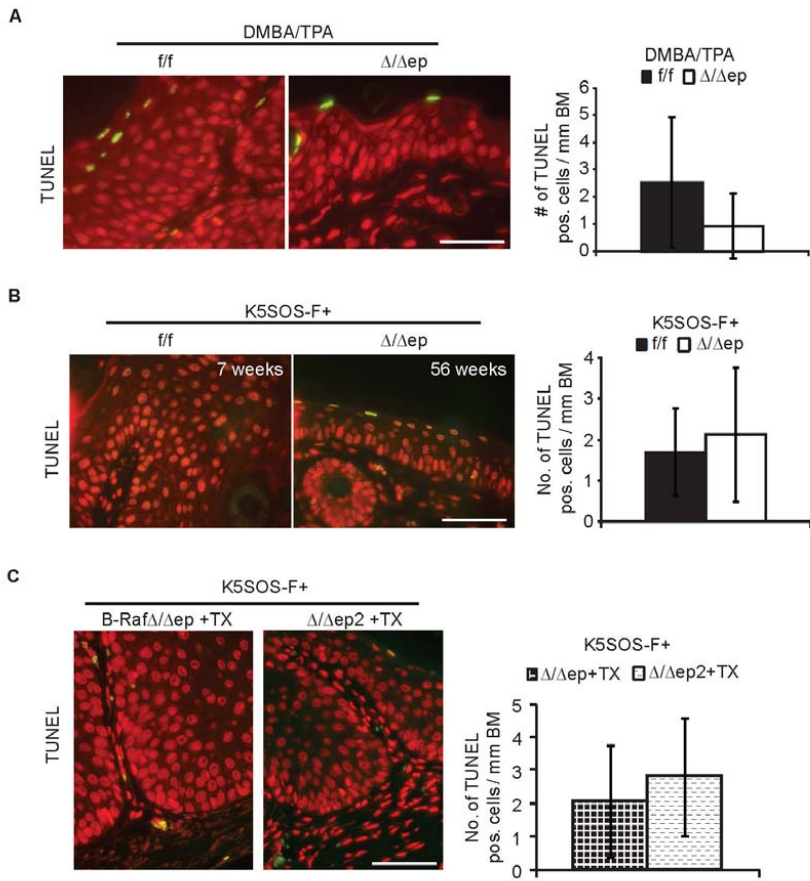
Figure S1- Raf ablation does not induce apoptosis.

Apoptotic cells were detected by TUNEL staining as previously described (Ehrenreiter et al., 2009). Only few TUNEL positive cells could be detected in size-matched chemically induced (A) or *K5SOS-F+* (B) *f/f* and *Δ/Δep* tumors, and (C) in established tumors 6 days after B-Raf (*Δ/ΔepTX*) or compound B-Raf and Raf-1 ablation (*Δ/Δep2TX*). The scale bars represent 100μm. The plots next to the Figures represent the results of the analysis of at least three animals/ genotype (± SD). The number of apoptotic cells remained constant throughout the observation period (10 weeks for *Δ/ΔepTX*, 3 weeks for *Δ/Δep2TX* animals).

2
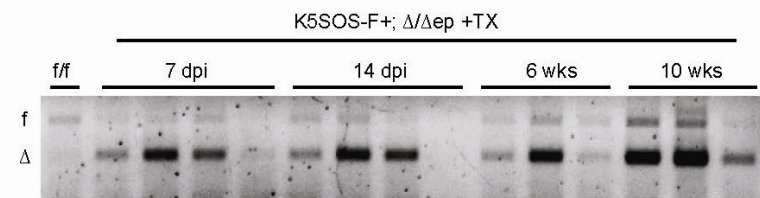
Figure S2

Figure S2- Efficient conversion of B-Raf *f/f* alleles to *Δ/Δep* in tamoxifen injected animals.
50.000-100.000μm^2 of tumor tissue of tamoxifen injected animals were dissected using laser microdissection and genotyped by PCR.
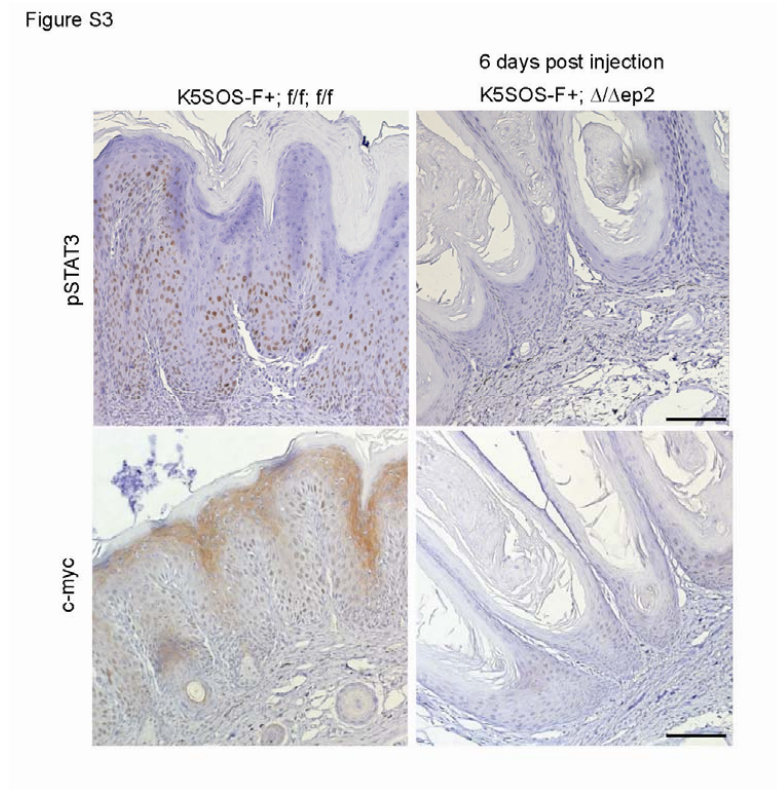
3

Figure S3 - Concomitant ablation of B-Raf and Raf-1 decreases the phosphorylation of STAT3 and the expression of Myc in *K5-SOS-F*-driven tumors.

STAT3 phosphorylation and Myc expression (lower panel) are dramatically reduced in regressing *K5-SOS-F;Δ/Δep2TX* tumors (day 6 after tamoxifen treatment). STAT3 phosphorylation and Myc expression were determined by immunohistochemistry. Positive cells are stained in brown. The scale bar represents 100 μm.

4

Part IV. Summary & Discussion

Summary

Together, the data presented in published and submitted manuscripts reveal essential, novel aspects and regulatory mechanisms involved in epidermal carcinogenesis. They further confirm the well established role of Raf in Erk/MAPK activation in the context of tumor formation and expand the signaling repertoire of Raf to kinase-independent functions.

While special emphasis is put on the essential kinase-dependent and -independent roles of Raf in Ras-driven skin-tumorigenesis, a collaborative effort has been included which examines the essential role that STAT3 signaling plays in HPV8-induced epidermal tumors.

The review provides a good starting point to introduce the mammalian epidermis, comprised of subcutaneous tissue, dermis and epidermis, that protects the body from water loss and the environment. It lays out the concept of the tight and essential regulation of proliferation and differentiation processes in the epidermis, a stratifying squamous tissue comprised of several layers of keratinocytes, to maintain epidermal homeostasis. This balance includes controlled proliferation in the basal layer keratinocytes, default differentiation upon migration to the suprabasal layers, the stratum spinosum and granulosum and the terminal differentiation to form enucleated squames that are continuously shed. Therefore, the basal layer keratinocytes need to constantly replenish cells of the outer compartments leading to a turnover of a about a month. Stringent control of these processes is required and any alteration might lead to severe conditions like inflammation, skin-barrier defects or hyperplasia and even cancer (Blanpain and Fuchs, 2009, Khavari and Rinn, 2007, Lock and Hotchin, 2009).

Especially during Ras-driven tumorigenesis the proliferation in the undifferentiated basal layer compartment is highly increased and the differentiation of the suprabasal layers, the stratum spinosum and granulosum is attenuated.

The review continues to discuss the relevance of the Erk/MAPK pathway in epidermal carcinogenesis. It mainly focuses on the Ras-driven carcinogenesis and the oncogene addiction mediated by the kinase independent function of Raf-1 to regulate Rok-α-mediated differentiation that is discussed in Niault et al. (2009) and Ehrenreiter et al. (2009).

"From autoinhibition to inhibition in trans: the Raf-1 regulatory domain inhibits Rok-alpha kinase activity" sheds light on the mechanism and the relevance underlying the Raf-1/Rok-α interaction. Both kinases regulate their activity through intramolecular binding of their regulatory domain to the kinase domain. This autoinhibition is relieved upon activation through upstream

Rho and Ras. Downstream of Rho and Ras it is the function of Raf-1 to antagonize Rok-α activity to promote motility and tumorigenesis. This inhibition, mediated *in trans* at the level of protein-protein interaction and independent of conventional signaling regulation (e.g. phosphorylation), represents a novel concept in kinase regulation.

This mechanism and its greater relevance was recently reviewed in Wimmer and Baccarini (2010) and holds great potential as a therapeutic target in newly designed inhibitors against Raf-1/Rok-α interaction.

"Raf-1 Addiction in Ras-Induced Skin Carcinogenesis" demonstrates the relevance of Raf-1-mediated Rok-α inhibition by showing its absolute and essential requirement for Ras-driven skin carcinogenesis. Mechanistically, it is shown that Raf-1 acts downstream of Ras as an endogenous inhibitor of Rok-α, a positive regulator of keratinocyte differentiation.

Ras activation is common to many human cancers and exerts its detrimental function through multiple major signaling pathways such as the PI3K pathway, the Ral-GDS pathway, the Tiam1 and the Erk/MAPK pathway. Since Ras is not druggable, it is of great scientific and therapeutic interest to elucidate the essential functions of its downstream effectors (Karnoub and Weinberg, 2008). For this purpose, conventional and conditional knockout systems have been generated that revealed, for example, that PI3K and the Ral-GDS pathway promote survival and the Tiam1/Rac pathway influences cell polarity and shape.

Our work is the first to show a role of a Ras effector in antagonizing differentiation; and perhaps more therapeutically relevant, we could show for the first time a dependence of established Ras-driven tumors on one single effector. The role of Raf-1 in Ras-driven tumorigenesis was investigated using a conditional epidermis-restricted knockout of Raf-1 (Ehrenreiter, 2005). The chemical two steps carcinogenesis that introduces a specific activating mutation in Ras, as well as the transgenic SOS-F model using a membrane-tethered SOS to constitutively activate Ras in the basal layer keratinocytes, are completely ineffective in epidermis-restricted Raf-1 knockout mice, demonstrating the crucial role of Raf-1 in tumor formation. Increased interaction between Raf-1 and Rok-α and decreased Rok-α kinase activity are found in tumor tissue lysates. Strikingly, ablation of Raf-1 in established tumors leads to hyperactivation of Rok-α and to total tumor regression, caused essentially by accelerated tumor cell differentiation. This increased differentiation is also seen in cultured primary keratinocytes, demonstrating that the effect is cell autonomous. Importantly, tumor formation can be induced in the normally tumor-refractory SOS-F-positive, Raf-1 knockout epidermis by treatment with a chemical Rok inhibitor, which counteracts the Rok-α activation induced by the lack of Raf-1. This result is important since the Rho/Rok pathway is often found upregulated in tumors promoting invasion, proliferation and inhibition of apoptosis (Fritz

et al., 1999, Fryer and Field, 2005) and substantial efforts have been undertaken to design inhibitors against Rok-α, which, in the light of our results, might lead to context-dependent adverse effects.

In conclusion, our data describe a non-oncogene addiction of Ras to Raf-1 in its function as an endogenous Rok-α inhibitor. This interaction promises to become a therapeutic target at least in tumors arising in stratified epithelia.

The paper "Keratinocyte-specific Stat3 heterozygosity impairs development of skin tumors in human papillomavirus 8 transgenic mice" shows the dependency of intact STAT3 signaling in HPV8-induced skin tumorigenesis. Although β-HPVs infections are widespread in the general population, they are normally unapparent or asymptomatic and only in immunosuppressed patients or patients with a rare skin disease (epidermodysplasia verruciformis) they have been implicated in the development of NMSC (e.g development of SCCs of the genital tract) (Stanley, 2010).

HPV16 and HPV18 induced tumors were found to overexpress STAT3 in humans (Sobti et al., 2009, Shukla et al., 2010). Almost complete ablation of STAT3 in mice compromised hair cycle and wound healing processes. It also effectively protected mice against the chemical two-steps carcinogenesis (Chan et al., 2004, 2008) but induced a higher susceptibility against UVB induced apoptosis (Sano et al., 2005).

In this study, epidermis-restricted STAT3 knockout mice were generated and crossed with a transgenic mouse model expressing the complete early genome region (CER) of β-HPV8, sufficient to induce hyperproliferation and tumor formation, in an epidermis-restricted manner. In contrast to the above mentioned mice generated by Chan et al., the STAT3 knockout is complete. This causes the mice to die around postnatal day 20-30 with severe defects in growth and hair development starting as early as 10 days after birth. Premature death is related to defective food uptake as the epidermal Cre promoter used (Keratin 5 or K5) is also expressed in the esophagus. Therefore, STAT3 heterozygous mice are used in this study.

The STAT3 heterozygosity rescues the epidermal thickening and hyperproliferation caused by the expression of HPV8-CER, examined in immunohistochemical analyses. More than 50% wildtype mice expressing the HPV8-CER develop tumors within 10 weeks of age, compared to a mere 13% of the STAT3 heterozygous mice. Moreover, the activation status of STAT3 investigated as well by immunohistochemical analyses show that the HPV8-mediated increase of phospho-STAT3 is diminished in heterozygous lesions.

Collectively, these results offer direct evidence of a critical role for Stat3 in HPV8-driven epithelial carcinogenesis and imply that targeting Stat3 activity in keratinocytes may be a viable

strategy to prevent and treat HPV-induced skin cancer. This might even apply to a broader spectrum of tumors as STAT3 was also found to play a critical role in intestinal tumors (Bollrath et al., 2009). The connection with our data showing that Raf-1 impinges on STAT3 activation levels via Rok-α/LIMK/Cofilin interaction implies that the Raf-1/Rok-α interaction might also play a role in HPV-induced skin tumorigenesis.

In "Essential ERK-dependent and -independent roles of Raf in Ras-driven skin carcinogenesis" the often predicted assumption that Ras-mediated carcinogenesis critically depends on Raf to activate ERK and induce proliferation is verified for the first time, at least in epidermal carcinogenesis. In combination with a Raf-1 knockout in a solid tumor it is further elucidated that both kinases act independently on different signaling pathways regulating proliferation and differentiation processes and that the ablation of both pathways synergizes to cause an abrupt and total regression.

In this study the same mouse tumor models and knockout strategies as in Ehrenreiter et al. (2009) are combined with a conditional epidermal B-Raf knockout (Chen et al., 2006) to test its role in the context of skin tumor formation. Again the chemical and the transgenic model show similar results, namely a substantial block in tumor formation and progression, although unlike the Raf-1 knockout this block is not complete. Inducible ablation of B-Raf in established tumors halts tumor growth and progression and frequently leads to a slight reduction of tumor volume. This is achieved by a reduction of the Erk activation shown by immunoblotting and immunofluorescence analysis *in vitro* and by immunohistochemical analysis *in vivo*. Apparently, the reduced Erk activation strongly impacts the proliferation potential and therefore leads to an increase in default differentiation. This increased differentiation is obvious in the upregulation of differentiation markers *in vitro* and *in vivo*, but is less prominent than in the wild-type controls and does not reach the levels observed in the Raf-1 knockout.

The concomitant ablation of B-Raf and Raf-1 in established tumor leads to an abrupt halt in tumor growth and an impressively fast, complete regression within 18 days. Analysis of the underlying processes revealed that the knockout of B-Raf exerts its effect on proliferation via reduced Erk activation independently of the effects of the Raf-1 knockout that induces differentiation via the established Rok-α interaction. Although independent, the affected processes have synergistic effects on tumor maintenance leading to impressively fast regression of the double knockout tumors.

These results suggest that B-Raf and Raf-1 have non-redundant roles in Ras-driven tumorigenesis and that therapies targeting both Raf-dependent pathways may be effective against a broader range of malignancies and reduce the risks of adverse effects and/or resistance.

Altogether the data obtained highlights the Raf/MEK/ERK pathway as one of the key effectors on Ras-driven skin tumorigenesis and attributes essential but distinct and independent functions to B-Raf and Raf-1. Best summarized in the graphical abstract of the submitted paper Kern et al. (2011).

Discussion

At the time when I started my thesis already a vast amount of data had emerged dealing with the Erk/MAPK pathway signaling and with the roles of Raf. Much of this data was generated *in vitro* using cell lines or using lower organisms that do not express all three isoforms of Raf found in mammals.

It was known, for instance, that the conventional ablation of a single Raf gene substantially perturbs development. The mildest phenotype is that of A-Raf knockout mice, which are born and can survive up to 21 days but display neurological and intestinal abnormalities (Pritchard et al., 1996). In contrast, both B-Raf and Raf-1 are essential in embryonic development, and their ablation leads to embryonic lethality. *b-raf* deficient embryos die at midgestation; a conditional epiblast-restricted knockout rescues this embryonic lethality indicating that this is due to placental defects caused by lack of ERK activation. The epiblast-restricted *b-raf* knockout animals also show a progressive growth retardation and died within 21 days after birth of an aggressive neurodegenerative disease. Moreover, a neuronal precursor-restricted knockout of *b-raf* mimicked most of the defects of the epiblast-restricted knockout and further analysis revealed an essential role of B-Raf and its downstream effector ERK in oligodendrocyte differentiation and myelination (Galabova-Kovacs et al., 2006b, 2008). Raf-1 deficient embryos are growth retarded and die at midgestation with ERK-independent anomalies in the placenta, lungs and in the fetal liver, the latter due to increased apoptosis (Mikula et al., 2001). Unlike B-Raf knockout embryos, animals lacking Raf-1 cannot be rescued by epiblast-restricted ablation, indicating that defects other than those observed in the placenta are responsible for embryonic lethality. These divergent phenotypes show that Raf isoforms cannot compensate for each other in the context of a developing organism.

The results of the conventional ablation studies suggest that A-Raf, although ubiquitously expressed, plays a minor signaling role compared to B-Raf and Raf-1. The *in vivo* studies also confirm that the main role of B-Raf is that of a MEK/ERK activator, since in every tissue affected by B-Raf ablation the ERK pathway was impaired (Galabova-Kovacs et al., 2006b, 2008, Sobczak et al., 2008). In contrast, the ablation studies have shown novel functions of Raf-1 in pathway

cross-talk and signal fine-tuning. Several kinase-independent functions of Raf-1 came to light, as a regulator of the pro-apoptotic kinases ASK1 (Chen et al., 2001) or MST2 (O'Neill et al., 2004) and of the cytoskeleton-based kinase Rok-α (Ehrenreiter, 2005, Piazzolla et al., 2005). Taken together, the *in vivo* studies show that the Raf isoforms serve distinct functions in different tissues. Thus, one of the main open questions was what tissue specific functions Rafs have, how they exert their specific functions and whether these are linked to the kinase activity or rather results from protein-protein interactions.

With this background we generated epidermis-restricted conditional knockouts of B-Raf and Raf-1 using the well established Cre/loxP system. The conditional knockout of either Raf revealed no obvious phenotype apart from a wavy hair and curly whiskers in the case of Raf-1. This means that, in normal intact epidermis, the loss of one isoform can be compensated for by the other or by other signaling molecules. Therefore, and since Rafs are prominent effectors of Ras, often mutated or overexpressed in human cancers, we investigated whether B-Raf or Raf-1 ablation plays a role in Ras-mediated skin carcinogenesis. Remarkably, the epidermal Raf-1 knockout was absolutely and the epidermal knockout of B-Raf almost completely refractory to Ras-induced tumor formation. More importantly, ablation of either B-Raf or Raf-1 had an remarkable effect on established tumors. Raf-1 ablation led to complete regression within 7-8 weeks, whereas acute B-Raf ablation halted tumor growth. In depth analysis revealed that Ras-mediated tumorigenesis completely relies on the kinase-independent function of Raf-1 to regulate Rok-α activity and suppress differentiation. Raf-1 ablation in tumors triggers differentiation due to Rok-α hyperactivation. Further analysis revealed the Rok-α/LIMK/Cofilin/STAT3/c-myc link to be an important mediator of the differentiation mediated regression. To our knowledge this finding is the first *in vivo* proof that Ras is dependent on a single effector, not only for tumor initiation but also for tumor maintenance, a prime example of non-oncogene addiction.

In contrast to this kinase-independent protumorigenic function of Raf-1, B-Raf was necessary for Ras-driven tumorigenesis in its function as a Mek/Erk activator. This is the first demonstration of an essential *in vivo* role of B-Raf in the context of Ras-mediated carcinogenesis, long predicted by *in vitro* studies.

Further, I could show that the concomitant ablation of both B-Raf and Raf-1 in a solid tumor independently affects the processes regulated by the two Rafs (proliferation and differentiation, respectively) resulting in a synergism that causes an immediate tumor regression within 2-3 weeks.

Taken together, I could show for the first time that B-Raf as well as Raf-1 have fundamental functions in Ras-driven tumor formation and that either Raf plays an essential role as single effector of Ras in tumor maintenance. These findings substantially contribute to the elucidation of

the *in vivo* roles of the two Raf proteins, especially in the context of Ras-mediated epidermal tumorigenesis. This is in contrast with recently published evidence showing that the development of Ras-driven lung adenocarcinomas depends on Raf-1, but not on B-Raf (Blasco et al., 2011). Because in the lung carcinogenesis model oncogenic Ras signaling was switched on concomitantly with Raf deletion, the therapeutic implications of these studies are limited. Nevertheless, these results had started to shift the attention of the scientific community towards Raf-1 as the main Ras effector, with possible consequence for the design of molecule-based therapies. Our data put this into perspective, demonstrating that the requirement for B-Raf in Ras-driven carcinogenesis depends on the target tissue. In addition, our findings reveal that the regulation of Rok-α by Raf-1 based on protein-protein interaction plays a remarkable role *in vivo* during tumorigenesis. This newly discovered paradigm of kinase regulation *in trans* could be a more general theme in pathway crosstalk in signaling; and as this would be more difficult to compensate for, it might become a promising therapeutic target. The rapid regression observed in double-knockout tumors advocates the development of therapies targeting both Raf kinase-dependent and protein-protein interaction-dependent pathways.

Overall the data presented answer fundamental questions regarding the function of Raf in Ras-driven skin-carcinogenesis and provide suitable models to study the underlying mechanisms.

These *in vivo* models might be used, for instance, to understand the paradoxic ERK activation and the development of drug-related epidermal tumors induced by Raf inhibitors used in the therapy of melanoma. Many hypotheses have been put forward to explain how Raf inhibitors used in the clinic obliterate ERK activation in melanoma cells containing the B-RafV600E mutation, while causing instead ERK activation in B-Raf wildtype cells. Based upon *in vitro* investigations it has been proposed that in low doses the inhibitors lead to the formation of B-Raf-Raf-1 heterodimers in which one of the two protomers is inhibited but induces the allosteric activation of the other. It has also been suggested that upstream activation (e.g. by Ras) favors inhibitor-induced heterodimerization and ERK activation, and it has been predicted that treatment with inhibitors may convert cells harboring other oncogenic mutations, particularly Ras mutations, in tumor cells. The onset of therapy-induced keratoachantomas and squamous cell carcinomas in patients treated with Raf inhibitors seem to bear out this prediction (Chapman et al., 2011). Treating the transgenic SOS-F tumor mice with Raf inhibitor will answer whether this hypothesis is true, and whether the proposed Ras activation is an essential prerequisite for tumor formation or merely catalyzes it. Combining this schedule with the B-Raf and Raf-1 knockout models will answer whether the deleterious effects of the inhibitors are mediated through a specific Raf kinase, and whether the proposed mechanism of heterodimerization of B-Raf and Raf-1 plays a relevant role in tumor

formation *in vivo*. In this respect the role of A-Raf, which may play the role of an uninvolved bystander or that of an opportunistic participant in inhibitor treated cells, could be addressed. Using Raf single- and double-knockout cells it could be tested whether the observed Erk activation in the presence of the inhibitor is mediated by A-Raf forming homodimers or heterodimers with other Rafs or with Raf-like scaffolds such as KSR (Brennan et al., 2011).

Another emerging area in cancer research are cancer stem cells (CSCs). The conditional epidermis-restricted Raf knockout models could be used to investigate whether B-Raf and Raf-1 ablation affects the stem cell compartments of the skin (the hair follicles and the epidermis). A possible role of B-Raf as the main Erk activator is suggested by the observation that in undifferentiated human embryonic stem cells (hESC) the inhibition of the ERK/MAPK pathway with U0126 leads to massive cell death and differentiation *in vitro* (Dreesen and Brivanlou, 2007). The epidermal knockout of Raf-1, on the other hand, exhibits a mild phenotype of curly whiskers and wavy hair which might point towards a defect in the stem cell compartment of the hair follicles. Moreover, the SOS-F tumor mice combined with the inducible epidermal knockout system would be a great tool to investigate the effects of acute Raf ablation on the CSCs. If acute Raf ablation would lead to differentiation of CSCs, this would substantially strengthen the already strong therapeutic potential of Raf.

Collectively and beyond their potential biomedical value, our data contribute to the growing knowledge that the complexity of signal transduction extends far beyond simple on/off switches. The Raf/MEK/ERK pathway is a prime example of this, and although studied for decades, it still represents a complex field of research with the promise of many more exciting and surprising findings to come.

Part V. Material and Methods

11   Material & Methods

11.1   Preamble

The following material and methods section is mainly restricted to methods carried out in our laboratory or in which we were directly involved. All materials and methods are of course found in the corresponding sections of the publications.

11.2   Plasmids

The following plasmids were used in transient expression experiments: pXJ40-HA-FL Rok-α, ΔPH/CRD, Rok-αK, Rok-αreg (Leung et al., 1996), pEFmyc FL Raf-1, pCMV5 FL Raf-1, Raf-1reg, Raf-1reg R89L provided by W. Kolch; (Kubicek et al., 2002, O'Neill et al., 2004), pEXV FL Raf-1, R89L, CC/SS, CAAX provided by J.F. Hancock; (Roy et al., 1997), pEGFP Raf-1reg provided by R.M. Lafrenie; (Zhang et al., 2002), pRSV FL Raf-1, Raf-1reg, and Raf-1–K (Bruder et al., 1992). For expression in bacteria, pGEX Raf-1reg (aa 1–187) was subcloned from pGEX Raf-1reg (aa 1–258; O'Neill et al. 2004) by PCR amplification and ligation. All CC/SS mutations were generated by site-directed mutagenesis and verified by sequencing. Monomeric RFP1 (mRFP1)–Rok-α constructs were generated by PCR amplification of pXJ40-HA–Rok-α and subcloned into the pcDNA mRFP1 vector. pGEX KG MLC2 and RhoA V14 Flag tagged were provided by E. Sahai and A. Ridley, respectively. Cell culture and transfection 3T3-like MEFs derived from c–Raf-1Δ/Δ and WT embryos (Mikula et al., 2001), COS-1, MCF-7, and MDA-MB-468 cells were maintained in DMEM with 10% FCS and transiently transfected using Lipofectamine reagents (Invitrogen) according to the manufacturer's instructions.

11.3   Migration assay

Migration was assessed in a modified Boyden chamber as described previously (Ehrenreiter, 2005). Migrating and nonmigrating EGFP-transfected cells were visualized and quantified ($\geq$450 cells/sample) by epifluorescence microscopy.

11.4   Immunofluorescence

Raf-1, Rok-α, involucrin, vimentin, actin, ezrinpT567, and Fas were performed as described previously (Ehrenreiter et al., 2009, Piazzolla et al., 2005). For Raf-1 and Rok-α staining, cells plated on fibronectin (Invitrogen) were permeabilized (0.01% Triton X-100), fixed in 4% PFA, and blocked with 0.2% gelatin before incubation with primary antibodies (Raf-1 and Rok-α; BD) and staining with the appropriate Alexa Fluor 488– or 594–conjugated secondary antibodies (Invitrogen). Rhodamine-conjugated phalloidin (Invitrogen) was used to visualize actin filaments. To visualize vimentin, intermediate filaments cells were fixed in methanol containing 5 mM EDTA and permeabilized with 0.5% Triton X-100. Cells were subsequently stained with vimentin antibody (Sigma-Aldrich) followed by Alexa Fluor 594–conjugated secondary antibodies. For ezrin pT567 staining, cells were fixed in cold methanol/5 mM EDTA and blocked (10% goat serum/1% BSA) before incubation with phospho-ezrin–radixin–moesin antibody (pT567; Cell Signaling Technology) followed by Alexa Fluor 594–conjugated secondary antibodies. For Fas staining, cells were fixed in cold methanol/5 mM EDTA for 10 min at room temperature followed by Alexa Fluor 594–conjugated secondary antibodies. Antifade reagent (ProLong Antifade; Invitrogen) was used as a mounting medium. Confocal microscopy was performed at room temperature with a microscope (Axiovert 100M; Carl Zeiss, Inc.) fitted with a Plan Apochro- mat 63×/1.40 NA oil objective and equipped with the confocal laser- scanning module (LSM 510; Carl Zeiss, Inc.). Immersol (518; Carl Zeiss, Inc.) was used as imaging medium. Images were acquired using the LSM 510 software (version 2.3; Carl Zeiss, Inc.). Representative z stacks are shown. 600 transfected cells were counted for the quantification.

11.5   Cell line lysates, immunoprecipitation, and immunoblotting

Cells were washed with ice-cold PBS and lysed in 200 mM Tris-HCl, pH 7.4, 2 mM EDTA, and 1% Triton X-100 with protease and phosphatase inhibitors. Lysates and HA–Rok-α immunoprecipitates were prepared from subconfluent cells 24–48 h after transfection and analyzed by immunoblotting using the following antibodies: Rok-α (Millipore), HA (12CA5), Rok-α, Raf-1, SOS (BD), pCofilinS3, Cofilin, pMLCT18/S19 (Santa Cruz Biotechnology, Inc.), pERK, pEzrinT567, ezrin–radixin–moesin (Cell Signaling Technology), tubulin (Sigma-Aldrich), and pan-RasV12 (EMD). The amount of Raf-1 proteins in the immunoprecipitation was quantified by densitometry (ImageQuant [GE Healthcare] or AlphaEase [Alpha Innotech]) and normalized to the amount of immunoprecipitated Rok-α.

11.6   Protein expression and purification

GST–Raf-1reg proteins were expressed in Escherichia coli Rosetta (DE3; EMD) by induction with 1 mM IPTG and incubation in minimal medium overnight at 22 °C. GST–Raf-1reg proteins were purified by binding to glutathione Sepharose beads (GE Healthcare) and eluted with 20 mM reduced glutathione in 50 mM Tris-HCl, pH 8.0. Recombinant Raf-1reg and MLC2 were obtained by thrombin cleavage (6 U/ml overnight at 4 °C) as previously described (Wyckoff et al., 2006).

11.7   GST pull-down and Rok-α *in vitro* kinase assays

GST–Raf-1reg immobilized on glutathione Sepharose was incubated with Rok-α–K (Millipore) for 15 min at 30 °C, washed, and eluted by boiling in SDS sample buffer. Complex formation was determined by immunoblotting with anti-5His (QIAGEN) or anti-GST antibodies. Rok activity was assayed using 7 µM MLC2 as a substrate. Phosphorylation was detected by immunoblotting with pMLCT18/S19 antibody, normalized to MLC2 content, and quantified using an infrared imaging system (Odyssey; LI-COR Biosciences).

11.8   Mouse strains

Mice carrying the floxed exon 11 of B-Raf, kindly provided by A. Silva, or mice with the floxed exon 3 of Raf-1 (Mikula et al., 2001), were maintained on a 129/Sv background and crossed to transgenic mice, expressing the Cre recombinase under the control of the keratinocyte specific keratin 5 (K5 Cre2) promoter, kindly provided by J. Takeda, to obtain epidermis restricted Raf ablation (Tarutani et al., 1997, Chen et al., 2006, Sibilia et al., 2000, Sano et al., 2005, Ehrenreiter, 2005, Indra et al., 1999). K5-Cre;b-raf f/f (b-rafΔ/Δep) and K5-Cre-er(T);b-raf f/f (Δ/ΔepTX) and K5-Cre;b-raf f/f;c-raf-1 f/f (double Δ/Δep) as well as K5-Cre-er(T); b-raf f/f;c-raf-1 f/f (doubleΔ/ΔepTX), plus or minus the K5-SOS-F+ trangene (Sibilia et al., 2000) were bred by crossing the appropriate genotypes. All animal experiments were approved by the Austrian Animal Care Committee and conducted in accordance with the guidelines for the use and care of laboratory animals.

11.9   Two steps carcinogenesis

For chemical two-stage carcinogenesis, mice were shaved 3 days before initiation with DMBA (25 mg/200ml acetone; Sigma) applied to the dorsal skin. Beginning 3 days later, TPA (6 mg/100ml acetone; Sigma) was applied twice per week for 20 weeks. Control mice were treated with ace-

tone. Onset, number, and size of tumors were monitored at least twice a week. All animal experiments were performed in accordance with a protocol authorized by the Austrian Ministry of Science and Communications, following the approval by the national Ethical Committee for Animal Experimentation.

11.10   Phenotypic analysis of the tumor model strains

The pheonotypic analysis of the tumor model included determining onset of tumor formation, tumor volume and the timeframe of tumor growth. Mice were monitored at least once per week, counting tumors as well as measuring tumor volume. The length and width of each individual tumor were measured with calipers. Tumors in various sizes were dissected from euthanized mice, fixed in paraformaldehyde and paraffin embedded as described below.

11.11   Genotyping

Mice and isolated keratinocytes were routinely genotyped. To this aim, tail tissue DNA was prepared digesting either 3-5 mm of mouse tail or cell pellets in 500 µl tail buffer (50 mM Tris-HCl, pH 7.5; 100 mM EDTA, pH 8.0; 100 mM NaCl; 1 % SDS) and 20 µl Proteinase K (Sigma) overnight in a waterbath at 55°C. On the next day 200 µl of saturated NaCl solution was added, samples mixed thoroughly and then centrifuged at 13.000 rpm (SIGMA) for 10 minutes. The supernatant was transferred into a new tube and the DNA precipitated by adding 200 µl isopropanol, vortexing the sample and then centrifuging at 13.000 rpm for 5 minutes. The DNA pellet was washed twice with 70% ethanol, centrifuged again at 13.000 rpm for 5 minutes. Pellets were airdryed for about 15-20 minutes to remove the ethanol. Finally 50-100 µl of TE (10 mM Tris-HCl, pH 7.5; 1 mM EDTA) was added and the samples incubated for 2 hours at 55°C shaking. The following primers were used for genotyping:

b-raf: primer 1, 5'-GCATAGCGCATATGCTCACA-3'; primer 2, 5'-CCATGCTCTAACTAGTGCTG-3'; and primer 3, 5'-GTTGACCTTGAACTTTCTCC-3'. Primers 1 and 2 amplify a 357-bp fragment of the endogenous b-raf allele and a 413-bp fragment of the floxed allele, whereas primers 1 and 3 amplify a 282-bp fragment of the targeted b-raf allele using the following cycle protocol of 1x 94 °C - 4 min, 35 cycles: 94 °C - 45 sec; 52 °C - 45 sec and 72 °C - 1 min concluding with 1x 72 °C - 7 min. (Galabova-Kovacs, Matzen et al. 2006)

c-raf-1: primer 1, 5'-TTC CGC CTC TCC GGG CTT ACA GC-3' and primer 2, 5'-GAG AGA TAA AGG GTT TCT TCG CTT CC -3'. Primers 1 and 2 amplify a 500-bp fragment of the c-raf-1 allele using the same cycle protocol as for b-raf.

sos: primer 1, 5'-TTC CGC CTC TCC GGG CTT ACA GC-3' and primer 2, 5'-GAG AGA TAA AGG GTT TCT TCG CTT CC -3'. Primers 1 and 2 amplify a 500-bp fragment of the sos-f allele using the following cycle protocol of 1x 94 ℃ - 4 min, 40 cycles: 94 ℃ - 30 sec; 60 ℃ - 40 sec and 65 ℃ – 1,5 min concluding with 1x 65 ℃ - 5 min.

cre: primer 1, 5'-taa tcg cca tct tcc agc ag -3' and primer 2, 5'-caa ttt act gac cgt aca c -3'. Primers 1 and 2 amplify a 1000-bp fragment of the Cre allele using the following cycle protocol of 1x 94 ℃ - 4 min, 40 cycles: 94 ℃ - 45 sec; 58 ℃ - 40 sec and 72 ℃ – 1 min concluding with 1x 72 ℃ - 5 min.

11.12   Laser Capture Microdissection

To confirm the efficient conversion of the b-raf f/f to Δ/Δ alleles in tamoxifen-injected animals a Leica LMD6500-Laser Capture Microdissection / Imaging Unit was used to dissect 50.000 - 100.000 μm2 from rehydrated 7 μm thick tumor sections from PEN-MembranSlides. The collected tissue was digested and genotyped using the standard PCR protocol with extended cycle numbers.

11.13   Staining of paraffin sections

Dorsal skin and tumors were dissected from euthanized mice and fixed overnight in 4% paraformaldehyde (Merck), transferred to 70% ethanol before dehydration the next day and paraffin embedding the day after, using an embedding machine (Thermo Electron Corp.). Big tumor samples of the two steps carcinogenesis were cut into pieces prior fixation to facilitate fixation. Paraffin embedded samples were subjected to sectioning using a Leica microtome. Tail sections were decalcified by incubating trimmed paraffin blocks for 10-15 minutes on green towels soaked with 2 N HCl to facilitate sectioning. Histological analyses were performed on 3 μm thick sections allowed to dry at 45℃ overnight. Briefly, paraffin was removed by 2x 10 minutes incubation in Xylene (J.T.Baker) and the sections rehydrated through incubation of 2x in 100% ethanol, 2x 90% ethanol and 1x 70% ethanol each 10 minutes. After endogenous peroxidase blocking using 1% H2O2 in 50% MeOH p.a. in dH2O antigen retrieval as stated was performed depending on the antibodies used. Sections were placed in Chamber Slides (Lab-Tek), blocked with 3% normal goat serum (Vector) in TBST (1xTBS (150 mM NaCl, 10 mM Tris pH 8.0) Tween20 (final 0.1%) for 30 minutes and then incubated with the primary antibody overnight at 4℃. The next day the samples treated with rabbit antibodies were washed, incubated with DAKO EnVision peroxidase system for 30 minutes, washed again, and incubated in 0.01% diaminobenzidine (DAB, Sigma). Samples treated with mouse antibodies were incubated using the ABC Staining Kit (Vector Laboratories). All samples

were counterstained with Hematoxylin (Sigma, 1:5) and dehydrated again by reversed order of the rehydration procedure. Stained sections were mounted with mounting medium (Merck) and stored at 4 °C or RT, respectively until examined under a light microscope (Zeiss Axio Vision).

11.14   Histology

Hematoxylin (Sigma) and eosin (Sigma) stainings were performed on 3 μm thick sections of 4% paraformaldehyde-fixed and paraffin-embedded tissues, prewarming samples for 1 hour at 55 °C and then using a staining Pathisto machine. Sections were mounted with mounting medium (Merck) and stored at RT until examined under a light microscope (Zeiss Axio Vision).

11.15   Immunohistochemistry

Immunohistochemical stainings were performed on 3 μm thick sections of 4% paraformaldehyde-fixed and paraffin-embedded tissues. Tail sections were decalcified by incubation of trimmed paraffin blocks for 10–15 min on paper towels soaked in 1 N HCl. Staining with the following antibodies was performed: Keratin 5 (BabCo/Covance), Keratin 10 (BabCo/Covance), pErk (Cell Signaling Technology), biotinylated-BrdU (Zymed), BrdU (Abcam), c-myc (Milipore), E-cadherin (Santa Cruz), integrin-β1 (BD Biosciences), Ki67 (Novocastra), pCofilin (Ser3, Santa Cruz), and pSTAT3 (Tyr705, Cell Signaling). Epitope retrieval was routinely performed by boiling the samples in 10 mM ctiric acid, pH 6.0 for 15 minutes and let them cool down. Epitopes for BrdU detection were retrieved incubating the sections in 1x Trypsin and 2.5 N HCl at 37 °C for 10 minutes each. Detection was performed as described above. BrdU incorporation was determined in mice injected with BrdU (12.5 mg/g body weight) 1 hr prior to tissue isolation.

11.16   Proliferation

Proliferation was detected using 5-bromo-2-deoxyuridine (BrdU, Roche) incorporation. Mice were injected intraperitoneally with 12.5 mg BrdU per g body weight 1 hour before sacrificing. Mouse tissue was treated for sectioning as described above. The antigen was retrieved by Trypsin and HCl treatment, before incubation with biotinylated-anti-BrdUrd mAb. The sections were incubated, using the ABC Staining Kit (Vector Laboratories) according to the manufacturer's recommendations, followed by incubation with DAB substrate. Sections were counterstained with hematoxylin, dehydrated, mounted and examined using a light microscope (Zeiss Axio Vision). Using the Zeiss Axio Vision software the length of the basement membrane was determined and the cells positively stained for BrdU counted manually.

11.17   TUNEL assay

Apoptotic cells were detected using the Terminal deoxynucleotidyl transferase mediated dUTP nick end labeling (TUNEL) in situ cell death detection kit from Roche, according to the manufacturer's recommendations. Tissue sections were subjected to antigen retrieval using proteinase K, followed by the addition of terminal deoxynucleotidyl transferase (TdT) enzyme and fluorescein-dUTP. Samples were counterstained with propidium iodide (PI, Fluka) and mounted with DAKO fluorescence mounting medium (DAKO). Positive control slides were pretreated with DNase. Images were acquired using the MetaVue 5.0r6 software (Universal Imaging Corporation) on a fluorescence microscope (Carl Zeiss MicroImaging, Inc.). Again, the basement membrane was measured and TUNEL positive cells counted.

11.18   Isolation and culturing of primary keratinocytes

Primary mouse keratinocytes from 3 day old mice were isolated as described in the following section. Mice were sacrificed and shaved, the skin was peeled off and placed 0,125% trypsin PBS (8 g of NaCl, 0.2 g of KCl, 1.44 g of Na2HPO4, 0.24 g of KH2PO4; pH 7.4) overnight at 4 °C. The next day, the epidermis was separated from the dermis and stirred for 20 minutes 500 rpm in harvesting medium (S-MEM, 8 % FCS, 100 U/ml penicillin/streptomycin; 100 µg/ml streptomycin, 100 U/ml nystatin (Roche)). The cell suspension was filtered through 70 µm teflon meshes (BD). Cells were washed once and resuspended in KGM Ca2+-free culturing medium (CLONTECH Laboratories, Inc.) supplemented with 2% chelated FCS, 0.4 µg/ml hydrocortisone, 5 µg/ml insulin, 5 µg/ml transferrin (Sigma-Aldrich), 10 ng/ml EGF, 60 µg/ml bovine pituitary extract, gentamycin (50 µg/ml), and 100 U/ml nystatin (Roche)). The final concentration of Ca2+ of the KGM was 0.05 mM. The cell number was determined and cells plated at a densitiy of 4-5x10^6 cells per 100 mm cell culture dish (FALCON). Culturing medium was exchanged the next day to remove dead cells and thereafter every second day.

Primary mouse keratinocytes from 21 day old mice were isolated as follows. Mice were sacrificed and shaved, the skin was peeled of including the skin from the tail and the ears and placed onto antibiotics PBS solution (1x PBS, 100 U/ml penicillin/streptomycin, 100 µg/ml streptomycin, 1x fungizone (Sigma) and 100 U/ml nystatin (Roche)). The antibiotics PBS solution was replaced by 0.8% trypsin (Sigma) PBS and the skin incubated for 1 hour at 37 °C. The epidermis was separated from the dermis and placed into 10-15 ml of DNAse medium (S-MEM, 8 %FCS, 250 µg/ml DNase (Sigma)) and left shaking at 37 °C in a waterbath for 1 hour. The cell suspension was filtered through 70 µm teflon meshes (BD). Cells were washed once and resuspended in cultur-

ing medium (MEM (Sigma), 5 µg/ml Insulin (Sigma), 10 ng/ml EGF (Roche), 10 µg/ml Transferrin (Sigma), 10 µM Phosphoethanolamine (Sigma), 10 µM Ethanolamine (Sigma), 0.36 µg/ml Hydrocortisone (Calbiochem), 1x Glutamine (Invitrogen, Glutamax-I), 1x Pen/Strep (Invitrogen), 8% chelated FCS (BioRad, Chelex 100 Resin)). Cell number was determined and cells plated at a density of 6-7x10^6 cells per 100 mm cell culture dish. The culture medium was exchanged the next day to remove dead cells and thereafter every second day.

For inducing differentiation, cells were trans- ferred into starvation medium (containing only 2% chelated FCS and no growth factors) and treated with 1.2 mM CaCl2 for different time periods. The Rok-α inhibitor Y-27632 (Calbiochem) and the MEK inhibitor U0126 (Cell Signaling) were added to the medium at a final concentration of 10 mM.

11.19   Rok-α immunoprecipitation and *in vitro* kinase assays

Crude epidermis lysates were prepared from the tail of 17-day-old mice. In brief, the skin was digested with trypsin to separate the epidermis from the dermis. The epidermis was placed in lysis buffer (200 mM Tris-HCl [pH 7.4], 2mMEDTA, and1%Triton X-100, supplemented with protease and phosphatase inhibitors) and homogenized with the PreCellys24 homogenizer (PeqLab). Rok-α immunoprecipitates were prepared from 1200 mg of protein with a Rok-a antibody (Upstate) and analyzed by immunoblotting or assayed for Rok-α kinase activity with the long S6 kinase (Upstate) as a substrate according to the manufacturer's instructions. The Rho kinase inhibitor Y-27632 (20 mM final) was used for assessment of Rok-α-specific kinase activity.

11.20   Western blot analysis of primary cell lysates / crude lysates

Primary keratinocytes were routinely cultured and grown to about 70-80% confluency. Cells were washed twice with icecold PBS and lysed using 100 µl lysis buffer (Frackelton buffer (10 mM Tris-HCl, 50 mM NaCl, 1% Triton X-100), 30 mM sodium pyrophosphate, 100 µM Na3VO4, 1 mM phenylmethylsulfonyl fluoride). After a 20 min centrifugation at 15.000 rpm (20.000g) the supernatant was transferred to new tubes and protein concentration measured using the Bradford method (Biorad). Or basic 2X Laemmli Buffer (4% SDS, 20% glycerol, 10% 2-mercaptoethanol, 0.004% bromphenol blue, 0.125 M Tris HCl, pH is approximately 6.8) was used to lyse small amounts of cells. After 10 min incubation time cells were scraped, transferred into tubes and boiled for 10 min at 95℃.

Samples with 10-50 µg of proteins were prepared, using 5x loading buffer (320 mM Tris, 5% SDS, 0,025% Bromphenolblue, 50% glycerol, pH 6.8) and 1x loading buffer to adjust volume

differences. The samples were then boiled for 5 minutes at 95°C and then stored at -20°C. The remaining lysates were stored at -80°C. For western blot analysis the samples were boiled for a couple of minutes and then separated by 10% SDS–PAGE, using a Biorad apparatus running at 25 mA per gel for the stacking gel (125 mM Tris pH 6.8., 10% SDS, 30 % Acrylamide/N', N'-Bismethyleneacryl- amide, 10% TEMED, 10% APS) and 50 mA per gel for the separating gel (375 mM Tris pH 8.8., 10% SDS, 30 % Acrylamide/N', N'-Bismethyleneacrylamide, 10% TEMED, 10% APS), using a 1x running buffer (25 mM Tris, 250 mM Glycine, 0,1% SDS). To estimate protein sizes, a prestained marker ProteinLadder (Fermentas) was used. The separated proteins were then electrophoretically transferred to a membrane (Amersham), using a transfer apparatus from Biorad running at 10 V for 1 hour, then 30 V overnight and finishing with 50 V for the last hour using a 1x transfer buffer (2x running buffer, 10% Methanol p.a. in dH2O). The transfer was verified by Ponceau S staining. The blots were probed with the appropriate primary antibodies Rok-α (Millipore), Cofilin (Abcam), panRasV12 (Calbiochem), 14-3-3, B-Raf, pCofilin, pMLC2 (Santa Cruz), SOS1, Raf-1, panERK, Raf-1, Rok-α (BD/Transduction Labs), Mek, pMEK, pERK (Cell Signaling) prior to incubation with peroxidase-conjugated secondary antibodies and detection by an enhanced chemiluminescence system (Pierce).

Part VI. References

References

Alam, M. and Ratner, D. (2001). Cutaneous squamous-cell carcinoma. *The New England journal of medicine* 344(13):975–83.

Arkenau, H.T., Kefford, R. and Long, G.V. (2010). Targeting BRAF for patients with melanoma. *British journal of cancer* 104(3):392–398.

Bardwell, a.J., Frankson, E. and Bardwell, L. (2009). Selectivity of docking sites in MAPK kinases. *The Journal of biological chemistry* 284(19):13165–73.

Blanpain, C. and Fuchs, E. (2009). Epidermal homeostasis: a balancing act of stem cells in the skin. *Nature reviews. Molecular cell biology* 10(3):207–17.

Blasco, R.B., Francoz, S., Santamaría, D., Cañamero, M., Dubus, P., Charron, J., Baccarini, M. and Barbacid, M. (2011). c-Raf, but not B-Raf, is essential for development of K-Ras oncogene-driven non-small cell lung carcinoma. *Cancer cell* 19(5):652–63.

Bollag, G., Hirth, P., Tsai, J., Zhang, J., Ibrahim, P.N., Cho, H., Spevak, W., Zhang, C., Zhang, Y., Habets, G., Burton, E.A., Wong, B., Tsang, G., West, B.L., Powell, B., Shellooe, R., Marimuthu, A., Nguyen, H., Zhang, K.Y.J., Artis, D.R., Schlessinger, J., Su, F., Higgins, B., Iyer, R., D'Andrea, K., Koehler, A., Stumm, M., Lin, P.S., Lee, R.J., Grippo, J., Puzanov, I., Kim, K.B., Ribas, A., McArthur, G.a., Sosman, J.A., Chapman, P.B., Flaherty, K.T., Xu, X., Nathanson, K.L. and Nolop, K. (2010). Clinical efficacy of a RAF inhibitor needs broad target blockade in BRAF-mutant melanoma. *Nature* 4(2):1–5.

Bollrath, J., Phesse, T.J., von Burstin, V.a., Putoczki, T., Bennecke, M., Bateman, T., Nebelsiek, T., Lundgren-May, T., Canli, O., Schwitalla, S., Matthews, V., Schmid, R.M., Kirchner, T., Arkan, M.C., Ernst, M. and Greten, F.R. (2009). gp130-mediated Stat3 activation in enterocytes regulates cell survival and cell-cycle progression during colitis-associated tumorigenesis. *Cancer cell* 15(2):91–102.

Brennan, D.F., Dar, A.C., Hertz, N.T., Chao, W.C.H., Burlingame, A.L., Shokat, K.M. and Barford, D. (2011). A Raf-induced allosteric transition of KSR stimulates phosphorylation of MEK. *Nature* 472(7343):366–9.

Bruder, J.T., Heidecker, G. and Rapp, U.R. (1992). Serum-, TPA-, and Ras-induced expression from Ap-1/Ets-driven promoters requires Raf-1 kinase. *Genes & Development* 6(4):545–556.

Chan, K.S., Sano, S., Kataoka, K., Abel, E., Carbajal, S., Beltran, L., Clifford, J., Peavey, M., Shen, J. and Digiovanni, J. (2008). Forced expression of a constitutively active form of Stat3 in mouse epidermis enhances malignant progression of skin tumors induced by two-stage carcinogenesis. *Oncogene* 27(8):1087–94.

Chan, K.S., Sano, S., Kiguchi, K., Anders, J., Komazawa, N., Takeda, J. and DiGiovanni, J. (2004). Disruption of Stat3 reveals a critical role in both the initiation and the promotion stages of epithelial carcinogenesis. *The Journal of clinical investigation* 114(5):720–8.

Chapman, P.B., Hauschild, A., Robert, C., Haanen, J.B., Ascierto, P., Larkin, J., Dummer, R., Garbe, C., Testori, A., Maio, M., Hogg, D., Lorigan, P., Lebbe, C., Jouary, T., Schadendorf, D., Ribas, A., O'Day, S.J., Sosman, J.A., Kirkwood, J.M., Eggermont, A.M.M., Dreno, B., Nolop, K., Li, J., Nelson, B., Hou, J., Lee, R.J., Flaherty, K.T. and McArthur, G.A. (2011). Improved Survival with Vemurafenib in Melanoma with BRAF V600E Mutation. *The New England journal of medicine* 364(26):110605080854063.

Chen, A.P., Ohno, M., Giese, K.P., Kühn, R., Chen, R.L. and Silva, A.J. (2006). Forebrain-specific knockout of B-raf kinase leads to deficits in hippocampal long-term potentiation, learning, and memory. *Journal of neuroscience research* 83(1):28–38.

Chen, J., Fujii, K., Zhang, L., Roberts, T. and Fu, H. (2001). Raf-1 promotes cell survival by antagonizing apoptosis signal-regulating kinase 1 through a MEK-ERK independent mechanism. *Proceedings of the National Academy of Sciences of the United States of America* 98(14):7783–8.

Davies, H., Bignell, G.R., Cox, C., Stephens, P., Edkins, S., Clegg, S., Teague, J., Woffendin, H., Garnett, M.J., Bottomley, W., Davis, N., Dicks, E., Ewing, R., Floyd, Y., Gray, K., Hall, S., Hawes, R., Hughes, J., Kosmidou, V., Menzies, A., Mould, C., Parker, A., Stevens, C., Watt, S., Hooper, S., Wilson, R., Jayatilake, H., Gusterson, B.a., Cooper, C., Shipley, J., Hargrave, D., Pritchard-Jones, K., Maitland, N., Chenevix-Trench, G., Riggins, G.J., Bigner, D.D., Palmieri, G., Cossu, A., Flanagan, A., Nicholson, A., Ho, J.W.C., Leung, S.Y., Yuen, S.T., Weber, B.L., Seigler, H.F., Darrow, T.L., Paterson, H., Marais, R., Marshall, C.J., Wooster, R., Stratton, M.R. and Futreal, P.A. (2002). Mutations of the BRAF gene in human cancer. *Nature* 417(6892):949–54.

Dhomen, N., Reis-Filho, J.S., da Rocha Dias, S., Hayward, R., Savage, K., Delmas, V., Larue, L., Pritchard, C. and Marais, R. (2009). Oncogenic Braf induces melanocyte senescence and melanoma in mice. *Cancer cell* 15(4):294–303.

REFERENCES

Dreesen, O. and Brivanlou, A.H. (2007). Signaling Pathways in Cancer and Embryonic Stem Cells. *Stem Cell Reviews* 3(1):7–17.

Ehrenreiter, K. (2005). Raf-1 regulates Rho signaling and cell migration. *The Journal of Cell Biology* 168(6):955–964.

Ehrenreiter, K., Kern, F., Velamoor, V., Meissl, K., Galabova-Kovacs, G., Sibilia, M. and Baccarini, M. (2009). Raf-1 addiction in Ras-induced skin carcinogenesis. *Cancer cell* 16(2):149–60.

Ferlay, J., Shin, H.R., Bray, F., Forman, D., Mathers, C. and Parkin, D.M. (2010). Estimates of worldwide burden of cancer in 2008: GLOBOCAN 2008. *International journal of cancer. Journal international du cancer* 127(12):2893–917.

Flaherty, K.T., Puzanov, I., Kim, K.B., Ribas, A., McArthur, G.A., Sosman, J.A., O'Dwyer, P.J., Lee, R.J., Grippo, J.F., Nolop, K. and Chapman, P.B. (2010). Inhibition of mutated, activated BRAF in metastatic melanoma. *The New England journal of medicine* 363(9):809–19.

Fritz, G., Just, I. and Kaina, B. (1999). Rho GTPases are over-expressed in human tumors. *International journal of cancer. Journal international du cancer* 81(5):682–7.

Fryer, B.H. and Field, J. (2005). Rho, Rac, Pak and angiogenesis: old roles and newly identified responsibilities in endothelial cells. *Cancer letters* 229(1):13–23.

Galabova-Kovacs, G., Catalanotti, F., Matzen, D., Reyes, G.X., Zezula, J., Herbst, R., Silva, A., Walter, I. and Baccarini, M. (2008). Essential role of B-Raf in oligodendrocyte maturation and myelination during postnatal central nervous system development. *The Journal of cell biology* 180(5):947–55.

Galabova-Kovacs, G., Kolbus, A., Matzen, D., Meissl, K., Piazzolla, D., Rubiolo, C., Steinitz, K. and Baccarini, M. (2006a). ERK and beyond: insights from B-Raf and Raf-1 conditional knockouts. *Cell cycle (Georgetown, Tex.)* 5(14):1514–8.

Galabova-Kovacs, G., Matzen, D., Piazzolla, D., Meissl, K., Plyushch, T., Chen, A.P., Silva, A. and Baccarini, M. (2006b). Essential role of B-Raf in ERK activation during extraembryonic development. *Proceedings of the National Academy of Sciences of the United States of America* 103(5):1325–30.

Hatzivassiliou, G., Song, K., Yen, I., Brandhuber, B.J., Anderson, D.J., Alvarado, R., Ludlam, M.J.C., Stokoe, D., Gloor, S.L., Vigers, G., Morales, T., Aliagas, I., Liu, B., Sideris, S., Hoeflich, K.P., Jaiswal, B.S., Seshagiri, S., Koeppen, H., Belvin, M., Friedman, L.S. and Malek, S. (2010).

RAF inhibitors prime wild-type RAF to activate the MAPK pathway and enhance growth. *Nature* 464(7287):431–5.

Heidorn, S.J., Niculescu-Duvas, I., Milagre, C., Whittaker, S., Reis-Filho, J.S., Springer, C.J., Nourry, A., Dhomen, N., Hussain, J. and Pritchard, C. (2010). Kinase-Dead BRAF and Oncogenic RAS Cooperate to Drive Tumor Progression through CRAF. *Cell* 140(2):209–221.

Honma, M., Benitah, S.A. and Watt, F.M. (2006). Role of LIM kinases in normal and psoriatic human epidermis. *Molecular biology of the cell* 17(4):1888–96.

Indra, a.K., Warot, X., Brocard, J., Bornert, J.M., Xiao, J.H., Chambon, P. and Metzger, D. (1999). Temporally-controlled site-specific mutagenesis in the basal layer of the epidermis: comparison of the recombinase activity of the tamoxifen-inducible Cre-ER(T) and Cre-ER(T2) recombinases. *Nucleic acids research* 27(22):4324–7.

Karnoub, A.E. and Weinberg, R.a. (2008). Ras oncogenes: split personalities. *Nature reviews. Molecular cell biology* 9(7):517–31.

Kern, F., Niault, T. and Baccarini, M. (2010). Ras and Raf pathways in epidermis development and carcinogenesis. *British journal of cancer* pp. 1 – 6.

Khavari, T.a. and Rinn, J. (2007). Ras/Erk MAPK signaling in epidermal homeostasis and neoplasia. *Cell cycle (Georgetown, Tex.)* 6(23):2928–31.

Kolch, W. (2000). Meaningful relationships: the regulation of the Ras/Raf/MEK/ERK pathway by protein interactions. *The Biochemical journal* 351 Pt 2:289–305.

Kubicek, M., Pacher, M., Abraham, D., Podar, K., Eulitz, M. and Baccarini, M. (2002). Dephosphorylation of Ser-259 regulates Raf-1 membrane association. *The Journal of biological chemistry* 277(10):7913–9.

Leung, T., Chen, X.Q., Manser, E. and Lim, L. (1996). The p160 RhoA-binding kinase ROK alpha is a member of a kinase family and is involved in the reorganization of the cytoskeleton. *Molecular and cellular biology* 16(10):5313–27.

Lock, F.E. and Hotchin, N.a. (2009). Distinct roles for ROCK1 and ROCK2 in the regulation of keratinocyte differentiation. *PloS one* 4(12):e8190.

Mason, C.S., Springer, C.J., Cooper, R.G., Superti-Furga, G., Marshall, C.J. and Marais, R. (1999). Serine and tyrosine phosphorylations cooperate in Raf-1, but not B-Raf activation. *The EMBO journal* 18(8):2137–48.

REFERENCES

Mercer, K.E. and Pritchard, C.a. (2003). Raf proteins and cancer: B-Raf is identified as a mutational target. *Biochimica et Biophysica Acta (BBA) - Reviews on Cancer* 1653(1):25–40.

Mikula, M., Schreiber, M., Husak, Z., Kucerova, L., Rüth, J., Wieser, R., Zatloukal, K., Beug, H., Wagner, E.F., Baccarini, M., Ruth, J. and R\\"uth, J. (2001). Embryonic lethality and fetal liver apoptosis in mice lacking the c-raf-1 gene. *The EMBO journal* 20(8):1952–62.

Mitin, N., Rossman, K.L. and Der, C.J. (2005). Signaling interplay in Ras superfamily function. *Current biology : CB* 15(14):R563–74.

Narayanan, D.L., Saladi, R.N. and Fox, J.L. (2010). Ultraviolet radiation and skin cancer. *International journal of dermatology* 49(9):978–86.

Niault, T., Sobczak, I., Meissl, K., Weitsman, G., Piazzolla, D., Maurer, G., Kern, F., Ehrenreiter, K., Hamerl, M., Moarefi, I., Leung, T., Carugo, O., Ng, T. and Baccarini, M. (2009). From autoinhibition to inhibition in trans: the Raf-1 regulatory domain inhibits Rok-alpha kinase activity. *The Journal of cell biology* 187(3):335–42.

O'Neill, E., Rushworth, L., Baccarini, M. and Kolch, W. (2004). Role of the kinase MST2 in suppression of apoptosis by the proto-oncogene product Raf-1. *Science (New York, N.Y.)* 306(5705):2267–70.

Pawlak, G. and Helfman, D. (2002). MEK mediates v-Src-induced disruption of the actin cytoskeleton via inactivation of the Rho-ROCK-LIM kinase pathway. *Journal of Biological Chemistry* 277(30):26927.

Pearson, G., Robinson, F., Beers Gibson, T., Xu, B.E., Karandikar, M., Berman, K. and Cobb, M.H. (2001). Mitogen-activated protein (MAP) kinase pathways: regulation and physiological functions. *Endocrine reviews* 22(2):153–83.

Piazzolla, D., Meissl, K., Kucerova, L., Rubiolo, C. and Baccarini, M. (2005). Raf-1 sets the threshold of Fas sensitivity by modulating Rok-alpha signaling. *The Journal of cell biology* 171(6):1013–22.

Poulikakos, P.I., Zhang, C., Bollag, G., Shokat, K.M. and Rosen, N. (2010). RAF inhibitors transactivate RAF dimers and ERK signalling in cells with wild-type BRAF.Suppl. *Nature* 1.

Pritchard, C.A., Bolin, L., Slattery, R., Murray, R. and Mcmahon, M. (1996). Post-natal lethality and neurological and gastrointestinal defects in mice with targeted disruption of the A-Raf protein kinase gene. *Current biology : CB* 6(5):614–7.

Quintanilla, M., Brown, K., Ramsden, M. and Balmain, A. (1986). Carcinogen-specific mutation and amplification of Ha-ras during mouse skin carcinogenesis. *Nature* 322(6074):78–80.

Rajakulendran, T., Sahmi, M., Lefrançois, M., Sicheri, F. and Therrien, M. (2009). A dimerization-dependent mechanism drives RAF catalytic activation. *Nature* 461(7263):542–5.

Raman, M., Chen, W. and Cobb, M.H. (2007). Differential regulation and properties of MAPKs. *Oncogene* 26(22):3100–12.

Ridky, T.W. and Khavari, P.A. (2004). Pathways sufficient to induce epidermal carcinogenesis. *Cell cycle (Georgetown, Tex.)* 3(5):621–4.

Riva, C., Lavieille, J.P., Reyt, E., Brambilla, E., Lunardi, J. and Brambilla, C. (1995). Differential c-myc, c-jun, c-raf and p53 expression in squamous cell carcinoma of the head and neck: implication in drug and radioresistance. *European journal of cancer. Part B, Oral oncology* 31B(6):384–91.

Roy, S., Lane, a., Yan, J., McPherson, R. and Hancock, J.F. (1997). Activity of plasma membrane-recruited Raf-1 is regulated by Ras via the Raf zinc finger. *The Journal of biological chemistry* 272(32):20139–45.

Rushworth, L.K., Hindley, A.D., O'Neill, E. and Kolch, W. (2006). Regulation and role of Raf-1/B-Raf heterodimerization. *Molecular and cellular biology* 26(6):2262–72.

Sano, S., Chan, K.S., Kira, M., Kataoka, K., Takagi, S., Tarutani, M., Itami, S., Kiguchi, K., Yokoi, M., Sugasawa, K., Mori, T., Hanaoka, F., Takeda, J. and DiGiovanni, J. (2005). Signal transducer and activator of transcription 3 is a key regulator of keratinocyte survival and proliferation following UV irradiation. *Cancer research* 65(13):5720–9.

Sebbagh, M., Hamelin, J., Bertoglio, J., Solary, E. and Bréard, J. (2005). Direct cleavage of ROCK II by granzyme B induces target cell membrane blebbing in a caspase-independent manner. *The Journal of experimental medicine* 201(3):465–71.

Shukla, S., Shishodia, G., Mahata, S., Hedau, S., Pandey, A., Bhambhani, S., Batra, S., Basir, S.F., Das, B.C. and Bharti, A.C. (2010). Aberrant expression and constitutive activation of STAT3 in cervical carcinogenesis: implications in high-risk human papillomavirus infection. *Molecular cancer* 9(1):282.

Sibilia, M., Fleischmann, A., Behrens, A., Stingl, L., Carroll, J., Watt, F.M., Schlessinger, J. and Wagner, E.F. (2000). The EGF receptor provides an essential survival signal for SOS-dependent skin tumor development. *Cell* 102(2):211–220.

REFERENCES

Sobczak, I., Galabova-Kovacs, G., Sadzak, I., Kren, A., Christofori, G. and Baccarini, M. (2008). B-Raf is required for ERK activation and tumor progression in a mouse model of pancreatic beta-cell carcinogenesis. *Oncogene* 27(35):4779–87.

Sobti, R.C., Singh, N., Hussain, S., Suri, V., Bharti, A.C. and Das, B.C. (2009). Overexpression of STAT3 in HPV-mediated cervical cancer in a north Indian population. *Molecular and cellular biochemistry* 330(1-2):193–9.

Stanley, M. (2010). Pathology and epidemiology of HPV infection in females. *Gynecologic oncology* 117(2 Suppl):S5–10.

Tarutani, M., Itami, S., Okabe, M., Ikawa, M., Tezuka, T., Yoshikawa, K., Kinoshita, T. and Takeda, J. (1997). Tissue-specific knockout of the mouse Pig-a gene reveals important roles for GPI-anchored proteins in skin development. *Proceedings of the National Academy of Sciences* 94(14):7400–7405.

Wimmer, R. and Baccarini, M. (2010). Partner exchange: protein-protein interactions in the Raf pathway. *Trends in biochemical sciences* 35(12):660–8.

Wyckoff, J.B., Pinner, S.E., Gschmeissner, S., Condeelis, J.S. and Sahai, E. (2006). ROCK- and myosin-dependent matrix deformation enables protease-independent tumor-cell invasion in vivo. *Current biology : CB* 16(15):1515–23.

Yamaguchi, O., Watanabe, T., Nishida, K., Kashiwase, K., Higuchi, Y., Takeda, T., Hikoso, S., Hirotani, S., Asahi, M., Taniike, M., Nakai, A., Tsujimoto, I., Matsumura, Y., Miyazaki, J.i., Chien, K.R., Matsuzawa, A., Sadamitsu, C., Ichijo, H., Baccarini, M., Hori, M. and Otsu, K. (2004). Cardiac-specific disruption of the c-raf-1 gene induces cardiac dysfunction and apoptosis. *The Journal of clinical investigation* 114(7):937–43.

Zaravinos, A., Kanellou, P., Baritaki, S., Bonavida, B. and Spandidos, D.a. (2009). BRAF and RKIP are significantly decreased in cutaneous squamous cell carcinoma. *Cell cycle (Georgetown, Tex.)* 8(9):1402–8.

Zhang, B.H. and Guan, K.L. (2000). Activation of B-Raf kinase requires phosphorylation of the conserved residues Thr598 and Ser601. *The EMBO journal* 19(20):5429–39.

Zhang, L., Bewick, M. and Lafrenie, R.M. (2002). Role of Raf-1 and FAK in cell density-dependent regulation of integrin-dependent activation of MAP kinase. *Carcinogenesis* 23(7):1251–8.

Part VII. Acknowledgements

Part VIII. Curriculum Vitae

Name	Florian Kern
Date; Place of birth	3.4.1981; Vienna, Austria

1987 – 1991	Elementary School, Biedermannsdorf, Austria
1991 – 1999	High School, Bundesgymnasium und Bundesrealgymnasium Mödling Keimgasse, Austria
1999 – 2000	Rotary Youth Exchange, Port Macquarie High School, Port Macquarie, Australia
2000 – 2001	Civil Service with the Austrian Red Cross
2001 - 2007	Studies of Molecularbiology at the University of Vienna, Austria
2004	Undergraduate student in the laboratory of Prof. Georg Schmetterer, Department of Physical Chemistry at the University of Vienna, Austria. Research project "Isolation and purification of Phycocyanin from Cyanobacteria".
2004	Undergraduate student in the laboratory of Prof. Rudolf Valenta, Department of Pathophysiology at the General Hospital (AKH), Vienna, Austria. Research projects on celiac disease and milk allergy.
2005 - 2006	ERASMUS: Undergraduate student in the laboratory of Mª Angeles Muñoz Fernandez, Department of Immunology at the General Hospital Gregorio Marañon, Madrid, Spain. Research project "HIV-2 (CBL-23) induces COX-2 in astrocytes (U-87)".
2006 – 2007	Diploma thesis in the laboratory of Univ. Prof. Dr. Manuela Baccarini, Max F. Perutz Laboratories at the Vienna Biocenter, Austria. "The role of B-Raf in Ras mediated skin tumorigenesis".
Since 2007	PhD thesis in the laboratory of Univ. Prof. Dr. Manuela Baccarini, Max F. Perutz Laboratories at the Vienna Biocenter, Austria. "The role of Raf in Ras mediated skin carcinogenesis".

Publications:

Álvarez S., Blanco A., **Kern, F.**, Fresno M., Muñoz-Fernández, M.A. (2008). HIV-2 induces NF-ϰB activation and cyclooxygenase-2 expression in human astroglial cells. Virology, 380 (2008) 144–151. doi:10.1016/j.virol.2008.07.008

Ehrenreiter, K., **Kern, F.**, Velamoor, V., Meissl, K., Galabova-Kovacs, G., Sibilia, M., & Baccarini, M. (2009). Raf-1 addiction in Ras-induced skin carcinogenesis. Cancer cell, 16(2), 149-60. doi:10.1016/j.ccr.2009.06.008

Niault, T., Sobczak, I., Meissl, K., Weitsman, G., Piazzolla, D., Maurer, G., **Kern, F.**, et al. (2009). From autoinhibition to inhibition in trans: the Raf-1 regulatory domain inhibits Rok-alpha kinase activity. The Journal of cell biology, 187(3), 335-42. doi:10.1083/jcb.200906178

De Andrea, M., Rittà, M., Landini, M. M., Borgogna, C., Mondini, M., **Kern, F.**, Ehrenreiter, K., et al. (2010). Keratinocyte-specific stat3 heterozygosity impairs development of skin tumors in human papillomavirus 8 transgenic mice. Cancer research, 70(20), 7938-48. doi:10.1158/0008-5472.CAN-10-1128

Kern, F., Niault, T., & Baccarini, M. (2010). Ras and Raf pathways in epidermis development and carcinogenesis. British journal of cancer, 1 - 6. Nature Publishing Group. doi:10.1038/sj.bjc.6606009

Kern F., Doma E., Rupp C., Niault T., and Baccarini M. (submitted 2011). Essential ERK-dependent and -independent roles of Raf in Ras-driven skin carcinogenesis. Submitted to Cancer Cell August 4th 2011